UNIVERSITÀ DEGLI STUDI DI PADOVA
DIPARTIMENTO DI PSICOLOGIA GENERALE

SCUOLA DI DOTTORATO DI RICERCA IN SCIENZE PSICOLOGICHE

CICLO XXVI

REACH TO GRASP MOVEMENT: A SIMULTANEOUS RECORDING APPROACH

DIRETTORE DELLA SCUOLA: Ch.ma Prof.ssa Francesca Peressotti
SUPERVISORE: Ch.mo Prof. Umberto Castiello

DOTTORANDO: Teresa De Sanctis

TABLE OF CONTENTS

LIST OF ABREVIATIONS

μ	=	Magnetic Moment
ACG	=	Anterior Cingulate Gyrus
AG	=	Angular Gyrus
AIP	=	Anterior Intraparietal (monkey)
aIPS	=	Anterior Intraparietal Sulcus (humans)
BA	=	Brodmann Area
BOLD	=	Blood Oxygenation Level Dependent
CBF	=	Cerebral Blood Flow
Cu	=	Cuneus
dPMC	=	Dorsolateral Premotor Cortex
DTI	=	Diffusion Tensor Imaging
EC	=	Euler Characteristic
EEG	=	Electroencephalography
ERP	=	Evoked Related Potentials
F1	=	Primary Motor Area (monkey)
F2	=	Dorsal Premotor Cortex (monkey)
F5	=	Ventral Premotor Cortex (monkey)
FIR	=	Finite Impulse Response
fMRI	=	Functional Magnetic Resonance Imaging
FWE	=	Family Wise Error
FWHM	=	Full Width at Half Maximum
GL	=	Grasping Large
GLM	=	General Linear Model
GS	=	Grasping Small
H	=	Hemisphere
HRF	=	Hemodynamic Response Function
ICA	=	Independent Component Analysis
IPL	=	Inferior Parietal Lobule
ISI	=	Inter Stimulus Interval
J	=	Angular Momentum
LH	=	Left Hemisphere

LIP = Lateral IntraParietal
M = Net Magnetization
M1 = Primary Motor Cortex
MCG = Middle Cingulate Gyrus
MeFG = Medial Frontal Gyrus
MFG = Middle Frontal Gyrus
MIP = Maximum Intensity Projection
mIP = Medial Intraparietal Area
mIPS = Medial Intraparietal sulcus
MLE = Maximum Likelihood Estimator
MR = Magnetic Resonance
MRI = Magnetic Resonance Imaging
MVPA = Multivoxel Pattern Analysis
PCU = Precuneus
PET = Positron Emission Tomography
PFC = Prefrontal Cortex
PFG = Precentral Frontal Gyri
PG = Precision Grip
PGA = Peak Grip Aperture
PMC = Premotor Cortex
PMd = Premotor Dorsal Cortex
PMv = Ventral Premotor Cortex
PPC = Posterior Parietal Cortex
PreCg = Precentral Gyrus
PreCu = Precuneus
PRR = Parietal Reach Region
rCBF = Regional Cerebral Blood Flow
RF = Radio Frequency
RFT = Random Field Theory
RFX = Random Effect Analysis
RH = Right Hemisphere
RL = Reaching Large
ROI = Region of Interest
RS = Reaching Small
RT = Reaction Time

SFG	=	Superior Frontal Gyrus
SI	=	Somatosensory Cortex
SII	=	Secondary Somatosensory
SMA	=	Supplementary Motor Cortex
SMG	=	Supramarginal Gyrus
SNR	=	Signal to Noise Ratio
SPL	=	Superior Parietal Lobule
SPM	=	Statistical Parametric Mapping
SVC	=	Small Volume Correction
TE	=	Echo Time
TMS	=	Transcranial Magnetic Stimulation
TR	=	Repetition Time
WHG	=	Whole Hand Prehension

SYNOPSIS

In our everyday life, we interact continually with objects. We reach for them, we grasp them, we manipulate them. All these actions are apparently very simple. Yet, this is not so. The mechanisms that underlie them are complex, and require multiple visuomotor transformations entailing the capacity to transform the visual features of the object in the appropriate hand configuration, and the capacity to execute and control hand and finger movements.

In neural terms, grasping behavior can be dissociated into separate reach and grip components. According to this view, computations regarding the grasp component occurs within a lateral parietofrontal circuit involving the anterior intraparietal area (AIP) and both the dorsal (PMd) and the ventral (PMv) premotor areas. The general agreement is that the processes occurring in AIP constitute the initial step of the transformation leading from representation of objects to movement aimed at interacting with such objects. Evidence supporting this view comes from neurophysiological studies showing that the representation of three-dimensional object features influences both the rostral sector of the ventral premotor cortex (area F5) and the ventro-rostral sector of the dorsal premotor area (area F2vr; for review see Filimon, 2010). With respect to the reach component, there is agreement that it is subserved by a more medial parieto-frontal circuit including the medial intraparietal area (mIP) termed as the parietal reach region (PRR), area V6A, and the dorsal premotor area F2. Human neuroimaging studies go in the same direction. They showed the involvement of the anterior portion of the human AIP in grasping behavior and they proposed human homologues of both the ventral and dorsal premotor cortices during grasping. Whereas, reaching activates the medial intraparietal and the superior parieto-occipital cortex (for review see Castiello & Begliomini, 2008).

Altogether these studies suggest that in humans, like in monkeys, reach to grasp movements involve a large network of interconnected structures in the parietal and frontal lobes. And, that

this cortical network is differentially involved for the control of distinct aspects characterizing the planning and the control of reach to grasp movement. Nevertheless, how the neural control systems interact with the complex biomechanics of moving limbs - as to help us to identify the operational principles to look for in reach to grasp studies and, more in general, in motor control - remains an open question. In this respect, it is only through the use of converging techniques with different characteristics that we might fully understand how the human brain controls the grasping function. What is so far lacking in the literature on cortical control of grasp in humans is a systematic documentation of the time course of neural activity during performance of reach to grasp movement. To fill this gap the present thesis will consider the co-registration of behavioural and neural events in order to provide deeper insights into the neuro-functional basis of reach to grasp movements in humans.

In Chapter 1 an overview on the state of the art in many disciplines investigating reach to grasp processes will be provided, with particular attention to neurophysiology, from which most of the knowledge regarding the neural underpinnings of reach to grasp movements comes from. Furthermore, kinematical as well as neuroimaging, and evoked related potentials (ERP) investigations will be reviewed. Particular emphasis will be given to neuroimaging studies, especially those exploring grasping movements by functional magnetic resonance imaging (fMRI), as the technique adopted to conduct the studies presented in this thesis (Chapter 1). Basic principles of co-registration techniques, which are at the core of the methodological aspect of the present thesis, will be reviewed (Chapter 2). In this respect, a description of the methodologies adopted in the present thesis together with general information regarding signal processing and data analysis for these different techniques will be provided in specific appendices (III, IV). Then, three studies focusing on the co-registration of kinematical with ERP (Chapters 3 and 4) and FMRI with ERP (Chapter 5) will be presented and discussed. In Chapter 3 the co-registration of ERP and kinematical signals will be considered with specific reference to

hand shaping, that is the grasp component of the targeted movement. A similar co-registration approach will be adopted in Chapter 4 for investigating the underlying circuits of reaching. The focus for Chapter 5 will be the co-registration of ERPs and fMRI signals as to reveal the time course of activation of the differential cortical areas related to the planning, initiation and on-line control of reaching and grasping movements and how such activity varies depending on object size. A general discussion (Chapter 6), contextualizing the results obtained by the studies presented in this thesis will follow.

SINOSSI

Durante la nostra vita quotidiana interagiamo continuamente con gli oggetti circostanti. Raggiungiamo, afferriamo e manipoliamo questi oggetti. Tutte queste azioni sono apparentemente molto semplici. Tuttavia non è proprio così. Il meccanismo sottostante queste azioni è molto complesso, e richiede una serie di trasformazioni visuomotorie che implicano la capacità di trasformare le caratteristiche visive di un oggetto nell'appropriata configurazione della mano oltre all'abilità di eseguire e controllare i movimenti di mano e dita.

In termini neurali il movimento di prensione può essere scomposto in due componenti: raggiungimento e prensione. Seguendo questa dicotomia è stato proposto che i sistemi neurali sottostanti la prensione avvengano all'interno del circuito parietofrontale laterale che coinvolge l'area intraparietale anteriore (AIP), ed entrambe le aree premotorie, premotoria dorsale (Pmd) e premotoria ventrale (PMv). Generalmente i processi che si verificano in AIP rappresentano la fase iniziale della trasformazione che conduce dalla rappresentazione degli oggetti al movimento finalizzato all'interazione con gli oggetti stessi. Le prove a sostengo di questa ipotesi provengono dagli studi neurofisiologici; che mostrano come la rappresentazione delle caratteristiche di un oggetto tridimensionale influenza entrambe la sezioni rostrale della coretccia premotoria ventrale (area F5) e la sezione ventro-rostrale dell'area premotoria dorsale (area F2vr). Per quanto concerne la componente di raggiungimento, è stato proposto un circuito parieto-frontale, principalmente mediale, che coinvolge l'area intraparietale mediale (MIP) definita anche come la regione parietale deputata al raggiungimento (PRR), area V6A e l'area premotoria dorsale F2. Nell' uomo studi di neuroimmagine confermano quelli neurofisiologici e dimostrano il coinvolgimento della porzione anteriore del corrispettivo umano del AIP durante il movimento di prensione ed inoltre hanno postulato omologhe aree per entrambe le cortecce premotorie ventrali e dorsali durante la prensione stessa. Mentre il movimento di raggiungimento attiva la corteccia intraparietale e la coretccia parieto-occipitale sueperiore.

Complessivamente questi studi suggeriscono che negli esseri umani, cosi come nelle scimmie, I movimenti di raggiungimento e prensione coinvolgono una vasta rete di strutture a livello dei lobi parietale e frontale. Inoltre il coinvolgimento di questa rete neurale si modula durante la pianificazione ed il controllo del movimento. Tuttavia la modalità con la quale i sistemi neurali interagiscono con gli aspetti biomeccanici deputati al controllo del movimento rimane una questione aperta. A tal proposito è solo attraverso l'utilizzo di tecniche convergenti con diverse caratteristiche che possiamo comprendere pienamente come il cervello umano esercita il controllo del movimento. Ciò che finora appare carente nella letteratura sul controllo corticale del movimento di prensione negli esseri umani è difatti una documentazione sistematica dell'andamento temporale dell'attività neurale e cinematica durante l'esecuzione del movimento di raggiungimento e prensione. Con l'intento di colmare questa lacuna il presente lavoro di tesi esaminerà la registrazione simultanea di eventi comportamentali e neurali al fine di fornire più profonde intuizioni sulle basi neuro-funzionali del movimento di raggiungimento e prensione negli esseri umani.

Nel Capitolo 1 verrà fornita una panoramica sullo stato dell'arte nelle molte discipline che studiano il processo di raggiungimento e prensione, con particolare attenzione alla neurofisiologia, dalla quale scaturisce la maggior parte delle conoscenze circa le basi neurali di questo tipo di azione nell'uomo. A tal proposito, sanno riesaminati studi riguardanti la cinematica, cosi come le neuroimmagini e i potenziali evocati (ERP).

I principi alla base delle tecniche di registrazione simultanea, che costituiscono la base metodologica del presente lavoro di tesi, saranno invece esaminati nel Capitolo 2. A tal proposito una descrizione delle metodologie d'indagine utilizzate nel presente lavoro di tesi assieme alle informazioni generali riguardanti l'elaborazione del segnale e l'analisi dei dati per queste diverse tecniche saranno forniti nelle apposite appendici (III, IV). Successivamente saranno presentati e discussi tre studi incentrati sulla registrazione simultanea dei correlati neurali del movimento di

raggiungimento prensione in partecipanti umani rilevati tramite cinematica, ERP e fMRI (capitoli 3, 4 e 5). Nel Capitolo 3 la registrazione simultanea dei segnali ERP e cinematico con specifico riferimento alla coreografia raggiunta dalla mano durante il raggiungimento. Lo stesso approccio di registrazione simultanea sarà adottato nel Capitolo 4 per indagare l'esistenza di circuiti specifici per il movimento di raggiungimento. L'obiettivo del Capitolo 5 sarà invece la registrazione simultanea dei segnali ERPs ed fMRI al fine di rilevare il decorso temporale dell'attivazione delle differenti aree corticali relative alla pianificazione e al controllo dei movimenti di raggiungimento e di prensione. Seguirà una discussione generale (Capitolo 6) volta alla contestualizzazione dei risultati riportati nel presente lavoro di tesi.

1. REACHING AND GRASPING MOVEMENT

This chapter will provide an overview on the state of the art of knowledge regarding reaching and grasping movements in different research domains. First, evolutionary and developmental contextualization will be outlined. Then studies conducted on reaching and grasping will be reviewed, including results obtained by behavioural, neurophysiological and neuropsychological approaches. Particular attention will be given to results obtained by investigations conducted using kinematics, functional magnetic resonance imaging (fMRI) and electroencephalography (EEG) as they specifically refer to the approach and techniques adopted to conduct the studies included within the present thesis.

1.1. The evolutionary approach

Morphological correlates of human reach to grasp movement emerged with our first ancestors, that is when the pentadactyl hand with the divergent thumb appeared. Because of this morphological evolution, the hand became able to grasp and manipulate objects, increasing the primate's ability to actively interact with objects. Manipulation of objects (or parts of them) became possible, through the opposition of the thumb to the other fingers (Haines, 1955). Through a very subtle coordination mechanism, fingers became able to close themselves around the object, firmly holding it. Another important aspect is concerned with the presence of the nails which support friction pads (Martin, 1990), and allow for foraging among slender branches for fruits and insects.

The evolution of reach to grasp abilities became more sophisticated in our more recent ape-like

ancestors. Theirs long and mobile arms, together with fingers allowed them to hang by one hand on branches, while the other hand was free to reach the surrounding space and grasp for fruits and leaves (Rose, 1992). Hand morphology has thus changed. On one side, fingers longer than before were theoretically obstructing effective thumb/fingertips, on the other side fingers became also able to move independently, and the thumb became able of opposition to the index finger (Stern, 1987).

With bipedalism hands became free, and reach to grasp movements were increasingly applied to the use of tools (Napier, 1961). More specifically, investigation on prehension dynamics started with Napier's study (1956, 1961) on *precision* and *power* grip (see below). His observations went well over a physical description of manual actions, showing how sophisticated and refined the control of an act such as reaching towards and grasp an object is. It is fascinating that we can observe the recapitulation hand functional evolution during millenniums reflected in human hand functional ontogeny.

1.2. A developmental perspective

Coordinated prehension in humans develops relatively late during ontogeny. The opposition of the thumb to the index finger, for example, does not emerge before ten months of age (Woodward et al., 2000). This is why a skilled manipulation of objects, as the opposition between thumb and index finger, needs a sophisticated control of finger-tip forces to become efficient. The ability to control these forces occurs through both feedback and feed forward mechanisms (Gordon et al., 1991; Johansson et al., 1998). The first attempts to perform a precision grip by young children are typically characterized by excessive force exertion and large variability. Furthermore, the movement is not fluid, but it appears to be segmented in different phases. Young children seem not to be able to take advantage from their previous "manipulative"

experience with objects as to calibrate the force output in the following attempts (Forssberg, 1992). In the second year of life, children become able to use sensory information in a more reliable and effective way, becoming able to optimize the force output and to implement feed-forward control (Gordon et al., 1991).

Children's grasping performance is not comparable to an adult performance until an age ranging from six to eight years. Then, subtle improvements occur until adolescence. Altogether these aspects of the maturation process suggest that grip coordination may coincide with the development and maturation of the neural structures responsible for the control of prehension. Along these lines, Zoia and colleagues (2006) reported that the reaching component of children is characterized by longer movement duration and deceleration time together with a lower maximum height of wrist trajectory than in adult. Furthermore, the maximal finger aperture is larger in children than adults. These findings suggest that the strategies adopted to reach towards and grasp objects are remarkably different during different stages of development (Kuhtz-Buschbeck et al., 1998a; 1998b; Zoia et al., 2007).

1.3. Behavioral studies

When thinking about a reach to grasp movement, we usually represent a hand reaching towards and then grasp an object which has specific attributes and a specific relationship with the environment (e.g. a pen on the table). In order to perform this act, the arm is transported towards the object, and the hand and fingers adopt a configuration which allows for an appropriate contact with it (see Figure 1.1.). Following contact, forces must be applied and calibrated as to maintain the grasp stable.

Figure 1.1. Preshaping of the hand during the reaching process towards the object. (Source: Castiello, 2005; modified with permission from Jeannerod, 1984)

Behavioural studies on reach to grasp movements in humans have been chiefly carried out by using three-dimensional (3D) motion analysis systems which allow for the acquisition of kinematical measures in terms of acceleration and velocity profiles together with spatial trajectories of arm and fingers (see Appendix I). These studies have demonstrated that the mechanics of grasping in humans is significantly influenced by object attributes.

Jeannerod (1982) defined the change in *grip aperture* - the separation between the thumb and the index finger – as the central plank of a grasping movement. This landmark is a pretty constant reference point in grasping kinematics, and occurs usually within the 60-70% of the overall reach to grasp time, and is highly correlated with the size of the object. Thus, during the reaching phase, there is a sort of hand preshaping, in which the hand accommodate to the size, the shape and the intended use of the object. The preshaping phase occurs thus independently of tactile and kinaesthetic inputs, because it refers to the approaching phase. These preliminary observations led to a big increase of kinematic studies on prehension, focusing not only on object size and type of prehension (e.g., Gentilucci et al., 1991; Jakobson et al., 1992; Castiello, 1996) – which are at the core of the present thesis - but also to other objects properties, such as fragility (Savelsbergh, 1996), size of the contact surface (Bootsma et al., 1994), texture (Weir et al., 1991a) and weight (Weir et al., 1991). As reviewed by Smeets and Brenner (1999), all these factors can influence the kinematics of grasping as outlined below.

1.4. Objects proprieties

A number of studies have investigated the effects of intrinsic object properties on hand kinematics suggesting that object's features have an effect on hand aperture (Smeets & Brenner, 1999). The level of accuracy with which an object is grasped depends on object size, weight, texture, fragility and contact surface size.

1.4.1. Effects of object size

Hand preshaping first involves a progressive opening of the grip with straightening of the fingers followed by a closure of the grip until it matches objects size (Jeannerod et al., 1981, 1984). The aperture between thumb and index finger (maximum grip aperture) during reach to grasp movement covaries linearly with object size. Marteniuk and colleagues (1990) found that for an increase of one centimeter in object size, the maximum grip size increases. These experimental findings suggest that maximum grip aperture was reached progressively sooner as stimulus size was decreased and that maximum grip aperture was highly related to the size of the to be grasped object (Marteniuk et al., 1990).

Moreover differences in kinematics have also been found depending on the relationship between object size and type of grip. For instance, Gentilucci and colleagues (1991), have shown how kinematic parameters varies depending on the type of grip used, namely precision grip (PG) and whole hand prehension (WHP). Results indicate that these two types of grip are characterized by specific kinematic signatures. The small stimuli naturally calling for a precision grip show for the grasp component an anticipated maximum and a lower grip aperture. And for the reaching component a longer movement duration and a lower amplitude of peak velocity.

1.4.2. Effects of object weight

In order to isolate the possible effects of weight, Weir and colleagues (1991) asked participants to reach, grasp, and pick up between the thumb and the index finger one of four dowels that were identical in appearance, but had different weights. This task could be performed under two different conditions of weight presentation, random trials (i.e., weight unknown) and blocked trials (i.e., weight known). The authors report that changing object weight did not change any key variable for the grasp component in neither condition (Weir et al., 1991a). However, more recent studies seem to suggest that the object's weight has an effect on hand aperture (Steenbergen et al, 1995; Smeets & Brenner, 1999; Brower et al., 2006). Maximum peak grip aperture (PGA) was earlier and larger for heavier than for lighter objects. The proposal is that because a heavy object requires a more accurate grasp as to avoid slippage, such accuracy requirement would call for a greater safety margin (obtained by a greater aperture) and a longer time to determine more firm contact points (obtained by an anticipated PGA) (Smeets & Brenner, 1999). Moreover the findings by Eastough and Edwards (2007) emphasize that the mass of the object significantly influence prior to contact grasp kinematics. Especially the heavy objects cause a greater peak of grip aperture to ensure a secure grip position on the object, an increased lift delay to ensure appropriate grip force and finally a reduced peak lift velocity as to ensure that the object is not dropped during the lift phase of prehension.

1.4.3. Effects of object texture

Another object's property which has attracted the interest of scientists is object texture. For instance, Johansson and Westling (1984) asked participant to reach, grasp, and pick up

between the thumb and the index finger one of three dowels covered in either plain metal (i.e., 'normal'), Vaseline (i.e., 'slippery'), or rough sandpaper (i.e., 'rough'). When reaching to grasp the slippery object, a larger grip earlier in the movement was evident compared with grasping rough-surfaced object (Johansson & Westling, 1984). These results have been confirmed in subsequent studies (Weir et al., 1991b; Fikes et al., 1994) and interpreted as a kinematic response to the accuracy requirement embodied in grasping slippery objects (Smeets & Brenner, 1999). Recent studies confirmed the importance of the role played by texture on prehension. For instance, texture helps to judge object shape (Moliner et al., 2007). This aspect underlines that a complete description of reach to grasp behaviors requires knowledge of surface texture if the qualitative and quantitative form of the movement is to be predicted/investigated/delineated (Flatters et al., 2012).

1.4.4. Effects of object fragility

The level of accuracy with which an object is grasped depends also on how fragile the object is. The effect of object's fragility has been investigated by Savelsbergh and colleagues (1996). In this study, the target object was either transparent or black. The impression of the participants was that the transparent object was more fragile than the black object. From a kinematic perspective, no differences were found on either time or amplitude of PGA; however the 'fragile' object was associated with longer movement duration with respect to the object appearing more firm (Savelbergh et al., 1996). Recently, Groniak et al. (2010) asked participants to move an object in different condition of fragility and grip. Results show that when participants moved more fragile objects, decreased object peak acceleration, increased movement time, and an attenuated relationship between the grip and load forces were evident (Gorniak et al., 2010).

1.4.5. Effects of contact surface size

It is possible that not all the surface of a graspable object would be suitable for hand-object contact. Therefore, the effect of contact surface size has been investigated in a series of studies in which participants were requested to reach, grasp, and pick up between the thumb and the index finger similar objects having different contact surface (e.g., rounded vs. flattened objects) (Zaal & Bootsma, 1993; Bootsma et al., 1994). It was found that PGA occurred earlier and it was bigger when reaching to grasp objects with smaller contact surfaces (Zaal & Bootsma, 1993). Altogether the studies on the effects of intrinsic object properties on reach to grasp kinematics had shown that, regardless the type of property being manipulated, a greater level of grasp stability determined a magnification of PGA, and an increase in reach duration. In other words, the need for more firm hand-object contact points translates into the determination of a safety margin which is operationalized through a lengthening of the time window within which contact points can be selected.

As can be noticed, a large amount of attention has been given to object properties and their influence on the kinematics of grasping. It has been shown that even tiny changes in object properties can result in a significant change in order to grap. Overall, these results demonstrate how detailed and sensitive the processes responsible for the "translation" of object properties into the motor program implemented during the "hand preshaping" stage are. In recent years, noticeable contributions to the understanding of these mechanisms have been provided by studies conducted in the neurophysiology domain.

1.5. Neurophysiological studies

The investigation conducted by registering the activity of single neurons in the cortex of the

behaving monkey allowed for a very detailed observation of reach to grasp related brain activity, with high levels of both spatial and temporal resolution. These studies have identified the main structures responsible for the control of reach to grasp movements. These are the primary motor cortex (F1), the premotor cortex (PMC) and the anterior intraparietal sulcus (AIP).

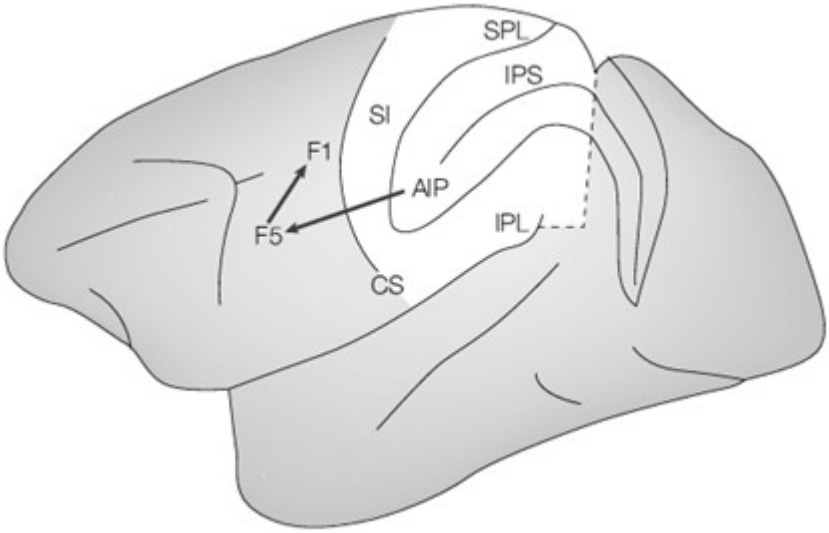

Figure 1.2. Lateral view of the monkey cerebral cortex. The visuomotor stream for grasping (AIP–F5) and the stream from F5 to F1 are indicated by large arrows. (Source: Castiello, 2005; modified with permission from Culham et al., 2003).

The ability to perform a successful grasping action depends primarily on the integrity of the primary motor cortex (F1): in fact, it has been shown how in monkeys lesions of this area produce a remarkable deficit in the control of individual fingers, which bring to a loss of the ability to coordinate individual fingers (Lawrence, 1976).

Information from the primary motor cortex is then conveyed to cells in the spinal cord via the corticospinal tract, a primary neural substrate for independent finger movements. Lesions to the corticospinal tract result in the impossibility to control fingers individually. However, this kind of lesion does not obstruct flexion during a power grip (Hepp-Reymond et al., 1996). Physiological evidences have also demonstrated that cortical motor neurons might be relatively more active during independent finger movements than during a power grip. In monkeys, large cortical motor

neurons projecting to the intrinsic hand muscles are active during the application of low levels of finely controlled force (precision grip), but can become counterintuitively inactive during a power grip (Muir et al., 1983).

The primary motor cortex projects also to the intermediate zone of the *cerebellum*, and for this reason it has been suggested that the cerebellum could play a role in the control of hand movement during grasping (Gibson et al., 1994; Robertson, 2000). This hypothesis has been tested in studies in which monkeys were trained to make two types of reaching movement: in one condition the monkey had to reach out while the hand gripped the handle of a device; in the other condition a raisin had to be grasped. The idea behind this experiment was that if the intermediate cerebellum is especially important for grasping, only reaching out to grasp a raisin should elicit discharge modulation in this area. The results agreed with the initial hypothesis, clearly showing that 93% of cells recorded from the interpositus nucleus of the cerebellum were more active during reaching out to grasp than when the hand simply gripped the handle (Gibson et al., 1994).

Another fundamental process for a successful grasp involves a transformation of the intrinsic properties of the object, visually described, into motor actions (Jeannerod et al., 1995). Two key cortical areas seem to be involved in visuomotor transformations for grasping in monkeys: area F5 and the AIP. Area F5 forms the rostral part of the monkey ventral PMv and consists of two main sectors: one on the posterior bank of the inferior arcuate sulcus (F5ab), the other on the dorsal convexity (F5c). The AIP is a small zone in the rostral part of the posterior bank of the intraparietal sulcus, and is directly connected to area F5ab (Matelli et al., 1985; Luppino et al., 1999; Matelli et al., 2001 – see Figure 1.2.).

Execution of distal motor acts such as grasping, holding, manipulating, and tearing is very effective in triggering F5 neuron responses. Interestingly, many hand grasping neurons also show

specificity for the type of prehension that is performed to grasp an object. Among these different types of grasp, PG, is the most represented type (Castiello & Begliomini, 2008). On the basis of this evidence, it has been proposed that in area F5 there is a "vocabulary" of elementary motor acts in which each "word" corresponds to a category of motor neurons that represents either the goal of the action or the way in which an action is executed, or the temporal segmentation of the action (Rizzolatti et al., 1988).

In monkeys that have been trained to grasp various objects, the activities of F5 (Figure 1.3.) and AIP (Figure 1.4.) neurons show strong similarities but also important differences (Rizzolatti et al., 1988; Taira et al., 1990; Rizzolatti et al., 1998; Rizzolatti et al., 2002). AIP and F5 neurons code for grasping actions that relate to the type of object to be grasped (for example, PG - Murata et al., 1997, 2000; Figures 1.3. and 1.4.). However, while AIP neurons seem to represent the entire action (see Figure 1.4.), F5 neurons seem to be concerned with a particular segment of the action (see Figure 1.3. - Rizzolatti et al., 1998; Murata et al., 2000). Another important difference is that visual responses to three-dimensional objects are found more frequently in AIP than in F5 (Murata et al., 2000). This suggests that AIP, although part of a parieto-frontal circuit dedicated to hand movements, contains a population of neurons that code 3D objects in visual terms.

On the basis of the functional role played by neurons in areas AIP and F5, Fagg and Arbib (1998) have developed a model in which area AIP provides multiple descriptions of 3D objects for the purpose of manipulation, whereas area F5 is mainly involved in selecting the most appropriate motor prototype among a motor vocabulary (Rizzolatti et al., 1988), for example, the type of grip that is effective in interacting with a target object. Confirmation that the AIP–F5 circuit is relevant for grasping comes from reversible, independent inactivation studies on these areas conducted in monkeys (Fogassi et al., 2001). Inactivation of either AIP or F5 markedly impaired hand shaping during reaching, and the hand posture after inactivation was inappropriate for the

object's size and shape.

The dorsal premotor cortex, area F2 (Matelli et al., 1985; Matelli & Luppino, 2001) occupies the caudal two thirds of superior area 6 (dorsal premotor cortex, PMd). It is located anterior to area F1, extends rostrally approximately 3 mm in front of the genu of the arcuate sulcus, and, laterally, up to the spur of the arcuate sulcus, which separates it from inferior area 6. Raos and others (2004) demonstrated that within area F2 a distal forelimb field also exists. This study provides compelling evidence that in the distal forelimb representation of area F2, there are neurons that are selective for the type of prehension required for grasping the object. The activity of these grasping neurons was not related to individual finger movements but to the grasping action as a whole. Specifically, Raos and colleagues (2004) proposed that F2 has the role of keeping in memory the motor representation of the object and combining it with visual information as to continuously update the configuration and orientation of the hand as it approaches the object to be grasped.

To sum up the representation of 3D features modulates activity within the premotor areas, which are known to be important for visual guidance of the hand (Rizzolatti et al., 1988; Raos et al., 2004). The PMv plays a primary role in selecting the most appropriate type of grip on the basis of the object affordances provided by AIP to which it is reciprocally connected, thus activating a motor representation of the object. This motor representation is then supplied to the PMd, which keeps memory of it and combines it with visual information provided by cortical areas of the superior parietal lobe to continuously update the configuration and orientation of the hand as it approaches the to be grasped object. The final output for action execution most likely involves both PMv and PMd (Castiello & Begliomini, 2008).

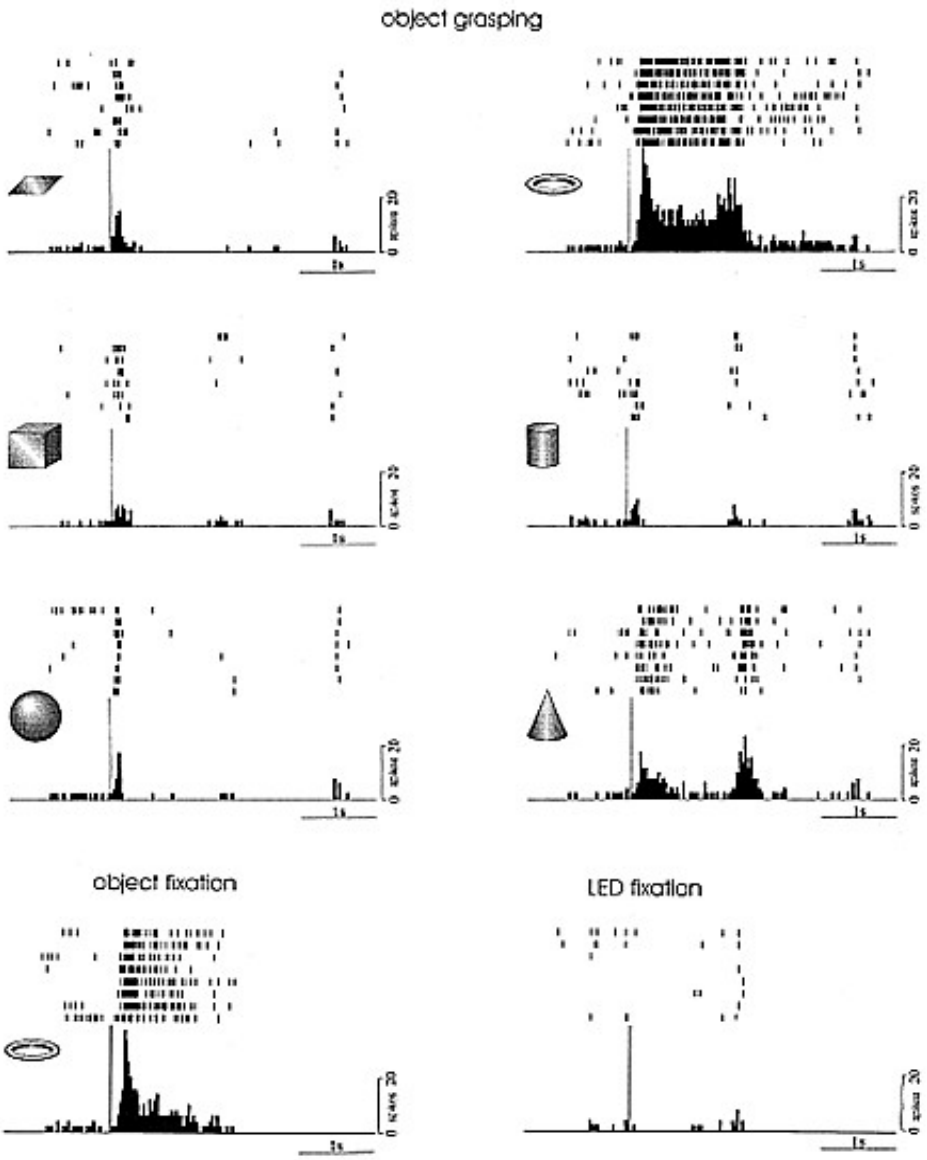

Figure 1.3. The upper part of the figure (object grasping) shows the neuron's activity during observation and grasping of different objects. The monkey was seated in front of a box, which housed six different objects. Objects were presented one at a time in a central position in random order. A red spot of light from a red/green LED was projected onto the object and the monkey was required to fixate it and press a key. Key pressing turned on the light inside the box and made the object visible. After the monkey held the key pressed for 1–1.2 s, the LED changed color (green, go signal) and the monkey was allowed to release the lever and grasp the object. Rasters and histograms are aligned with the key press (the moment when the object became visible). In the ring grasping panel, the second peak of discharge corresponds to the activity related to the grasping movement. The lower part of the figure (left) shows the activity of the same neuron during object fixation (only the responses to the ring are shown in the figure). In this condition, when the LED was turned on (green light), the monkey, as in the previous condition, was trained to fixate the spot of light and press the key. The object then became visible. However, when the LED changed color, the monkey had only to release the key. Rasters and histograms are aligned with the key press. The lower part of the figure (right) shows the activity of the same neuron during fixation of a spot of light. In this condition, the task was the same as in the object fixation condition, but carried out in the dark. No object was visible and the monkey simply was required to fixate the spot of light (Source: Rizzolatti et al., 2001).

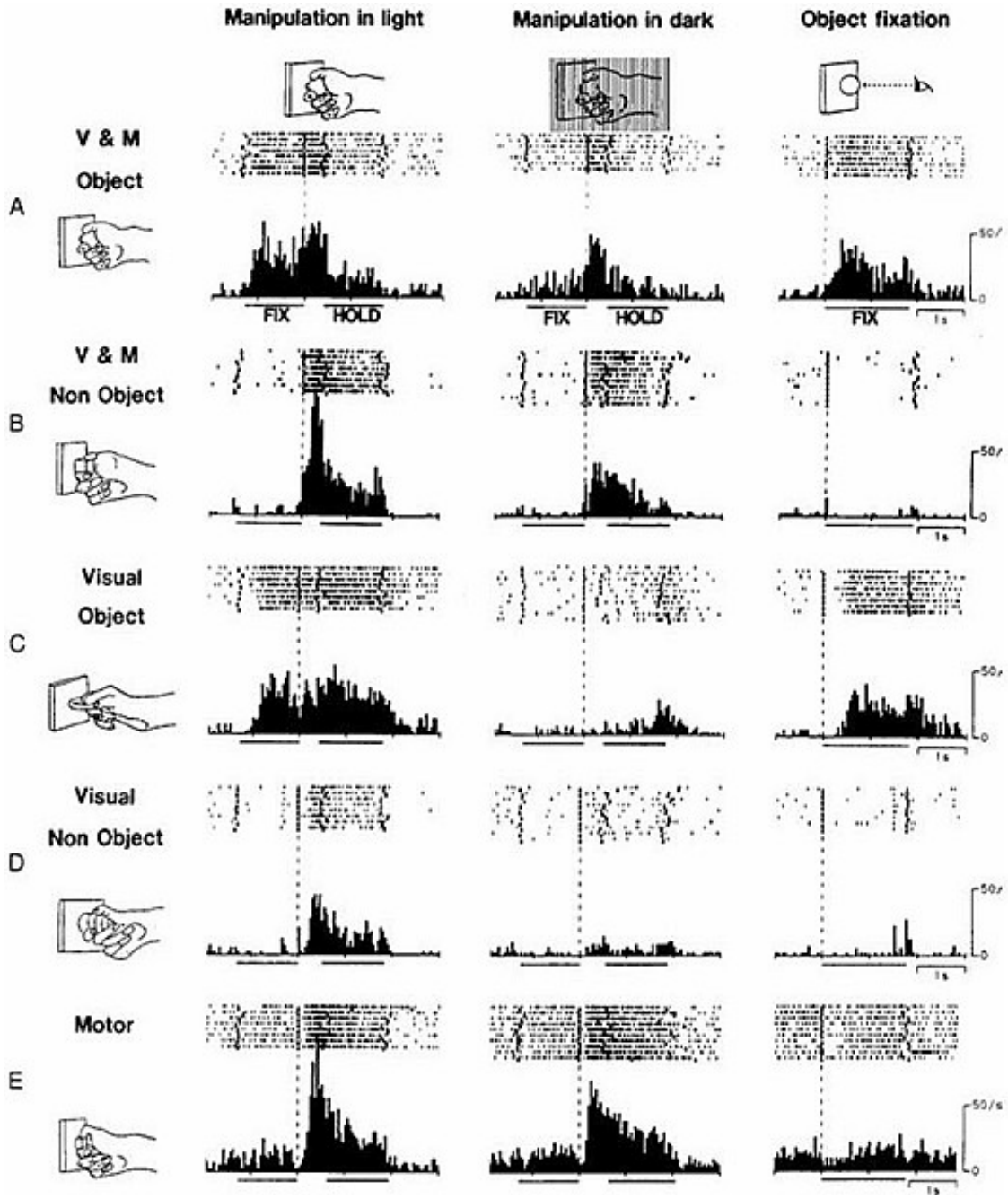

Figure 1.4. Five types of hand-manipulation-related neurons under the 3 different conditions.

1) Manipulation in light: object manipulation task in the light. 2) Manipulation in dark: object-manipulation task in the dark. 3) Object fixation: object-fixation task in the light. Raster and histograms were aligned with the moment at which the monkey released the key in the manipulation task and when the monkey pressed the key in the object-fixation task. In the manipulation task, beneath each raster indicate the onset of pressing down the key, release of the key, switching on of the microswitch of the object, and release of the object, respectively, and the line below the histogram shows the mean duration of the "fixation" period (FIX) and "hold" period (HOLD). In the fixation task, in the raster indicate key down and key release, respectively, and the line below the histogram shows the mean duration of the "fixation" period (FIX). Example of object-type visual-motor neuron (*A*), nonobject-type visual-motor neuron (*B*), object-typevisual-dominant neuron (*C*), nonobject-type visual-dominant neuron (*D*), and motor-dominant neuron (*E*) (Source: Murata et al., 2000).

Like vision, somesthesis is a crucial source of information for the motor system. Somatic receptors in muscles, joints and skin provide information regarding the current posture of the hand and its location and orientation with respect to potential targets for grasping. This information is necessary to compute a trajectory to bring the hand to the object and grasp it properly. To investigate the conjunction of visual and somatic processing, a series of studies compared the timing of spike trains recorded by single-unit recording in the somatosensory cortex (SI) and the AIP cortex of the same animals during a reach to grasp task (Gardner et al., 2002; Gardner et al., 2007a, b, c). Kinematics was also recorded during the task, with the goal to define the stages of the reach to grasp movement. Altogether these findings support hypotheses that predictive and planning components of prehension are represented in PPC and premotor cortex, concluding that neurons in parietal area 5, like those in area AIP, integrate object features, hand actions, and grasp postures during reach to grasp.

The results showed that the response of cells in AIP was influenced by the shape of the target object. Neurons in SI typically responded later than those in AIP, showing a significant increase in firing rates only after the hand touched the object, and firing when grasping was secure. However, SI neurons rarely differentiated the shape of the grasped object in the manner that occurred in AIP neurons.

Recent evidence indicates that action goal has the ability to affect reach to grasp neural activity (Bonini et al., 2010, 2011, 2012). Particularly, these experimental findings showed that grasping neurons in the inferior parietal area and in area F5 of the monkey can be differentially activated depending on the action (grasp-to-eat or grasp-to-place) in which the coded act is embedded (Bonini et al., 2010). A more recent study by the same group showed that both grasp-to-eat and grasp-to-place neurons did not change their selectivity in relation to the rewarding value of the

food obtained by the monkey for correct task accomplishment (Bonini et al., 2011). Finally, the same study also demonstrated that the neuronal selectivity of PFG and F5 grasping neurons is similar during the execution of both simple and complex action sequences and crucially depends on the availability of contextual information about the final action goal (Bonini et al., 2011).

The temporal dynamics of grip and goal selectivity showed that grasping neurons reflect first "how" the object has to be grasped (grip), to guide and monitor the hand shaping phase, and then "why" the action is performed (goal), very likely to facilitate subsequent motor acts following grasping. These findings suggest that, in the parieto-frontal system, grip types and action goals are processed by both parallel and converging pathways, and inferior parietal area (PFG) appears to be particularly relevant for integrating this information for action organization (Bonini et al., 2012).

Given the wealth of evidence for a grasping circuit involving several areas in the monkey brain, the natural question is whether a similar circuit exists in humans. For ethical reasons, invasive physiological recording of brain activity is rarely possible in humans. Nonetheless, considerable progress has been made towards understanding the neural substrates of grasping in humans, mainly from studies of patients with brain damage and neuroimaging experiments.

1.6. Neuroanatomical Mechanisms underlying reach to grasp movement in humans

1.6.1. Motor cortices and pathways

The ability to control movement is something that we usually take for granted. But even the most simple act, is controlled by our brain. Brain controls motor acts through three major regions in the frontal lobes, located in its caudal portion. This region of the frontal lobes is also known as agranular frontal cortex, because of the lack of granular cells (Rizzolatti & Luppino, 2001).

The agranular frontal cortex is constituted of several distinct motor areas: the supplementary motor cortex (SMA), and the PMC (Figure 1.5.). These areas have topographical representation of all the muscle groups of the body. Moreover other structures like basal ganglia, brain stem and cerebellum are involved.

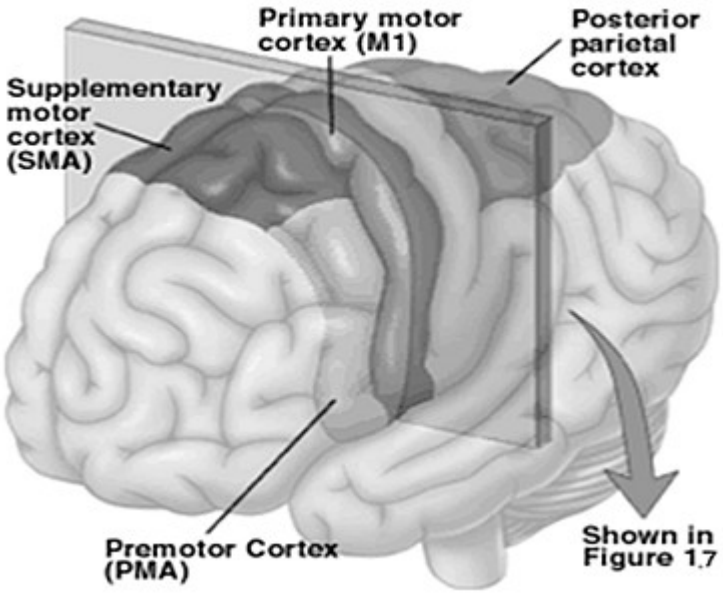

Figure 1.5. Main brain regions involved in motor control in humans.
(Source:http://brainconnection.positscience.com/the-anatomy-of-movement)

M1 is a subdivision of the agranular frontal cortex described by Brodmann (Brodmann, 1903) as areas 4 (Figure 1.6.). It is located anteriorly to the central sulcus, beginning laterally in the sylvian fissure and contains a somatotopical representation of the contrlateral part of the human body. In humans, Area 4 can be subdivided into area 4a (anterior) and 4p (posterior) on the basis of neurotransmitter binding patterns (Geyer et al., 1996).

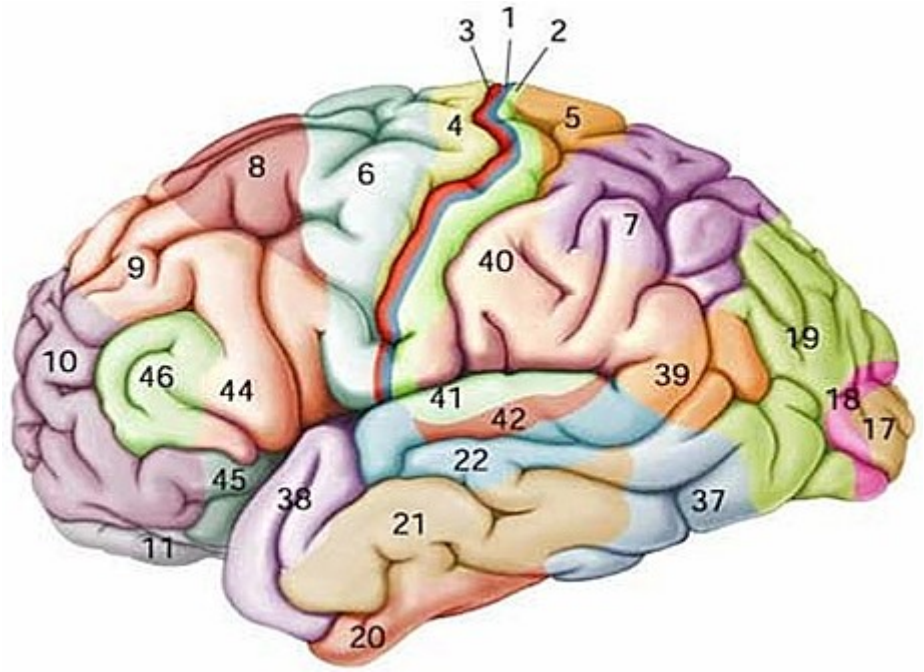

Figure 1.6. Brodmann map showing subdivision of the brain cortex on the basis of the cytoarchitectonis structure. (Source: http://mybrainnotes.com/memory-language-brain.html)

The representation of the hand is located dorsolaterally, between head and arm representations (Figure 1.7.). Areas of the body usually requiring greater precision of movement, such as face, thumb, fingers and hands have larger representations than other body areas like trunk or limbs for example. Stimulation of the primary motor cortex elicits relatively precise and simple muscles twitches in the contralateral part of the body.

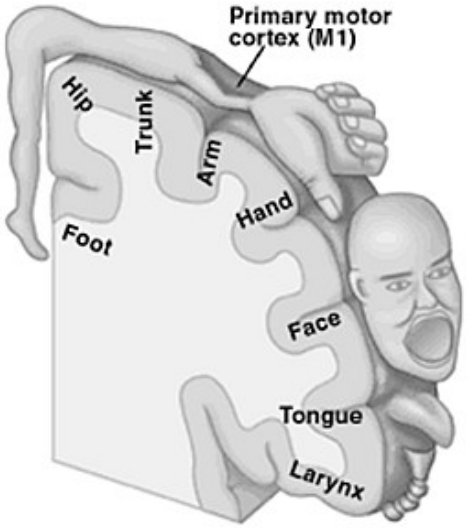

Figure 1.7. The motor homunculus in primary motor cortex. (Source: http://brainconnection.positscience.com)

PMC's, encompass Brodmann area 6, 44 and 45 and lie anterior to M1, extending inferiorly to the sylvian fissure and superiorly into the longitudinal fissure. Their neurons project directly to M1, the red nucleus, the reticular formation, the basal ganglia and, indirectly, to the cerebellum (Dum et al., 1991). The direct monosynaptic connections of PMC to lower areas suggest that this area can control movements independently of the M1. PMC stimulation results in patterns of movement involving muscle groups that are used to perform specific tasks.

Premotor cortices can be distinguished into two subregions, dorsolateral and ventrolateral, even if recent imaging studies suggest that the distinction may be even more detailed (Picard et al., 2001). The dorsolateral premotor cortex (dPMC) is located within the rostral precentral gyrus and caudal superior frontal gyrus (Rizzolatti et al., 1998). This area appears to be involved in action planning, response selection, movement preparation and visual guidance of motor responses, especially when the actions are cued by arbitrary associations (Wise et al., 2001).

The ventrolateral premotor cortex (vPMC) is located ventrally to the frontal eye fields (FEF) and caudally to Brodmann areas 44 and 45, even if the extent of this area is not well established (Grèzes et al., 2001). This area seems to be involved in action observation and object manipulation tasks (Grèzes et al., 2001).

The SMA is located anteriorly and superiorly to PMC. and roughly corresponds to Brodmann area 6. This area can be further divided into two further subregions, the *proper SMA* and the *pre-SMA* (Zilles et al., 1995). The proper SMA, appears to be involved in simple, externally triggered and well practiced motor tasks (Passingham,1996). Differently, the pre-SMA seems to be involved in more cognitive tasks, such as processing of cues rather than response selection (Picard et al., 2001). Its stimulation results in complex

bilateral movements (Rizzolatti & Luppino, 2001).

1.6.2. Somatosensory pathways

Somatosensation consists of touch proprioception, thermal sensation and pain. The inputs forming the basis for these sensations are collected from skin, joints, muscles and subcutaneous tissue. Like motor areas, also somatosensory areas have somatotopical organization, showing larger representations for areas densely innerved, like lips and fingertips (Hari et al., 1993).

The primary SI is located in the posterior bank of the central sulcus in the post-central gyrus. SI consists of four different areas (3a, 3b, 1 and 2), whose distinction is based on cytoarchitectonic differences. Areas 3b and 1 are specialized for processing of informations coming from mechanoreceptors of the skin; area 3a and 2 for proprioception. Like motor areas, also these areas are somatotopically organized,

The secondary somatosensory (SII) cortex lies in the upper bank of the sylvian fissure . Informations arrive to SII from both sides of the body, via thalamus, SI and also through other sensory areas, like visual and auditory cortices. Neurons of SII have ipsilateral projections to M1, SMA and PPC, and contralateral projections to SII (Burton et al., 1986). Direct simulation of SII produces in humans tingling sensations and desire to move both sides of the body (Blume et al., 1992).

The posterior parietal cortex (PPC) is located in the parietal lobe and compasses Brodmann areas 5, 7 and 40. It is implicated in integration of informations coming from different sensory modalities, and lesions to this area (especially on the right side) result in a neglect syndrome, where the patient ignores contralateral visual, auditory and tactile information.

It has been demonstrated that a particular region of the PPC, the AIP plays a key role in the context of grasping movements. Its contribution seems to be fundamental for the hand

shaping stage.

1.6.3. Subcortical pathways

The most important pathway from M1 to periphery is the **corticospinal tract**, also known as pyramidal tract. Its neurons originate mostly from M1, PMC and SMA: the axons from cortex pass through the internal capsule and then downward through the brain stem and the medulla, where most of the fibers decussate to the opposite side. The fibers then descend in the lateral tract and project to interneurons of the intermediate region of the cord gray matter and form the lateral tract. Some of the fibers do not cross in the medulla and form the ventral tract. The corticopsinal tract is crucial for discrete and fine tuned movements, especially those including hands and fingers (Rizzolatti et al., 2001).

Also basal ganglia are involved in motor control. They consist of interconnected subcortical structures (stratum, subthalamic nucleus, globus pallidus and substantia nigra). They receive inputs from somatosensory and motor cortices and are involved in the maintenance of muscle tone (Crossman, 2000).

The thalamus, acting as relay, transmitting information from basal ganglia, cerebellum to the cortex (Holsapple et al., 1991).

The cerebellum seems to be significantly implicated in motor learning (Doyon et al, 2003). It has a three-layered cortex, surrounding the cerebellar nuclei. It receives input from the spinocerebellar tract, conveying informations from muscle, joints, cutaneous receptors and spinal interneurons.The cerebellum als receives topographically organized inputs from the contralateral cerebellar cortex via the pontine nuclei. The majority of the fibers forming the cortico-pontine tract originate from sensorimotor and motor areas. Purkinije cells from the cerebellar cortex project to cerebellar nuclei (Allen & Tsukahara, 1974), which influence

movement via excitatory projections to the spinal cord and via the ventrolateral thalamus to motor cortices (Matelli et al., 1996). Cerebellar damage results in coordination deficits, such as ataxia and tremor, underlying the role of the cerebellum in fine-tuning motor behaviour.

1.7. Neuroimaging studies

1.7.1. Functional Magnetic Resonance Imaging

Brain imaging experiments investigating neural substrates of grasping in humans usually take results obtained from neurophysiology as a reference point. In these experiments, subjects are scanned during either reach to grasp actions, or only grasping actions using in general the (dominant) right hand (Castiello, 2005). Some studies using functional MRI (fMRI; see Appendix II) have focused on selected neuroanatomical regions, presumably the hypothetical human homologue of monkey AIP.

In one study Binkofski et al. (1998) compared a grasping movement towards a rectangular object (varying in orientation) to a pointing movement towards the same object. The results showed a specific activation of AIP for the grasping task; moreover also activations in the contralateral sensorimotor cortex, bilateral PMC and the PPC were detected. The portion of AIP activated by the grasping task appear to be the homologue of AIP area in the monkey. Lesions to this area lead to grasping deficits (Binkofski et al., 1998; Frey et al., 2005). This result was further confirmed by studies that used a ROI approach and an event-related design (Culham et al., 2003; James et al., 2003; Culham, 2004). In these experiments, a diverse and unpredictable sequence of objects (rectangular shapes of varied length and orientation) was presented to participants while lying in the MR scanner, using a custom equipment (see Figure 1.8.), and had to reach towards the long axis of the objects and grasp

them using a precision grip. The results provided clear evidence that AIP contributes to the ability to perform grasping actions towards objects.

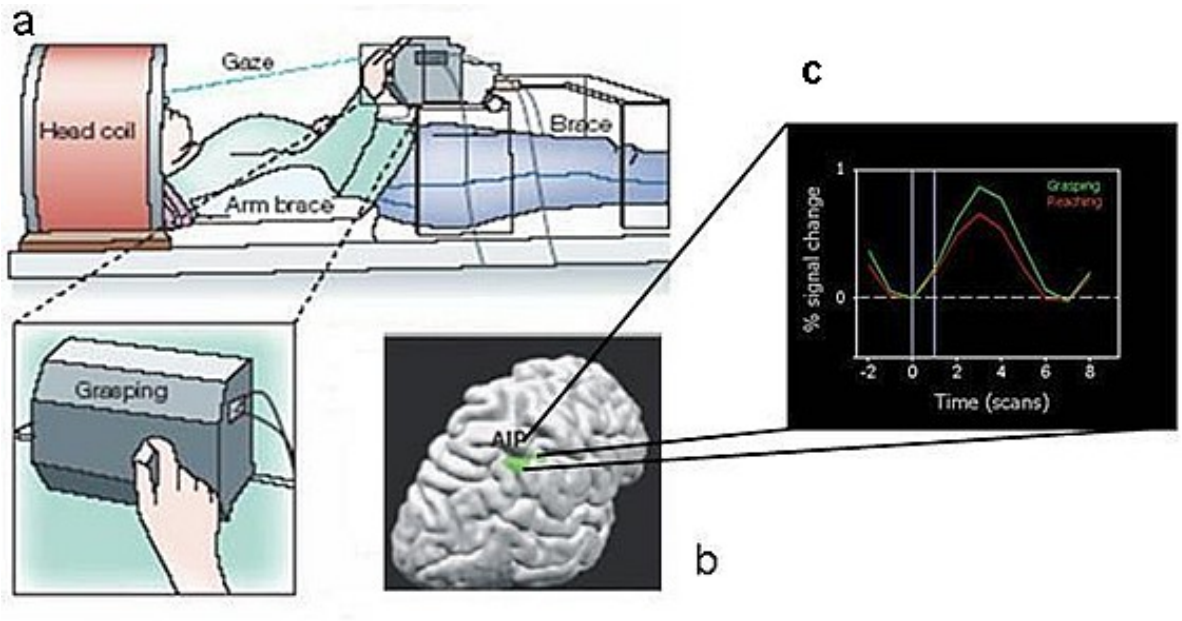

Figure 1.8. (Panel a) the pneumatic rotating drum was used to present objects that could be grasped with the right hand. (Panels b and c) The experiment showed the expected pattern of greater activation for grasping compared with reaching in the anterior intraparietal area. (Source: Panel a: Castiello, 2005; modified with permission from Culham, 2004; Panels b and c: Culham, 2004).

Unfortunately, the fact that subjects were constrained to a single type of grasp prevented a more complete comparison with the monkey AIP, which contains selective motor-dominant neurons that represent various patterns of hand movements appropriate to grasping particular objects. Grèzes and colleagues (2003) looked in humans for a neural network underlying grasping similar to those detected in area F5 of macaques. In three execution conditions, subjects performed a type of grasp a) appropriate for the viewed object; b) imitated a visually presented pantomime action; c) imitated a viewed hand grasping an object. A power grip on all trials while viewing a static background was adopted as a baseline condition. One of the objects used was a large object that would normally be grasped with a power grip; the other was small and would normally be grasped by a PG. The activated areas were

consistent with the monkey AIP–F5 visuomotor circuit. Unfortunately, the data were not analysed separately for the two types of grasp and the action was confined to the grasping component, as participants did not perform overt arm movements.

A more recent study considered different type of prehension movement (i.e., reaching, reach to grasp with precision grip and reach to grasp with whole hand grip) and different type of stimuli (i.e. small object and large object), results indicated that the left aIPS was active when the subjects naturally adopted a PG to grasp the small object but showed a much weaker response when subjects naturally adopted a WHG to grasp the large object (Begliomini et al., 2007a). Moreover in another related study, Begliomini and colleagues (2007b) paid particular attention to the dorsolateral and dorsomedial network; functional magnetic resonance imaging was used to explicitly test whether activity within this network varies depending on the congruency between the adopted grasp and the grasp called by the stimulus. Results show that the aIPS was more active for PG than for WHG independently of stimulus size. Conversely, both the dorsal premotor cortex and the primary motor cortex were modulated by the relationship between the type of grasp that was adopted and the size of the stimulus (Begliomini et al., 2007b). An additional experimental finding tested how handedness modulates activity within human grasping-related brain areas. Right- and left-handers subjects were requested to reach towards and grasp an object with either the right or the left hand using a PG while scanned. In this study the fMRI was accompanied by kinematic recordings as a behavioral counterpart. Significant activity within the right PMd, the right cerebellum and AIP bilaterally was found. This study emphasized the need of bilateral AIP activity for the performance of PG movements which varied depending on handedness (Begliomini et al., 2008).

Other issues involved in grasping relate to force production for specific grasping patterns. Ehrsson and colleagues (2000, 2001) compared human brain activity during a PG and a

power grip. The activity recorded in the contralateral primary sensorimotor cortex was higher during a power grip than a precision grip. By contrast, the activity in the PMv, the rostral cingulate motor area and at several locations in the PPC and the PFC was stronger during the PG than the power grip. Furthermore, the power grip was associated predominantly with contralateral activity, whereas the precision grip task involved extensive activation in both hemispheres. These findings indicate that, in addition to the primary motor cortex, premotor and parietal areas are important for control of fingertip forces during PG.

Grol and colleagues (2007) used dynamic causal modeling of functional magnetic resonance imaging time series to assess how parieto frontal connectivity is modulated by planning and executing prehension movements toward objects of different size and width. This experimental manipulation evoked different movements, with different planning and execution phases for different objects. Crucially, grasping large objects increased inter-regional couplings within the dorsomedial circuit, whereas grasping small objects increased the effective connectivity of a mainly dorsolateral circuit, with a degree of overlap between these circuits. These results argue against the presence of dedicated cerebral circuits for reaching and grasping, suggesting that the contributions of the dorsolateral and the dorsomedial circuits are a function of the degree of online control required by the movement (Grol et al., 2007).

In another study fMRI the human neural substrates of the transport component and its relationship with the grip component was examined. For the first time Cavina-Pratesi and colleagues (2010) have identified the neural substrates of the transport component which include the superior parieto-occipital cortex and the rostral superior parietal lobule. Summing up they found specialization for the grip component in bilateral AIP and left PMv, confirming the literature. Moreover they also found activity grasp related even when no transport was involved. They reported an integration of the two components within the PMd

and SMA postulating that these two regions are important in the coordination of the reach to grasp movement (Cavina-Pratesi et al., 2010).

Either species, human and macaques, the AIP is thought to be specialized for hand grip, whereas the superior parieto-occipital cortex and medial intraparietal cortex are specialized for arm transport. These areas then project to the PMv and PMd. Considering these results (Cavina-Pratesi et al., 2010) each substream show preferential connections with other areas, precisely the dorsomedial stream (more involved in peripheral vision and complex motions) appear well suited for processing locations away from fixation arm position and online corrections (Galletti et al., 2003; Grol et al., 2007); instead the dorsolateral stream (more involved in visual and haptic object properties) appear well suited for planning and control of grip (Cavina-Pratesi et al., 2010).

Gallivan and colleagues (2011) demonstrate that we can also decode movement intentions from human brain signals, before their initiation, testing object-directed grasp and reach movements with fMRI. Subjects performed an event-related delayed movement task toward a single centrally located object. For each trial, after visual presentation of the object, one of three hand movements was instructed: grasp the top cube, grasp the bottom cube, or reach to touch the side of the object (without preshaping the hand). They found that, despite an absence of fMRI signal amplitude differences between the planned movements, the spatial activity patterns in multiple parietal and premotor brain areas accurately predicted upcoming grasp and reach movements. Furthermore, the patterns of activity in a subset of these areas additionally predicted which of the two cubes were to be grasped. These findings offer new insights into the detailed movement information contained in human preparatory brain activity and advance our present understanding of sensorimotor planning processes through a unique description of parieto-frontal regions according to the specific types of hand movements they can predict.

Glover and colleagues (2012), focused on planning and execution movement phases. They provide evidence that the planning and control of even simple reaching and reach to grasp actions use different brain regions. They measured neural activity through fMRI during four experimental condition (passively observe a grasp target, plan a grasping movement without executing, plan and then execute a grasp movement, immediately execute a grasp movement). Two large, independent networks of brain activity were identified: a planning network (including the premotor cortex, basal ganglia, anterior cingulate, posterior medial parietal area, superior parietal occipital cortex and middle intraparietal sulcus) and a control network (including sensorimotor cortex, the cerebellum, the supramarginal gyrus and the superior parietal lobule)(Glover et al., 2012).

To better understand neural networks underlying reaching, the relationship between reaching and reach to grasp related responses and topographically organized areas of the human AIP was characterized using functional MRI. Reach to grasp specific activation was localized to the left AIP, partially overlapping with the most anterior topographic regions and extending into the postcentral sulcus. Reaching specific activation was localized to the left precuneus and SPL, partially overlapping with the medial aspects of the more posterior topographic regions. Although the majority of activity within the topographic regions of the IPS was nonspecific with respect to movement type, they found evidence for a functional gradient of specificity for reaching and grasping movements spanning posterior-medial to anterior-lateral PPC. In contrast to the macaque monkey, grasp- and reach-specific activations were largely located outside of the human IPS (Konen et al., 2013).

Lastly some studies also tested the role of subcortical structures involved in reach to grasp movement execution. In this respect, basal ganglia have to be considered as another important system that could possibly play a role in grasp selection or movement execution planning, or even related to the on line control of force or force pulses during movement

(Grafton, 2012). Related experimental findings have identified the basal ganglia and also the cerebellum as complementary actors in regulation of ongoing actions when precise updating is required (Tunik et al., 2009).

1.7.2. Electroencephalography

Evoked-Related Potentials (ERPs) measured by electroencephalography (EEG) provide a quantitative measure of the whole brain's electrical activity, revealing the time course of brain activity modulations throughout reach to grasp movement from planning to execution. Wheaton and colleagues (Wheaton et al., 2005a, b) reported the involvement of parietal activity preceding that of the frontal areas in praxis hand movements. In this study, the authors compared motor potentials related to the generation of self-paced simple movements (i.e., thumb adduction) with motor potentials related to self-paced tool-use movements (e.g., hammer pantomime). Motor-related potential showed significant greater amplitude and earlier onset for more complex movements. Specifically, they observed that the motor-related potential in the posterior parietal cortex anticipated that in the frontal areas, and continued as the movement onset approached. They postulated that the complexity of the movement per se (e.g., multiple joint coordination) requires higher neural computation demand, which took place in the parietal lobe.

More recently, Bozzacchi and colleagues (2012) defined the spatiotemporal activity of parietal and frontal areas in self-paced object-oriented actions. By examining motor-related potentials in planning reach to grasp movement, they clearly showed that parietal areas were involved in the early phase of planning. Such parietal activity started long before movement onset and was followed by a classical fronto-central component. The observed timing of parieto-frontal interaction in reach to grasp movements further confirmed previous evidence showing that parietal areas provide premotor areas with grasp-related information (Grol et

al., 2007).

Another study (Zaepffel & Brochier, 2012) recorded EEG in a precuing task to investigate the planning process underlying of reach to grasp movements in humans. Participants were requested to reach, grasp, and pull an object as fast as possible after a visual go signal. Only two parameters where manipulated : the hand shape for grasping (precision grip or side grip) and the force required to pull the object (high or low). Three seconds before the go signal considered as onset, a cue provided participants task instructions regarding force, grip, both of them or neither. Zaepffel and Brochier found higher late Contingent Negative Variation (lCNV; Gaillard, 1977; Rohrbaugh, and Gaillard, 1983; Leuthold, et al., 2004) amplitude over Cz and FC electrodes when the cue provided information regarding the type of grip to use and the level of force required to pull an object. Furthermore, whereas the force-related lCNV was more distributed over fronto-central electrodes, the grip-related lCNV was chiefly restricted to parietal and premotor areas. Aside from outlining the composite nature of the such ERP component in terms of high- and low-level planning processes, these findings confirmed that a functional parietal-premotor network is involved in the planning of grip. Moreover they recorded also reaction time to confirm that two distinct functional networks are involved with different time courses in the planning of grip and force (Zaepffel & Brochier, 2012).

To sum up, these studies suggest that in humans, like in monkeys, reach to grasp movements involve a large network of interconnected structures in the parietal and frontal lobes (Brochier & Umiltà, 2007; Castiello & Begliomini, 2008; Rizzolatti & Luppino, 2001). And, that this cortical network is differentially involved for the control of distinct aspects characterizing the planning and the control of reach to grasp movement. Nevertheless, how the neural control systems

interact with the complex biomechanics of moving limbs (as to help us to identify the operational principles to look for in reach to grasp studies and, more in general, in motor control) remains an open question. In this respect, it is only through the use of converging techniques with different characteristics that we might fully understand how the human brain controls the grasping function (Castiello & Begliomini, 2008). What is so far lacking in the literature on cortical control of grasp in humans is a systematic documentation of the time course of neural activity and kinematical signals during performance of grasp. To fill this gap the studies included within the present thesis investigated fMRI with ERPs and ERPs with kinematical signals in order to provide deeper insights into the neuro-functional basis of grasping in humans.

2. SOME CONSIDERATION ON EEG-fMRI INTEGRATION

2.1. Introduction to integration

Nowadays the integration between different investigation techniques represents a powerful research approach that provides a unique opportunity of maximizing the technical advantage of investigation techniques and at the same time minimizing the disadvantages of them.

Considering the increasing availability of functional neuroimaging technique and the main research goals to capture the complex nature of cerebral activity a multimodal approach became needful in order to better understand the mechanisms underlying this activity. In this respect integration of information from different domains become a powerful solution of experimental investigation as well an important methodological challenge (Rosa et al., 2010).

Particularly the combination of EEG with fMRI has been shown to be a valuable method since these two techniques are highly complementary (Rosenkranz & Lemieux, 2010). The poor spatial resolution but good temporal resolution of the EEG signal integrates the poor temporal resolution but the good spatial resolution of fMRI (see Appendices III and IV). Figure 2.1. illustrates the powerful integration of these investigation techniques, the dotted outline represents the sampling characteristics of the combination between the temporal resolution of EEG recording with the spatial resolution of fMRI (Ullsperger & Debener, 2010). Moreover the combination of these techniques appear one of the best choice as to study the systematic interactions in brain networks in vivo, considering their non-invasive nature (Mullinger & Bowtell, 2011).

To sum up, the integration of different techniques is promising to fill four main goals: first of all

to overcome the shortcomings of single methods and at the same time to make optimal use of their advantages and also obviously to compensate their disadvantages last but not least it provides a complete tool to the identification of common neuronal generators.

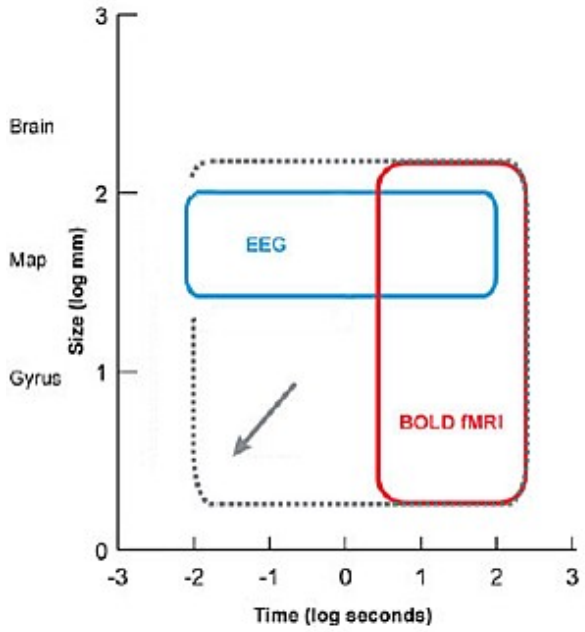

Figure 2.1. Resulted characteristic by integration between EEG-fMRI (modified from Ullsperger & Debener, 2010).

2.2. "EEG–fMRI", or EEG correlated fMRI:

The fundamental assumption behind any integration approach is that the signals recorded in both modalities are at least partly produced by the same neural generators (Debener et al., 2006).

Nunez and Silberstein (2000) more than ten years ago, when shift from theorization to implementation began, used to refer as co-registration as an apparently plausible approach for achieving both high spatial and high temporal resolution since both EEG and fMRI detect the same equivalent neural dipoles. Nowadays is preferable refer to EEG-fMRI as correlated, integrated or simultaneous in order to avoid applicable misunderstanding during the MRI data analysis process. (Mulert & Lemieux, 2010; Ullsperger & Debener, 2010).

The recent advent of safe and high quality EEG recording inside the MR scanner has given the

tools necessary to compare blood oxygenation level dependent (BOLD) image contrast and EEG derived localization information (Lenieux et al., 2001). fMRI enables brain regions engaged during cognitive processes to be localized with high spatial precision; EEG signal is directly coupled to neuronal electrical activity and has millisecond precision (Debener et al., 2006). Accordingly, great hope lies in the integration of EEG and fMRI to achieve both high temporal and high spatial resolution of human brain function (Babiloni et al., 2004).

Experimental findings propose that simultaneous EEG and fMRI recordings provide a major improvement that will advance considerably our understanding of how cognitive functions are implemented by the brain. Importantly, simultaneous EEG–fMRI recordings enable the investigation of trial-by-trial fluctuations of brain activity, which reveals important insights into the dynamics of cognitive functions (Debener et al., 2006).

2.3. Different levels of combination

EEG and fMRI recordings can be combined at three different levels separately, in an interleaved fashion, or in a simultaneously manner (Mullinger & Bowtell, 2011).

2.3.1. Separate (Off Line) - combination

The easiest, but less powerful manner of combination consists in a simple data combination after a separate data acquisition and preprocessing of the used investigation methodologies during the designed experimental task. This method of combination between EEG and fMRI data is usually termed ‘off line’ or ‘separate’ data integration (Mulert & Lemieux, 2010; Mullinger & Bowtell, 2011).

2.3.2. Interleaved - Combination

Like others combination techniques 'interleaved' recording offers a halfway between separate and simultaneous recordings. EEG recording periods are planned only during quite period of scanner, in order to avoid magnetic fields gradients effects. Interleaved recording enforcement may also extend during the acquisition time, but this increases the discomfort experienced by the subjects. Interleaved recording produces three main advantages: (i) it relies upon the fact that the BOLD response is delayed in comparison to the neuronal activity, (ii) it allows EEG data collection without contamination from gradient artefacts and (iii) it gives an easy and real time monitoring of the EEG response. Interleaved recording disadvantages emphasize that neither modality is continually monitoring brain activity and involves a longer experimental time (Mulert & Lemieux, 2010; Mullinger & Bowtell, 2011).

2.3.3. Simultaneous Combination

Simultaneous acquisition of EEG and fMRI represents the best way to ensure the perfect correspondence between electrical and hemodynamic responses, especially when the focus of the study is on unpredictable neuronal activity (Rosenkranz & Lemieux, 2010).

Unfortunately simultaneously recording also offer a series of disadvantages such as a quality of the data which can be worse than that obtained in separate recording sessions. Furthermore MRI data can be degraded by the presence of the EEG recording equipment and EEG are also superimposed to magnetic field effects (Mullinger & Bowtell, 2011). Therefore special measure must be taken to ensure that the interaction between the recording setting and the magnetic environment are minimized as to preserve image quality. Potential artifacts are handled by adopting special conducting materials with suitable magnetic proprieties and also through special data recording strategies and post-processing (Rosenkranz & Lemieux, 2010).

Nevertheless this approach technique is considered the best way of answering at a number of research questions which are usually difficult to address using others techniques. This is why the field of simultaneous EEG-fMRI is rapidly expanding (Mulert & Lemieux, 2010).

Table 2.1. reported below summarizes briefly all the technical challenges of simultaneously EEG-fMRI recording complemented by the proposed solution.

TECHINCAL CHALLENGE OF SIMULTANEOUS EEG FMRI RECORDINGS			SOLUTIONS
1. SOURCE OF ARTIFACTS	EEG DATA	– Gradient artefacts – Pulse artefacts – Head rotation – Static magnetic field became non-uniform	→ Appropriate experimental setup → Artefact correction (stepping stone technique, gradient artefact correction, optimal basis sets, independent component analysis)
	MRI DATA	– Perturbation of static magnetic field (compromise image quality and detection of activation) – Radio frequency field (from introduction of EEG cap and recording apparatus)	→ Correct selection of EEG materials → Data visual inspection
2. SAFETY		– Feromagnetic material – Optic isolation – Heating test	→ MRI compatible apparatus → Temperature recordings →Aavoid looping leads
3. EXPERIMENTAL DESIGN		– Eliminate potential intersession bias – Optimize the recorded effects in both psychophysiological signal relieved	→ Well planned and checked experimental design → Marker use can be helpful
4. DATA INTEGRATION		– Maximize signals (EEG, fMRI) – Maximize signal from artifact – Maximize the advantage of both methods	→ Independent Component Analysis (ICA) is a linear decomposition technique that aims to reveal the underlying statistical sources of mixed signals

2.3.4. Separate vs Simultaneous combination

On the basis of what stated above it is important to determine which approach is best suited to address specific experimental hypothesis.

For instance, it might be useful to consider that it might be challenging to provide identical sensory stimulation in two separate recording environments as EEG and fMRI laboratories (i.e. to reproduce scanner noise and so on). Moreover different recording sessions (i.e., EEG, fMRI) require different settings and such differences might induce different levels of

stimulation for the same task (Mulert & Lemieux, 2010). Besides differences in preparation time and task experience the recording environment might affect a participant's mood, vigilance, compliance and behavior, which could be reflected in different patterns of brain activity. In addition many cognitive processes are not well-suited to repeated testing because the same stimuli cannot be used twice (Debener et al., 2006; Ullsperger & Debener, 2010).

Indeed trial-by-trial analysis is only possible using simultaneous recording protocols in order to allow the investigation of the relationship between both signals thus allowing the removal of intersession biases and enable to identify common neural generators (Rosenkranz & Lemieux, 2010).

Simultaneous recording provide a series of advantage over the separate recording. Table 2.2 outlines the main features for both the considered acquisition protocols.

Table 2.2. Comparison of separate and simultaneous EEG–fMRI recording protocols (Debener et al., 2006).

Protocol feature	Separate	Simultaneous
Optimal signal quality	Yes	No
Possibility to optimize design	Yes	No
Avoidance of order effects	No	Yes
Identical sensory stimulation	No	Yes
Identical subjective experience	No	Yes
Identical behavior	No	Yes
Direct temporal correlation of EEG and fMRI signals	No	Yes

Briefly, simultaneous EEG-fMRI protocols guarantee identical sensory stimulation, identical perception and an identical sensory behavior. In other words, a unique way to study how intrinsic brain states interact with extrinsic event related processing.

While data acquired in separate sessions can be appropriate for some research questions,

only simultaneous EEG–fMRI offers the opportunity to relate both modalities to actual brain events, an issue that is relevant not only in the clinical field but also for addressing numerous research questions in basic and cognitive neuroscience (Mulert & Lemieux, 2010).

2.4. Data Quality

Usually the most observed mismatches between EEG and fMRI data can be interpreted as a decoupling of the electrophysiological and the hemodynamic activity or as a signal detection failure (i.e., false positive or false negative from either involved technique). To avoid this, every experimental phase has to be planned in detail and well checked during the experiment (Rosa et al., 2010).

One of the primary problem, in terms of the quality of recorded data, is that EEG data are represented by the gradient artifacts produced by the time varying magnetic field gradient and by the pulse artifacts from cardiac driven motion in the magnetic field. Moreover also the quality of fMRI data is affected during simultaneous recoding (i.e., the presence of EEG recording equipment and the suitability of experimental paradigm sometimes could affect the data collection because they are not suited for that particular situation)(Mullinger & Bowtell, 2011).

Further consideration should be given to other sources of artifacts which applies to both EEG and fMRI recording like head movements. The fact is that the artifacts of which each technique already suffers is carried over in simultaneous setting, but these artifacts can usually be minimized by the use of appropriate experimental design and setup (Mulert & Lemieux, 2010).

2.4.1. EEG data

The main responsible for the degradation of EEG signals in simultaneous recording setting, are the gradient and the pulse artifacts. Gradient artifacts are an electromotive force inducted by Faraday's cage that produces voltages at the level of the amplifier inputs which affects EEG signal. Side pulse artifacts is due to ballistocardiogram derived from periodic motion of blood flow linked to the cardiac rhythms in the magnetic field (Mulert & Lemieux, 2010; Mullinger & Bowtell, 2011).

2.4.2. fMRI data

The principal sources of data degradation during simultaneous EEG-fMRI data collecting are the perturbations stemming from the introduction of the EEG recording apparatus within the scanner room. In particular, the perturbation of the radio frequency field is caused by an interaction of the conducting elements of the EEG apparatus with the radio frequency magnetic field that is used to excite and detect the MR signal. Usually these effects increase with the strength of the magnetic field (Mulert & Lemieux, 2010; Mullinger & Bowtell, 2011).

2.5. Data Integration

Solved the data quality problem, the following step is related to data integration. Data integration modelling is still under debate, below various types of data integration models are summnarized. Figure 2.2. shows some of the the approaches to used for EEG-fMRI integration: (i) integration through prediction, (ii) integration through constrain, and (iii) integration through fusion with forward models.

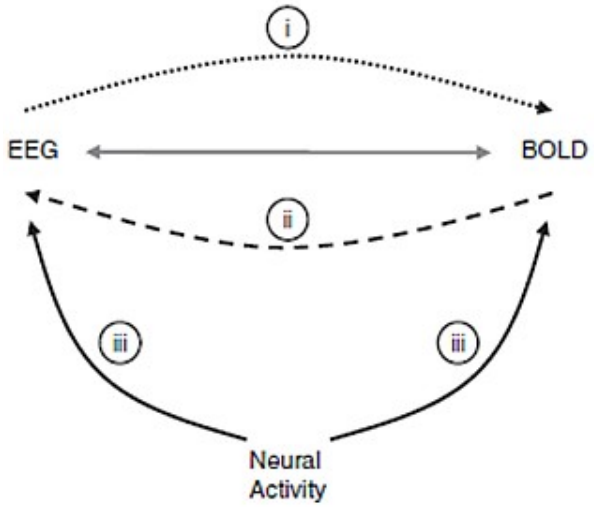

Figure 2.2. Approaches to EEG-fMRI integration. (Adapted from Rosa et al, 2010).

2.5.1 Integration through prediction

Integration through prediction involves using the EEG data to form a model of the expected BOLD signal changes. This means convolving the time-course of a particular component of the EEG signal with the haemodynamic response function, so as a regressor. Statistical analysis can then be used to identify voxels in the image whose signal variation is significantly correlated with the regressor, yielding a map depicting areas where the BOLD signals are consistent with the variation of the chosen EEG component (Mulert & Lemieux, 2010; Mullinger & Bowtell, 2011).

2.5.2 Integration through constraints

fMRI data are used to provide spatial constraints when localizing the sources of EEG signals. The premise for this approach is that combining EEG and fMRI allow an improvement in EEG source localization that may be achieved by using the spatial information from the BOLD data (Mulert & Lemieux, 2010; Mullinger & Bowtell, 2011).

Furthermore it should be noted that neither of the two approaches described above forms a

true integration, since in each case a separate analysis of the EEG or fMRI data is required as a first step (Mullinger & Bowtell, 2011).

2.5.3. Integration through fusion with forward models

A proper fusion of the data analysis, which would draw maximum benefit from simultaneous EEG/fMRI recording, requires a common temporal forward model that links the underlying neuronal dynamics of interest to the measured hemodynamic and electrical responses. Unfortunately experimental findings suggest that further work is needed before this approach can be fully exploited (Mulert & Lemieux, 2010; Mullinger & Bowtell, 2011).

Other modes of integration consider the level of synchrony between the data acquired for each modality and the ways in which the data from each modality are analyzed. These series of data can be brought together in various manners. For instance, some authors considered three different strategies of multimodal data integration (i.e., spatial co-registration, asymmetric data integration and symmetrical data fusion).

2.6. Example of data integration

Blind source separation algorithms such as independent component analysis (ICA, see Appendix V for more details) can deal effectively with EEG artifacts and help to unravel spatiotemporally overlapping brain activities (Ullsperger & Debener, 2010).

Although different analysis strategies have been applied to enhance the validity of the acquired data (i.e. electrical source imaging (ESI) or dynamic causal modeling (DCM); Rosenkranz & Lemieux, 2010) ICA seems one of the best solution to optimize the signal-to-noise ratio of

single-trial EEG estimates used to predict the BOLD response. In addition it offers different successful alternative to decompose and estimate components of interest. In addition it allows to identify, discard or correct artifacts (Debener et al., 2006). Figure 2.3. represents schematically a classical example of trial by trial EEG-fMRI analysis subsequent to EEG-fMRI simultaneous recording.

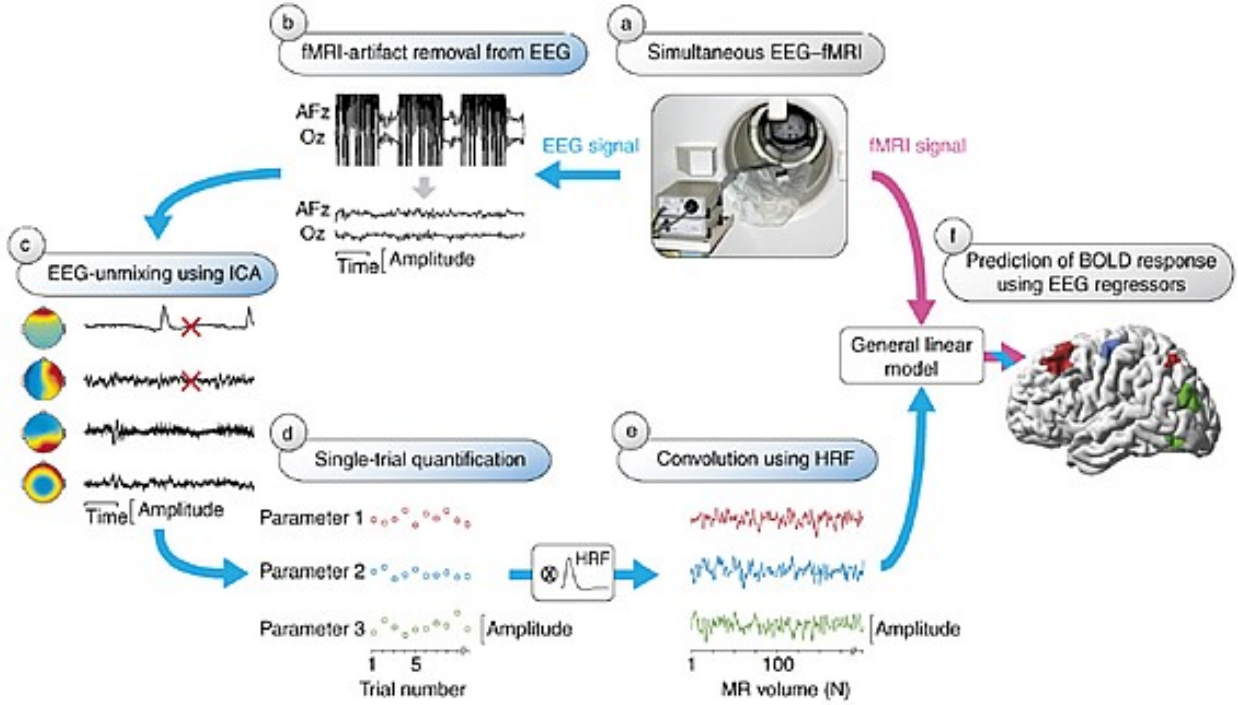

Figure 2.3. EEG-informed fMRI analysis. EEG (blue arrows) and fMRI (pink arrow) can be recorded simultaneously (a) and, subsequently, EEG signals are corrected for fMRI artifacts. This is illustrated for two (AFz and Oz) out of a larger number of EEG channels (b). ICA applied to the continuous EEG signal returns artifact-related and brain-related component activations and maps; typical artifact-related components are marked with red crosses (c). Selected components reflecting brain activity of interest can be used to obtain a measure for each recorded trial (d). After convolution with the hemodynamic response function (HRF), the single-trial amplitudes yield EEG regressors (e) that parametrically predict the BOLD response (f) (Debener et al., 2006).

3. CO-REGISTERING KINEMATICS AND EVOKED RELATED POTENTIALS DURING VISUALLY GUIDED REACH TO GRASP [1]

3.1. Introduction

In our everyday life, we interact continually with objects. We reach for them, we grasp them, we manipulate them. All these actions are apparently very simple. Yet, this is not so. The mechanisms that underlie them are complex, and require multiple visuomotor transformations entailing the capacity to transform the visual features of the object in the appropriate hand configuration, and the capacity to execute and control hand and finger movements.

Motion analysis of grasping shows that the motor configuration that is formed by the hand in contact with the object represents the end result of a motor sequence that begins well ahead of the action of grasping itself (Jeannerod, 1981, 1984; Gentilucci et al., 1991; Jakobson & Goodale, 1991; Chieffi & Gentilucci, 1993). The fingers begin to shape during transport of the hand towards the object. This process of preshaping first involves a progressive opening of the grip with straightening of the fingers, followed by a closure of the grip until it matches object size. The point in time where grip size is the largest (maximum grip size) is a clearly identifiable landmark that occurs well before the fingers come into contact with the object.

In neural terms, grasping behavior can be dissociated into separate reach and grip components (for reviews, see Castiello, 2005; Culham & Valyear, 2006; Brochier & Umiltà, 2007; Castiello & Begliomini, 2008; Filimon, 2010; Grafton, 2010). According to this view, computations regarding the grasp component occurs within a lateral parietofrontal circuit involving the AIP

1 *De Sanctis, T., Tarantino, V., Straulino, E., Begliomini, C. & Castiello, U. (2013). Co-Registering Kinematics and Evoked Related Potentials during Visually Guided reach to grasp Movements. PloS One, 8, e65508.*

and both the PMd and the PMv premotor areas (Moll & Kuypers, 1977; Godschalk et al.,1981; Weinrich & Wise, 1982; Passingham, 1987; Rizzolatti et al., 1988; Raos et al., 2004). The general agreement is that the processes occurring in AIP constitute the initial step of the transformation leading from representation of objects to movement aimed at interacting with such objects (Taira et al., 1990; Fagg & Arbib, 1998). Evidence supporting this view comes from neurophysiological studies showing that the representation of 3D object features influences both the rostral sector of the ventral premotor cortex (area F5) and the ventro-rostral sector of the dorsal premotor area (area F2vr; Raos et al., 2004). According to this model Area F5 plays a primary role in selecting the most appropriate type of grip on the basis of the object affordances provided by AIP to which it is reciprocally connected, thus activating a motor representation of the object. This motor representation is then supplied to area F2vr which keeps memory of it and combines it with visual information provided by cortical areas of the superior parietal lobe to continuously update the configuration and orientation of the hand as it approaches the to-be-grasped object. These properties suggest that F2vr neurons code the continuous activation of the object representation in motor terms, but that they are more dependent than F5 neurons on the visual information during actual grasp. With respect to the reach component, there is agreement that it is subserved by a more medial parieto-frontal circuit including the medial intraparietal area (mIP) termed as the parietal reach region (PRR), area V6A, and the dorsal premotor area F2 (Kalaska et al., 1997; Fattori et al., 2002; Battaglia-Mayer et al., 2003; Gregoriou & Savaki, 2003). Human neuroimaging and transcranial magnetic stimulation (TMS) studies go in the same direction (for reviews see Castiello, 2005; Castiello & Begliomini, 2008; Cavina-Pratesi et al., 2007; Gallivan et al., 2011). They showed the involvement of the anterior portion of the human AIP in grasping behavior (Grafton et al., 1996; Faillenot et al., 1997; Dohle et al., 1998; Ehrsson et al., 2000; Ehrsson et al., 2002; Culham et al., 2003; Frey et al., 2005; Begliomini et al., 2007; Begliomini et al., 2008; Davare et al., 2007) and they proposed human homologues of both the

ventral and dorsal premotor cortices during grasping (Begliomini et al., 2007; Begliomini et al., 2008; Davare et al., 2006). Whereas, reaching activates the medial intraparietal and the superior parieto-occipital cortex (Chapman et al., 2002; Connolly et al., 2003; Prado et al., 2005; Cavina-Pratesi et al., 2010).

A point worth noting is that such dichotomic view has recently been questioned. Evidence from single-cell data (Fattori et al., 2009; Fattori et al., 2010; Raos et al., 2004) and lesion studies (Battaglini et al., 2002)] suggests that areas V6a and F2 are also involved in managing specific aspects of grasping behavior such as grip posture and wrist orientation. Similarly, fMRI investigations reported grasping-related parieto-occipital and dorsal premotor cortex activations (Begliomini et al., 2007; 2008; Chapman et al., 2002) which might be considered the possible human homologue for areas V6A and F2, respectively. Moreover, it is noteworthy that a recent neuroimaging study, based on the quantification of the modulation of the effective parieto-frontal connectivity, argues against the existence of dedicated circuits for reaching and grasping (Grol et al., 2007). Rather, the authors suggest a differential level of effective connectivity in the AIP-PMv circuit depending on the type of grasped objects. Whereas grasping small objects is characterized by a high degree of on-line control requirement, grasping large objects led to an increased coupling in the so-called reaching circuit (V6A-PMd).

Complementary to these approaches, ERPs provide a quantitative measure of the whole brain's electrical activity, revealing the time course of brain activity modulations throughout reach to grasp movement from planning to execution. Wheaton and colleagues (2005 a, b) reported the involvement of parietal activity preceding that of the frontal areas in praxis hand movements. In this study, the authors compared motor potentials related to the generation of self-paced simple movements (i.e., thumb adduction) with motor potentials related to self-paced tool-use movements (e.g., hammer pantomime). Motor-related potential showed significant greater amplitude and earlier onset for more complex movements. Specifically, they observed that the

motor-related potential in the posterior parietal cortex anticipated that in the frontal areas, and continued as the movement onset approached. They postulated that the complexity of the movement per se (e.g., multiple joint coordination) requires higher neural computation demand, which took place in the parietal lobe.

More recently, Bozzacchi and colleagues (2012) defined the spatiotemporal activity of parietal and frontal areas in self-paced object-oriented actions. By examining motor-related potentials in planning reach to grasp movement, they clearly showed that parietal areas were involved in the early phase of planning. Such parietal activity started long before movement onset and was followed by a classical fronto-central component. The observed timing of parieto-frontal interaction in reach to grasp movements further confirmed previous evidence showing that parietal areas provide premotor areas with grasp-related information (Grol et al., 2007).

Another study (Zaepffel & Brochier, 2012) considering a precuing task found higher late Contingent Negative Variation (lCNV; Walter, 1964; Loveless & Sanford, 1974; Gaillard, 1977; Rohrbaugh & Gaillard 1983; Leuthold et al., 2004) amplitude over Cz and FC electrodes when the cue provided information regarding the type of grip to use and/or the level of force required to pull an object. Furthermore, whereas the force-related lCNV was more distributed over fronto-central electrodes, the grip-related lCNV was chiefly restricted to parietal and premotor areas. Aside from outlining the composite nature of the such ERP component in terms of high- and low-level planning processes, these findings confirmed that a functional parietal-premotor network is involved in the planning of grip (Zaepffel & Brochier, 2012).

To sum up, these studies suggest that in humans, like in monkeys, reach to grasp movements involve a large network of interconnected structures in the parietal and frontal lobes (Brochier & Umiltà, 2007; Castiello & Begliomini, 2008; Rizzolatti & Luppino, 2001). And, that this cortical network is differentially involved for the control of distinct aspects characterizing the planning

and the control of reach to grasp movement. Nevertheless, how the neural control systems interact with the complex biomechanics of moving limbs - as to help us to identify the operational principles to look for in reach to grasp studies and, more in general, in motor control - remains an open question. In this respect, it is only through the use of converging techniques with different characteristics that we might fully understand how the human brain controls the grasping function (Castiello & Begliomini, 2008). What is so far lacking in the literature on cortical control of grasp in humans is a systematic documentation of the time course of neural activity and kinematical signals during performance of grasp. To fill this gap our study investigated ERPs with kinematical signals in order to provide deeper insights into the neuro-functional basis of grasping in humans. Participants were requested to perform a natural reach to grasp movement towards a visually available target object which could be either of a small size, requiring a PG movement or of a larger size requiring a WHG in order to be grasped. Differently from previous studies (Wheaton et al., 2005), I did not investigate ERPs evoked by a cue signaling specific object's intrinsic features, but by the target stimulus itself. Such approach may allow to examine how information about an object's geometric properties is transformed into specific motor programs more directly. I hypothesize that the ERP analysis may reveal the time course of activation of the differential cortical areas related to the planning, initiation and on-line control of reach to grasp movements and how such activity varies depending on grasp types. Kinematic analysis will provide an objective standard for parsing hand movements into distinct stages and for determining their temporal occurrence. Hand movements kinematics, acquired by means of a 3D motion analysis system synchronized with the EEG recording system, will make possible the correlation across neural and kinematical temporal events.

3.2. Materials and Methods

3.2.1. Ethics statement

The experimental procedures were approved by the Institutional Review Board at the University of Padua, and were in accordance with the Declaration of Helsinki (Sixth revision, 2008). All participants gave their informed written consent to participate in the study.

3.2.2. Participants

Twenty-two students, recruited from the Faculty of Psychology at the University of Padua, took part in the study. They had a mean age of 23.68 years (SD = 2.49; range = 19-28; 11females); they were all right handed, as measured by the Edinburgh Handedness Inventory (Oldfield, 1971) with normal or corrected to-normal vision, and without neurological or psychiatric pathologies.

3.2.3. Apparatus and Procedures

The participant was seated on a height adjustable chair so that the thorax pressed gently against the front edge of the table and the feet were supported. The position of the head was controlled by means of a head-chin-rest. A pressure sensitive starting switch was positioned 15 cm anterior to the mid-line of the participant's thorax. With the hypothenar eminence of the right hand placed upon this switch, the starting position was slight shoulder flexion and 70-80° of internal rotation, 90° of elbow flexion, semipronation of the forearm, 5-10° wrist extension and opposition between the pads of the index finger and thumb. The experimental stimuli were either a small or a large wooden sphere (Figure 3.1.). The small sphere was of diameter 3 cm whereas the large sphere was of diameter 7 cm. The stimulus

was placed upon the working surface 30 cm directly in front of a pressure sensitive starting switch (Figure 3.1.). Visual availability of the stimulus was controlled via Plato Liquid-crystal shutter glasses (translucent Technologies, Toronto, ON, Canada) worn by the participant throughout the test (Figure 3.1.).

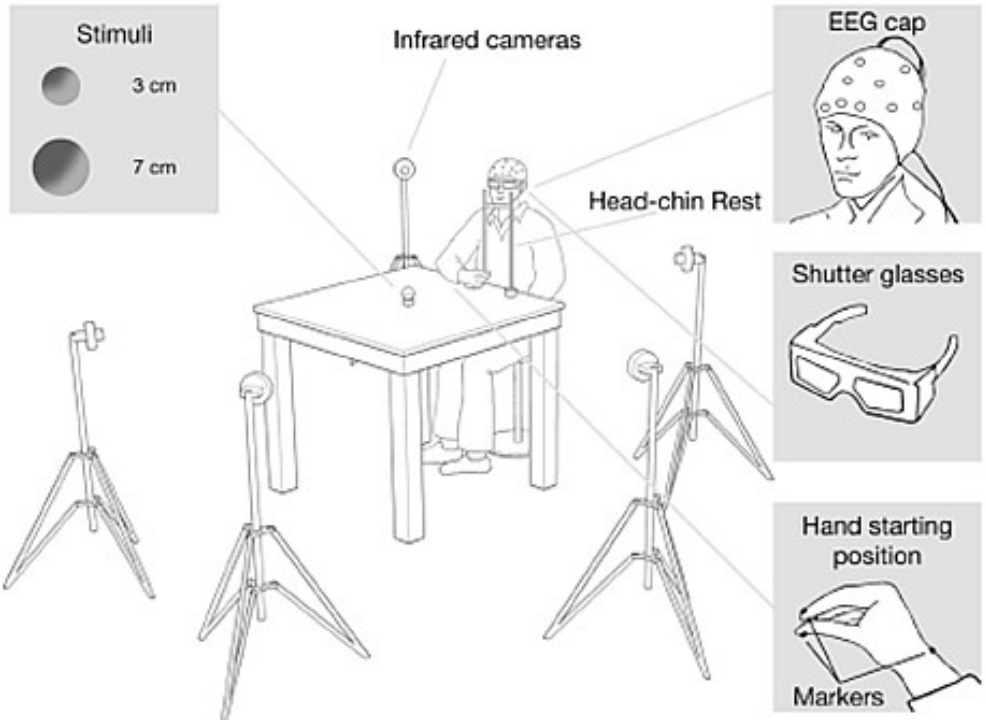

Figure 3.1. Experimental setup.

Under computer control, the shutters change from translucent to transparent within 10 ms and return to translucent in 2 ms. All participants naturally adopted a PG to grasp the small stimulus and WHG to grasp the large stimulus. And they were requested to maintain their gaze fixed towards the stimulus location. There were two experimental conditions, a grasping large (GL) condition in which participants grasped the large stimulus adopting a WHG. And a grasping small (GS) condition in which participants grasped the small stimulus adopting a PG. During a training session task instructions were given to participants. The experimenter explained the task consisting in reaching towards and grasping the presented stimulus. Once the participant was comfortable with the task they

performed a total of 80 trials, 40 for the GL and 40 for the GS conditions. The sequence of events was the following. At the start the shutter glasses were in a closed (opaque) state. At the time the shutter glasses opened (i.e., became translucent) the stimulus become visible and the participant was instructed to initiate the reach to grasp movement towards the stimulus. The shutter glasses remained open for the entire duration of the movement. Trials were administered in two blocks presented in a pseudorandom order. All failed trials were reintegrated and presented randomly later in the block. ERPs and kinematical recordings started at the time the shutters glasses became translucent (Figure 3.2.).

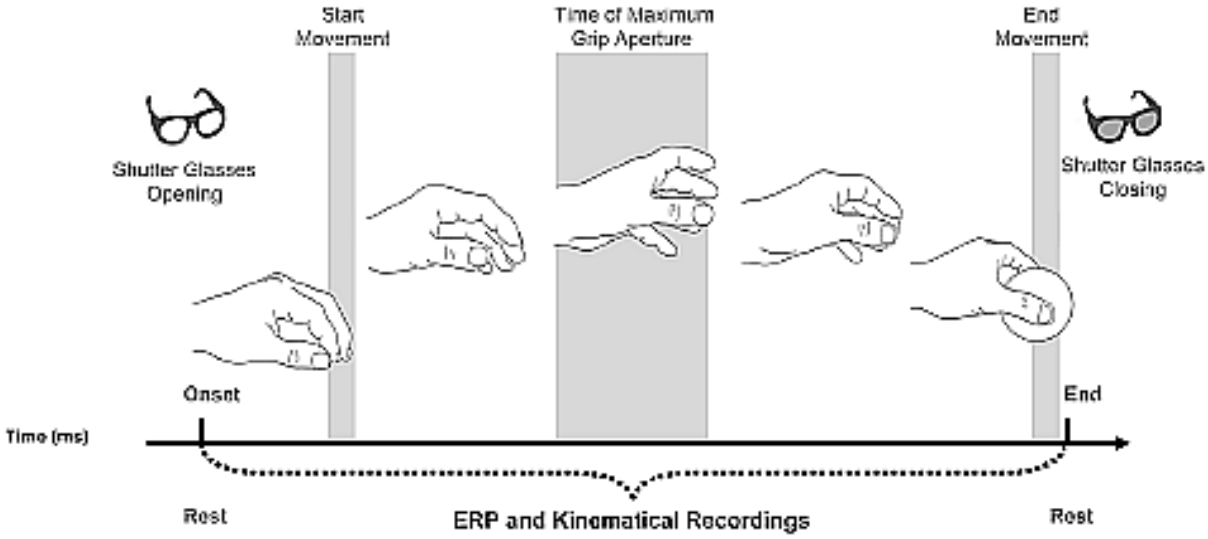

Figure 3.2. Hand choreography and type of recordings. Graphical representation of the choreography assumed by the hand during the movement and the timeline within which ERPs and kinematical data were acquired.

Kinematical recording and data processing: Reflective passive markers (0.25 cm diameter) were attached to the following points of the reaching limb: (a) wrist - radial aspect of the distal styloid process of the radius; (b) index finger - radial side of the nail; and (c) thumb - ulnar side of the nail (Figure 3.1.). Movements were recorded with the SMART system (BTS, Milan, Italy). This consisted of six infra-red cameras (sampling rate 200 Hz) inclined

at an angle of 45 degrees to the vertical, and placed around the table (Figure 3.1.). The calibrated working space was a parallelepiped (length 50 cm, breadth 50 cm, height 50 cm) from which the spatial error measured from stationary and moving stimuli was 0.4 mm. Coordinates of the markers were reconstructed with an accuracy of 1/3000 over the field of view and sent to a host computer. The SD of the reconstruction error was 1/3000 for the vertical (Y) axis and 1.4/3000 for the two horizontal (X and Z) axes. The SMART analyzer software package was used to assess the data. This gave a three-dimensional reconstruction of the marker positions. The data were then filtered using a finite impulse response (FIR) linear filter - transition band of 1 Hz (sharpening variable = 2; cutoff frequency 10 Hz). The reach component was assessed by analysing the trajectory and the velocity profile of the wrist marker. The manipulation component was assessed by analysing the trajectory of each of the hand markers, and the distance between these two markers. Reaction time was defined as the time interval between the opening of the crystal liquid lenses and the release of the start button upon which the hand was resting. Movement duration was calculated as the time between movement onset (defined as the time at which the wrist first began to move) and the end of the action (defined as the time when the fingers closed on the target and there were no further changes in the distance between the index finger and thumb). The period following this, whereby the stimulus was lifted, was not assessed. The dependent variables were (a) reaction time; (b) movement duration, (c) transport component parameters: time and amplitude of peak velocity of the wrist marker, and (c) grasp component parameters: time and amplitude of maximum grip aperture.

Electrophysiological recording and data processing: The electroencephalogram (EEG) was acquired by a portable amplifier system (SD-MRI, Micromed, Mogliano Veneto, Italy) from an array of 30 tin electrodes embedded in an elastic cap (ElectroCap International, Inc.) according to the 10–20 International System (AEEGS, 1991). The montage included

the following scalp positions: Fp1,Fpz, Fp2, F7, F3, Fz, F4, F8, FC3, FCz, FC4, T3, C3, Cz, C4,FT7, FT8, T3, T8, T5, CP3, CPz, CP4, P3, Pz, P4, T6, TP7,TP8, O1, O2. All electrodes were referenced to linked-mastoids. The ground electrode was placed in AFz. Impedance of all electrodes was kept below 5kΩ. The EEG signal were digitized at a sampling rate of 512 Hz (16 bit AD converter), and high-pass filtered at 0.15 Hz. Data processing was performed by BrainVision Analyzer 2 software (Brain Products GmbH, Gilching, Germany). Continuous EEG was off-line low-pass filtered at 30 Hz. Epochs were extracted separately for each of the two type of object stimuli (small, large), time-locked at the time the glasses were opened (i.e., stimulus appearance) and lasted 2000 ms. The considered time window encompassed the time at which the shutter glasses opened and the time at which the object was grasped (see Figure 3.2.). Artifacts were corrected by means of Independent Component Analysis (ICA) applied on all epochs together, regardless of stimulus size. The ICA correction was performed by using a toolbox in the EEGLAB software (9.0.3.4b version; Jung et al., 2000). The ICA allows for the identification of the independent components in the segmented EEG signal by taking simultaneously into account frequency, timing and location on the scalp. This procedure helps in isolating artifactual components, such as blinks and head muscles' contraction (Jeannerod et al., 1995; Castiello, 1996; Smeets & Brenner, 1999). In addition, epochs containing amplitude deflection greater than ±75μV was rejected for all the recorded channels prior to further analysis. The signal was then baseline-corrected against the mean voltage during the 200 ms prior to object appearance. Epochs containing erroneous movements were discarded. A total of 38.31 epochs (SD=1.84) for each size condition were included within the statistical analyses. Based on visual inspection of grand average waveforms and amplitude scalp maps, the following ERP components were statistically analyzed: amplitude and latency of P300, namely the positive peak evoked 200-400 ms following stimulus appearance at

parietal sites (P3, Pz, P4); amplitude and latency of N400, namely the negative peak occurring at 300-500 ms after object appearance at frontal (F3, Fz, F4), fronto-central (FC4, FCz, FC3), and central (C3, Cz, C4) sites; and mean amplitude of the sustained negativity observed in 400-800 and 1200-2000 time windows at frontal (F3, Fz, F4), fronto-central (FC4, FCz, FC3), central (C3, Cz, C4), and parietal (P3, Pz, P4) sites.

3.3. Data Analysis

Mean values for reaction time, movement duration and each kinematical measure were compared between grasping conditions (small, large) by means of paired t-test. ERP components were analyzed by means of separate repeated measure ANOVAs (see 'results' section). The alpha level of significance was fixed at 0.05. Before running the analyses, I checked for all the main assumptions behind this statistical parametric model (i.e., normality and sphericity). Kolmogorov-Smirnov test revealed that the normality assumption was satisfied. In all ANOVAs, Mauchly test showed that the sphericity assumption was not violated. The effect size of ANOVA results was quantified by means of partial eta-square values ($\eta 2p$). P-values of t-test and correlation results were corrected for multiple comparisons using a false discovery rate (FDR). Post-hoc comparisons of ANOVA were corrected by Bonferroni method. Correlation analyses by means of Pearson's r coefficient were performed between kinematical and ERP measures as well as between movement duration and ERPs events.

3.4. Results

3.4.1. Reaction time and movement duration

Reaction time did not differ between the GL and the GS conditions (517 ±137 vs 500 ±123 ms; $p > 0.05$). However, movements towards the smaller stimulus had a longer duration

than movements towards the larger stimulus [1141 ±164 vs 1114 ±196 ms; $F_{(1,23)} = 5.46$, $p < 0.02$; η^2 p = 0.41].

3.4.2. Kinematics

The manipulation of object size had predictable effects on the reaching and the grasping component, respectively. In particular, the reach component was characterized by a bell-shaped wrist velocity profile with a single peak. The latency of this peak did not differ significantly with stimulus size (475 ±123 vs 476 ±130 ms). For the grasp component, there was a direct relationship between the size of the stimulus and the maximum opening of the hand en route to the target, and between the size of the object and the time taken to open the hand maximally. The maximum grip aperture occurred earlier [519 ±48 vs 582 ±61 ms; $F_{(1,23)} = 16.06$, $p < 0.001$; η^2 p = 0.46] and it was smaller [123 ±3 vs 91 ±2 mm; $F_{(1,23)} = 106.93$, $p < 0.0001$; $\eta^2 p = 0.58$] for the GS than for the GL conditions.

3.4.3. Evoked Related Potentials

ERP waveforms of grand-average, locked to glasses opening (i.e., object appearance), were characterized by an early negative peak at around 100 ms, more marked at parietal and central electrode sites, which showed similar amplitude and latency for the two grasping conditions. Then, differences in ERP amplitude between the two conditions become evident. Specifically, a positive peak at around 300 ms (P300), maximally expressed at parietal electrode sites, showed higher amplitude for the GL than for the GS conditions. Subsequently, a negative electrical activity, peaking at around 400 ms, evident at central and frontal electrode sites, and sustained for a time-window lasting from 400 to 800 ms, clearly showed higher amplitude for the GS than the GL conditions. The polarity, the

temporal trend and the scalp distribution for such component suggests that this is likely linked to the motor component of action planning and to premotor areas, therefore I termed this component as motor-related N400 (m-N400). From 800 to about 1200 ms after object visual availability, a slow ERP deflection from negative to positive values at all electrode sites was found, which was characterized by a similar pattern for the two conditions (see Figures 3.3. and 3.4.). Then, a sustained positivity was evident from 1200 to 2000 ms, which was higher for the GS than for the GL condition. A time window corresponding to the time at which the object was approached and contact points have to be optimized.

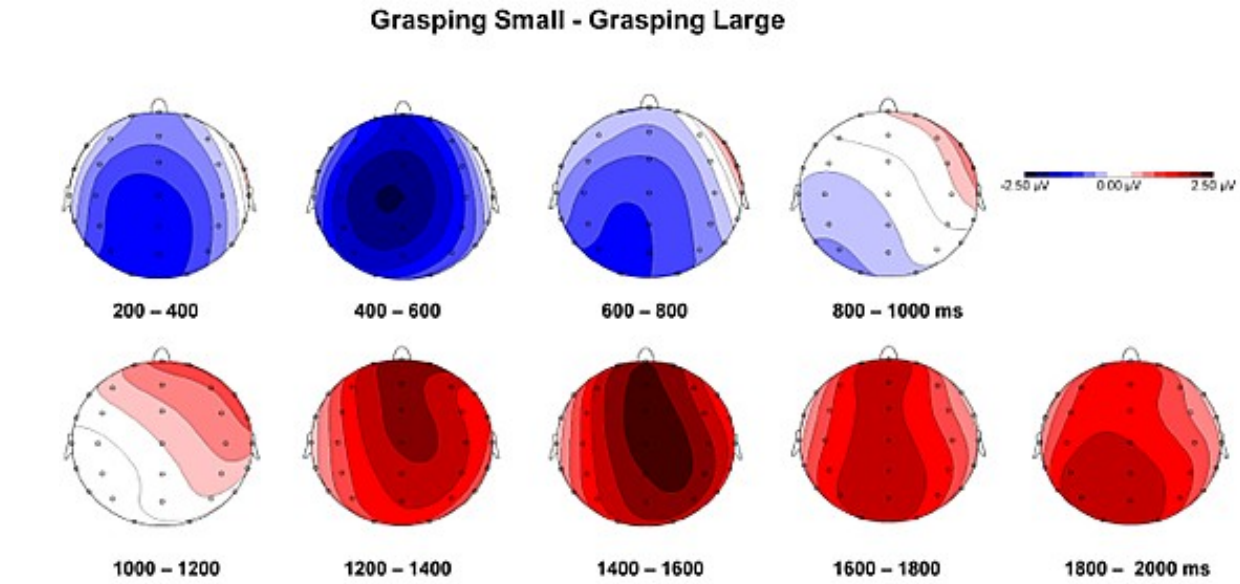

Figure 3.3. Scalp distribution of ERP differences between Grasping Small and Grasping Large conditions.

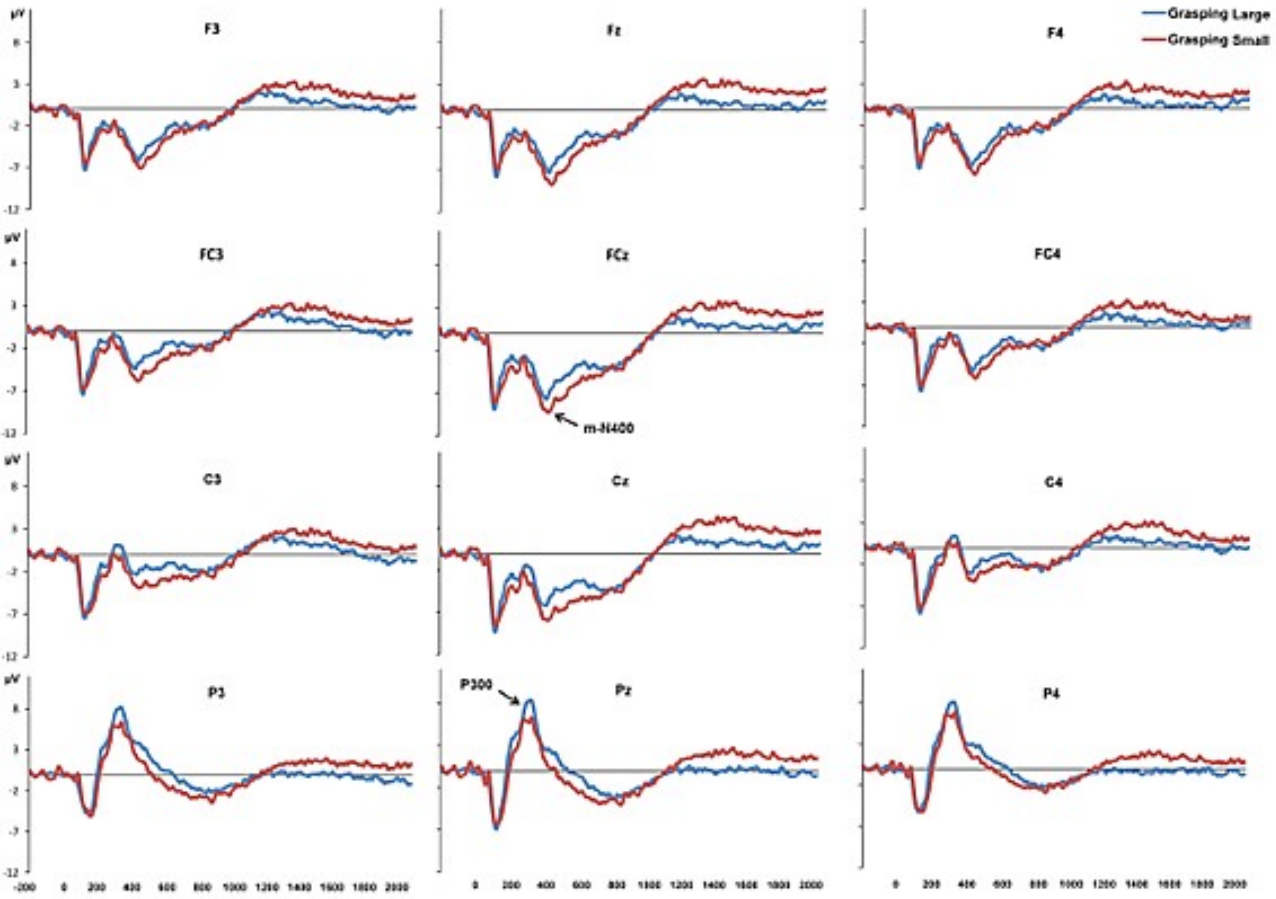

Figure 3.4. Grand-average ERP waveforms for the Grasping Small and the Grasping large conditions. The plots show ERPs time locked to glasses opening.

P300: Figure 3.4. depicts grand-average waveforms for the two grasping conditions at parietal sites P3, Pz, and P4, in which a P300 was evident. The amplitude and the latency of this component were analyzed by means of a 2 (stimulus size: small, large) × 3 (electrode position: left, midline, right) repeated-measure ANOVA. The analysis revealed a main effect of stimulus size [$F_{(1,21)} = 5.98$, $p = 0.024$; $\eta^2p = 0.24$]. A less positive amplitude for the GS than for the GL condition was revealed. No difference in peak latency between grasping conditions was found. Rather, electrode position significantly affected latency of the P300 component [$F_{(2,20)} = 4.22$, $p = 0.022$; $\eta^2p = 0.18$]. Post-hoc comparisons revealed that P300 peak reached maximal amplitude earlier for the left and midline sites (P3 and Pz, respectively) compared to the right site P4 ($p = 0.024$ and $p = 0.047$, respectively). No significant differences between P3 and PZ were detected. The scalp map in Figure 3.3., showing the topography of differential amplitude (GS – GL), confirms that within the 300-350 ms time window ERPs were higher for the GL compared to the GS condition.

M-N400: Figure 3.4. illustrates grand-average waveforms for the two grasping movements at the following electrode positions: F3, Fz, F4, FC4, FCz, FC3, C3, Cz, C4. Amplitude and latency of the negative ERP deflection peaking at around 400 ms (m-N400) were analyzed by means of a 2 (stimulus size: small, large) × 3 (anterior-posterior electrode position: frontal, fronto-central, and central) × 3 (left-right electrode position: left, midline, right) repeated-measure ANOVA. This analysis yielded a main effect of stimulus size [$F_{(1,21)} = 7.18$, $p = 0.014$; $\eta^2p = 0.25$], namely the m-N400 peak was found to reach higher amplitudes when participants were required to grasp the small compared to the large stimulus. A main effect of anterior-posterior electrode position was found [$F_{(2,20)} = 14.78$, $p < 0.001$; $\eta^2p = 0.41$]. Post-hoc comparisons revealed that, for both conditions, m-N400 amplitude was higher at frontal compared to fronto-central ($p = 0.30$) and central ($p = 0.002$) sites, and at fronto-central compared to central sites ($p = 0.001$). Furthermore, a

main effect of left-right electrode position [$F_{(2,20)} = 33.07$, $p < 0.001$; $\eta^2p = 0.61$] showed that, for both grasping conditions, m-N400 amplitude was higher at midline compared to left ($p < 0.001$) and right ($p < 0.001$) sites. The post-hoc analysis of the stimulus size × anterior-posterior electrode position interaction [$F_{(2,20)} = 3.76$, $p = 0.031$; $\eta^2p = 0.15$] revealed that for the GS condition the amplitude of the m-N400 did not differ between frontal and fronto-central sites ($p = 0.205$), meaning that the m-N400 was more equally distributed at frontal and fronto-central sites. Furthermore, the significant anterior-posterior × left-right electrode position interaction [$F_{(4,18)} = 18.27$, $p < 0.001$; $\eta^2p = 0.46$] revealed that for both grasping conditions, the m-N400 amplitude significantly increased from central to fronto-central to frontal sites only in left and right electrodes (all ps ≤ 0.040), whereas for midline electrodes it was equally larger. When considering latencies a main effect of stimulus size was found for them-N400 [$F_{(1,21)} = 8.65$, $p = 0.008$; $\eta^2p = 0.30$]. For all the considered electrode sites the m-N400 reached the maximum values later for the GS than for the GL condition. In summary, the m-N400 showed higher amplitude and later latency for the GS than for the GL condition at all considered electrode sites. Specifically, the maximum peak value was reached at FCz (GS: MAmpl = -12.13 μV, MSE = 1.13; MLat = 429.97 ms, MSE = 16.82; GL: MAmpl= -10.11 μV, MSE = 1.10; MLat = 383.55 ms, MSE = 18.37). The differential scalp distribution for the m-N400 component is depicted in Figure 3.3., where it clearly appears that this component reached its maximal (negative) amplitude values for the GS condition at frontal and central midline electrode sites.

400-800 ms: As shown in Figures 3.3. and 3.4., a sustained potential was observed from 400 to 800 ms at frontal, fronto-central, central, and parietal electrode sites (F3, Fz, F4, FC4, FCz, FC3, C3, Cz, C4, P3, Pz, P4). Mean ERP amplitude in this time window was analyzed. The 2 (object size) × 4 (anterior-posterior electrode position) × 3 (left-right

electrode position) ANOVA revealed that, as found for the m-N400 peak, such component showed an overall higher (more negative) mean ERP amplitude for the GS compared to the GL condition, in all frontal, fronto-central and central electrode sites [main effect of stimulus size: $F_{(1,21)} = 7.72$, $p = 0.011$; $\eta^2p = .27$]. A significant main effect of anterior-posterior electrode position [$F_{(2,20)} = 46.69$, $p < 0.001$; $\eta^2p = 0.69$] revealed that, for both grasping conditions, larger ERP amplitude was observed at frontal and fronto-central sites compared to central and parietal positions (all ps < 0.003). A significant main effect of left-right electrode position [$F_{(2,20)} = 31.50$, $p < 0.001$; $\eta^2p = 0.60$] showed that mean ERP amplitude within the 400-800 time-window was maximal at midline compared to both left and right sites (ps < 0.001). As for the m-N400, the significant stimulus size × anterior-posterior electrode position interaction [$F_{(2,20)} = 4.92$, $p = 0.012$; $\eta^2p = 0.19$] revealed that for the GS condition such sustained negativity was equally distributed between frontal and fronto-central sites (i.e., mean ERP amplitude between such sites did not differ, $p = 0.625$). The anterior-posterior × left-right electrode position interaction [$F_{(4,18)} = 13.76$, $p < 0.001$; $\eta^2p = 0.40$] revealed that, for both grasping conditions, ERP amplitude became significantly larger from parietal to central to fronto-central to frontal sites only for the left and the right electrodes (all ps < 0.050), whereas for the midline electrodes, where ERP amplitude reached the highest values, fronto-central and frontal sites did not differ from central sites, but were significantly higher than parietal sites (all ps < 0.001).

1200-2000 ms: Mean ERP amplitude extracted in this time window at frontal, fronto-central, central, and parietal electrode sites was analyzed. The ANOVA confirmed that higher ERP amplitude was found for the GS condition [main effect of stimulus size: $F_{(1,21)}= 28.08$, $p< 0.001$; $\eta^2p= 0.57$]. A significant main effect of anterior-posterior electrode position [$F_{(2,20)}= 10.28$, $p< 0.001$; $\eta^2p= 0.33$] showed that ERP in such time window were larger at frontal, fronto-central and central sites compared to parietal positions (all ps<

0.030). A significant main effect of left-right electrode position [$F_{(2,20)}$= 12.47, p< 0.001; η^2p= 0.37] revealed that mean ERP amplitude within the 1200-2000 ms time-window was maximal at midline compared to both left and right sites (all ps< 0.002).

3.4.4. Correlations between kinematic and ERP events

Mean amplitude and latency of P300 and m-N400 components were averaged at electrode sites in which they were maximally expressed. Specifically, at P3 and Pz for the P300 and at Fz and FCz for the m-N400. Then these values were correlated with movement duration and the considered kinematic measures, namely time to peak velocity and the time of maximum grip aperture. No significant correlations were detected when considering the relationship between kinematical and ERP events. However, as depicted in Figure 3.5., for both the GL and the GS experimental conditions, the individual mean latency for the m-N400 component significantly correlated with the individual mean for movement time [for GL: r(22) = 0.49, p = 0.022; for GS: r(22) = .46, p = 0.034].

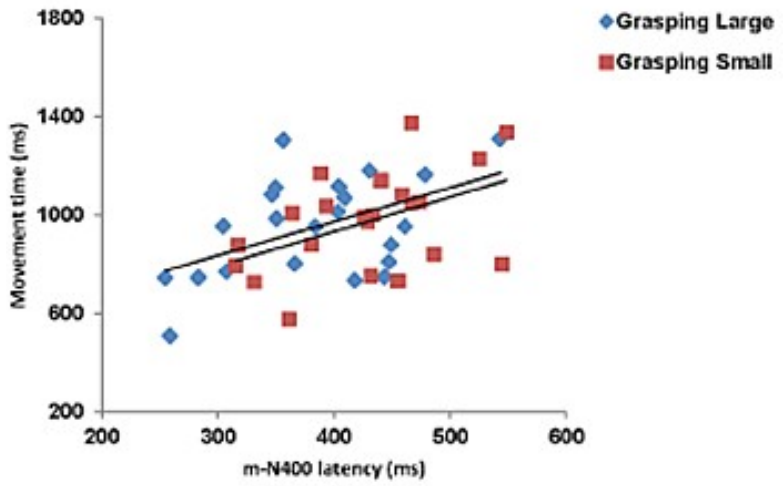

Figure 3.5. Correlation between movement time and ERP measures. Correlation between the individual data for movement time and the m-N400 latency for the Grasping Large and the Grasping Small conditions.

3.5. Discussion

We set out to investigate kinematics and ERP activity during reach to grasp movements performed towards either a large or a small stimulus. Overall the results indicate that the two grasping conditions determine a modulation in timing and amplitude of specific kinematic landmarks and ERP components.

In terms of behavioural performance, our results are in line with previous kinematical studies (Jeannerod, 1984; Gentilucci et al., 1991; Jakobson & Goodale, 1991; Jeannerod et al., 1995; Castiello, 1996; Smeets & Brenner, 1999). Literature findings consistently indicate that, with respect to whole hand grips, precision ones are characterized by a longer movement duration, and an anticipated and lowered amplitude of maximum grip aperture (e.g. Jeannerod, 1984; Jakobson & Goodale, 1991; Castiello, 1996). Customarily, no differences in the times to peak wrist velocity regardless of the type of grasp are usually found. In the same way, here the reaching component was characterized by a bell-shaped wrist velocity profiles with single peaks with no differences in the latency of these peaks depending on grasp type. The total duration of reach to grasp movements was longer and the time and amplitude of maximum grip aperture was earlier and smaller for the GS than for the GL condition. These findings indicate that the size of the stimulus influenced selectively the planning and the execution of the reach to grasp movement. This is an important aspect of the present study because in order to ascertain the effects that such differential processing might have on ERPs, it is necessary to demonstrate that the participants' movement show classic kinematic signatures depending on grasp conditions.

For an efficient grasp visual information regarding an object's physical properties (e.g., size) must be transformed and used to select an appropriate motor command. For both humans and monkeys the key cortical circuit involved in this transformation involves the anterior intraparietal area (AIP), the ventral and dorsal premotor cortices (PMv and PMd, respectively), and the primary motor cortex (M1) (Jeannerod et al., 1995; Murata et al., 1997; Ehrsson et al.,

2000; Murata et al., 2000; Rizzolatti & Luppino, 2001; Castiello, 2005; Raos et al., 2006; Begliomini et al., 2007; Grol et al., 2007; Umilta et al., 2007). AIP contains neurons that discharge in relation to specific object properties (Murata et al., 2000), whereas many grasp-related "canonical" neurons (Rizzolatti & Luppino, 2001) are found in PMv (Murata et al., 1997; Raos et al., 2006; Umilta et al., 2007). Experiments in monkey (Murata et al., 2000; Raos et al., 2006) and humans (for review see Castiello & Begliomini, 2008) appear to show that object properties are encoded as a gradient along the AIP-PMv-M1 axis, with the object being first represented in visual attributes and then in terms of an appropriate grasp.

With this in mind, our EEG recording revealed differences between grip types in the ERPs evoked by stimulus appearance. Such differences were concerned to, both visuo-spatial processing and motor planning. At first, differences in amplitude between conditions become evident over parietal sites following object appearance, at around 300 ms (P300), that is during the planning phase. Such difference remained significantly distinct during the execution phase up to 800 ms. In particular, the peak amplitude for the P300 component was higher for the GL than for the GS condition. This finding might reflect the greater amount of visuo-spatial information to be extracted from larger objects. In this view, object metric properties, such as size, are processed at parietal level. Although I cannot firmly determine the brain source of such activation, it is likely that it reflects AIP activity concerned with the amount of visual information related to the object, and it might be seen as the initial step of the transformation leading from representation of objects to movement. These findings fit with those reported in a recent study on the role of anterior intraparietal sulcus in sensorimotor integration of visually guided hand movements (Verhagen et al., 2012). Here it was shown that the suppression of alpha oscillation over the parieto-occipital electrodes occurred at 220-240 ms following object presentation. Furthermore, the evidence of a parietal involvement is in agreement with neurophysiological evidence showing that parieto-occipital neurons are sensitive to grip type

(Fattori et al., 2009; 2010). Assuming that our present results reflect this kind of activity, they might provide a further confirmation that motor plans requiring hand preshaping extend farther anteriorly into both the precuneus and the middle intraparietal sulcus (Gallivan et al., 2011). In the light of previous ERPs studies looking at brain sources of motor-related potentials (Zaepffel & Brochier, 2012) it is likely to suggest the involvement of additional areas, such as the superior parietal lobe.

Subsequent to the parietal activation I found a negative electrical activity, peaking at around 400 ms following object appearance (m-N400), which was evident over central and frontal electrode sites. The amplitude of this component was higher for the GS than the GL conditions and such difference was significant within a time-window lasting from 400 ms up to 800 ms following object presentation. The polarity, the slow temporal trend and the scalp distribution suggest that such component reflects motor planning and that it is linked to premotor activity (Shibasaki & Hallett, 2006).

Unlike previous ERP studies on motor planning (e.g., Müller-Gethmann et al., 2000; Wheaton et al., 2005b; Leuthold & Jentzsch 2009; Bozzacchi et al., 2012; Kourtis et al., 2012; Zaepffel & Brochier, 2012), I did not analyze self-paced movements and I did not adopt a precuing task, but I examined EEG deflections evoked by stimulus appearance which prompted a spontaneous grip movement. Nevertheless, the spatio-temporal characteristics of the m-N400 might be assimilated to an index of motor planning and it is strongly influenced by motor variables. Interestingly, stimulus size significantly affected the latency and the topographical location of such component. The m-N400 peak had a later onset and a wider fronto-central distribution for the GS than for the GL condition. This suggests that the planning phase needed for a precision grip movement takes longer and involves more (dorsal) areas. Taken together, these findings indicate that the parietal' visual information, encoded in an "object" reference frame, is subsequently multiplexed into a "grasp" reference frame within a premotor network possibly involving both

the PMd and the PMv. Beyond forming a critical node in the visuomotor planning circuit underlying grasping, recent evidence suggests that different premotor areas (e.g., PMd and PMv) might have dissociable processes. Experiments in humans and monkeys indicate that PMv is more involved in the distal components of the action, such as hand preshaping and specific grip responses (e.g., Davare et al., 2006). PMd, instead, appears to be more involved in the on-line control of movement (e.g. Raos et al., 2004; Begliomini et al., 2007). Given that most of these previous descriptions are based on the characterization of activity stemming during the movement itself, the decoding of different planned hand movements shown here provides a significant additional dimension to such descriptions, which fits with previous functional imaging reports (e.g., Gallivan et al., 2011).

The difference in amplitude between the GS and the GL condition may reflect the need for additional sensory-motor control mechanisms for the more accurate GS condition. A result that is in keeping with the evidence that accuracy has the ability to affect readiness potentials (Shibasaki & Hallett, 2006). In humans, evidence from developmental, psychophysical, neuropsychological and neuroimaging studies seems to suggest that precision grips (as for our GS condition) are characterised by a greater degree of complexity. Firstly, the ability to perform independent finger movements and grasp with the precision grip is not present when voluntary grasping emerges (e.g., Gordon et al., 1994). Secondly, consistent results within the adult reach to grasp behavioral literature (Castiello, 2005), and those obtained in the present study, indicate that the performance of a precision grip is characterized by the need for additional time. Berthier and colleagues (1996) also showed that as visual information and object size decreased, subjects had longer movement times, slower speeds, and more asymmetrical hand-speed profiles. This kinematic characterization reflects the adoption of a strategy following the principles of the Fitt's Law (Fitt, 1954), implying that the difficulty of the task is reflected in movement kinematics. Thirdly, in macaques, it has been revealed that of the premotor area F5 neurons active during

grasping, the most frequent were those involved in precision grips (Raos et al., 2004) whereas whole hand neurons were encountered much less frequently (Rizzolatti et al., 1988; Jeannerod et al., 1995). Finally, neuroimaging studies indicate that premotor activity increase more during the execution of a movement toward a small object than toward a large one reflecting the increased planning and on-line control required by grasping small objects (Begliomini et al., 2008; Grol et al., 2007). An alternative possibility related to the modulation of the N-400 activity might be concerned with inhibition. Previous studies from Kok and colleagues (1986), demonstrated a frontal N400 elicited by a No-Go stimulus in a Go\No-Go paradigm. In this view the greater N-400 activity for the condition in which a PG is performed would stem from inhibiting the opening of the whole hands in order to specify index finger and thumb when a precise grasping is requested. This idea would imply that the 'simpler' whole hand grasp would be prepared by default and then precision grip would be specified. Evidence that this process might be in place comes from reach to grasp perturbation studies in which the passage from whole hand to precision grip movements has been measured (Castiello et al., 1993).

Altogether, the present findings confirm a parietal processing related to the vision of a particular graspable object which provides premotor cortices with grasp-related information that allows neurons in these areas to be tuned to the upcoming grasp and on-line control. Importantly, they provide an addition to current literature by revealing the time course of the visuomotor transformation process starting from the 'parietal' visual object discrimination activity to the 'premotor' activity concerned with the assignment of specific hand configurations depending on object's size. Furthermore, they show that once such differential process, depending on grasp type/stimulus size ensemble within the 'parietal' and the 'frontal' component of the grasping circuit is started before movement initiation, it remains sustained throughout the entire action. This indicates that these areas participate in a sensorimotor network involved in grasp planning, prediction of sensory stimulation, and monitoring of appropriate execution of the desired actions.

And also suggest the role of the parietal (possibly the AIP region) and premotor cortices (possibly PMv and PMd) not only during the execution of reaching-to-grasp movements as previously reported (Rice et al., 2006; Xiao et al., 2006), but also during the planning phase. A result which is in line with neurophysiological evidence showing that the discharge of F5 neurons is tuned for specific grasps well before movement onset and this early tuning was carried over in the preshaping period of the task. In line with this evidence I found a marked differentiation across different grasps during the premovement phase which was carried over into early grasp phases (as witnessed by kinematical analysis) characterized by a premotor kind of activity. Altogether, these properties are consistent with the notion that premotor areas play a role in translating visual information about an object's physical properties into the appropriate motor plans to interact with the same object (Rizzolatti et al., 1988; Raos et al., 2006; Murata et al., 1997; Brochier et al., 2004).

Another aspect of the present findings is concerned with some relationship between kinematical and ERPs events. Of interest is that the ERPs differences noticed during the planning phase at both parietal and premotor level depending on grasp conditions persisted all along the unfolding of the action. And remained statistically different at the time key kinematic landmarks such as the time of maximum grip aperture occurred. A greater peak of maximum grip aperture and a modulation of the time occurrence for this peak corresponded to a significantly different level of activity for ERPs components. This signifies that when the stimulus become visually available sensory and motor processes specifically tailored to process the stimulus were established and maintained active as to organize the kinematical unfolding of the movement.

Although I did not find any significant correlation between the times at which peak ERPs components and the considered kinematical landmarks occurred, I found that for both the GL and the GS conditions the individual mean latency for the premotor m-N400 component significantly correlated with the individual mean for movement time. This might indicate that at the time the

'parietal' information regarding the visual aspect of the object are integrated within the premotor area (possibly PMv) with the motor prototypes adequate to successfully grasp it, the time to perform the action is kept into account. Similarly, an estimate of movement time, possibly performed at the level of PMd, might serve to plan the amount of on-line control required by the movement. This mode of programming might keep the timing of the commands independent from the spatial parameters of the movement. In other words, selection of the muscles needing to be activated to carry out a given task can be modified, or the kinematics can be modulated within a centrally generated temporal template that determines the co-ordination of a given action. This might appear to be the easiest and most readily chosen organizational option of the neural system to compensate for the postural and joint kinematic variability characterizing reach to grasp actions.

3.6. Conclusion

In the present study, I have explored the kinematic and ERP dynamics during a reach to grasp task. Together, kinematical and ERPs data confirm that the object size/type of grasp ensemble has the ability to modulate both the behavioural and the neural components underlying this kind of action. Analysis of the changes at the level of the ERPs components revealed that the parieto-frontal network is modulated differently by prehension movements towards differently sized objects at both planning and execution level. The correlation between movement time and ERPs components is suggestive of a mode of programming relying on a centrally generate template within which dynamic aspects of the movement are coordinated. In a broader perspective, this work underlines the use of EEG for the investigation of movements with unique cortical motor processes such as reach to grasp movements.

4.OBJECT SIZE MODULATES FRONTO-PARIETAL ACTIVITY DURING REACHING MOVEMENTS[2]

4.1. Introduction

In order to perform a successful reaching movement towards an object signals about limb starting position, eyes position and target location have to be combined and integrated into common, distributed spatial representations (Buneo et al., 2002; Battaglia-Mayer et al., 2003; Mascaro et al., 2003; Shadmehr & Wise, 2005). In both humans and monkeys a central role for such integration is played by a neural circuit involving the frontal and the parietal cortex, the so-called "dorsal visual stream" (for review see Culham et al., 2006).

By means of single-unit recording techniques, a number of studies have demonstrated the presence of visuomotor-related neurons within the parieto-occipital (Galletti et al., 1996, 1997; Battaglia-Mayer et al., 2000; Fattori et al., 2001, 2005) and intraparietal sulci (Grefkes & Fink, 2005), the PMd and the PMv cortices (Hoshi & Tanji, 2004a, b). Furthermore, a parietal reach region (PRR) lying in the medial bank of the intraparietal sulcus, a region likely corresponding to the medial intraparietal area (MIP) has been defined (Andersen & Buneo, 2002; Buneo et al., 2002; Connolly et al., 2003; Gail & Andersen, 2006).

Results from human neuroimaging studies appear to nicely fit with the neurophysiological results reported above. Reaching related activation has been revealed within motor, premotor areas (Decety et al., 1992; Grafton et al., 1996; Kawashima et al., 1996; Kertzman et al., 1997)

2 *Tarantino, V., De Sanctis, T., Straulino, E., Begliomini, C., Castiello, U. (2013). Object size modulates activity within the fronto-parietal network underlying reaching movements. European Journal of Neuroscience. In Press.*

and within specific sectors of the parietal cortex, namely the medial intraparietal sulcus (mIPS; Prado et al., 2005; Cavina-Pratesi et al., 2010; Konen et al., 2013) and the precuneus (PCu; Connolly et al., 2003; Grefkes et al., 2004; Astafiev et al., 2004; Grefkes & Fink, 2005; Filimon et al., 2009).

Complementary to these approaches, ERPs measured by electroencephalography EEG have shown P-300 like components related to reaching in premotor, motor and parietal areas (McDowell et al., 2002; Berndt et al., 2002; Naranjo et al., 2007; Bozzacchi et al., 2012).

Recently, a particular noticeable finding is that neural recording in monkey show that one of the areas of the dorsomedial pathway, the medial posterior parietal area V6A, hosts neurons that, in addition to being sensitive for the direction of arm reaching movements (Fattori et al., 2001, 2005), are also sensitive to intrinsic features of target objects such as shape (Fattori et al., 2012). A result which is in line with the evidence that in humans the kinematical organization of reaching is affected by the precision requirements related to intrinsic features of objects, such as size, despite a change in the distal program (i.e. hand shaping) is not implied (Gentilucci et al., 1991; MacKenzie et al., 1987).

To date, whether in humans the fronto-parietal network alerted during the planning and execution of reaching movements is modulated by the intrinsic features of objects has yet to be investigated. To fill this gap, our study investigated kinematical and EEG signals while participants performed a reaching action towards an object which could be either of a small or a large size.

4.2. Materials and methods

4.2.1. Ethics statement

The experimental procedures were approved by the Institutional Review Board at the University of Padua, and were in accordance with the Declaration of Helsinki (Sixth revision, 2008). All participants gave their informed written consent to participate in the study.

4.2.2. Participants

Twenty-two students, with the same characteristics of those who participated in the experiment reported in Chapter 3 took part in the Experiment.

4.2.3. Apparatus and Procedures

Apparatus and procedures were the same as those reported in Chapter 3 except that participants were requested to perform a reaching task in which they were asked to touch the object maintaining the hand in a closed fist (the fist posture was the same for both small and large objects, see Figure 4.1. Panel a). The fist's posture was chosen as to minimize distal involvement (see kinematical processing and data analysis section). Once the participants were comfortable with the task they performed a total of 80 trials, 40 trials towards the large object and 40 trials towards the small object. The sequence of events was the same as the experiment reported in Chapter 3 (see Figure 4.1. Panel b).

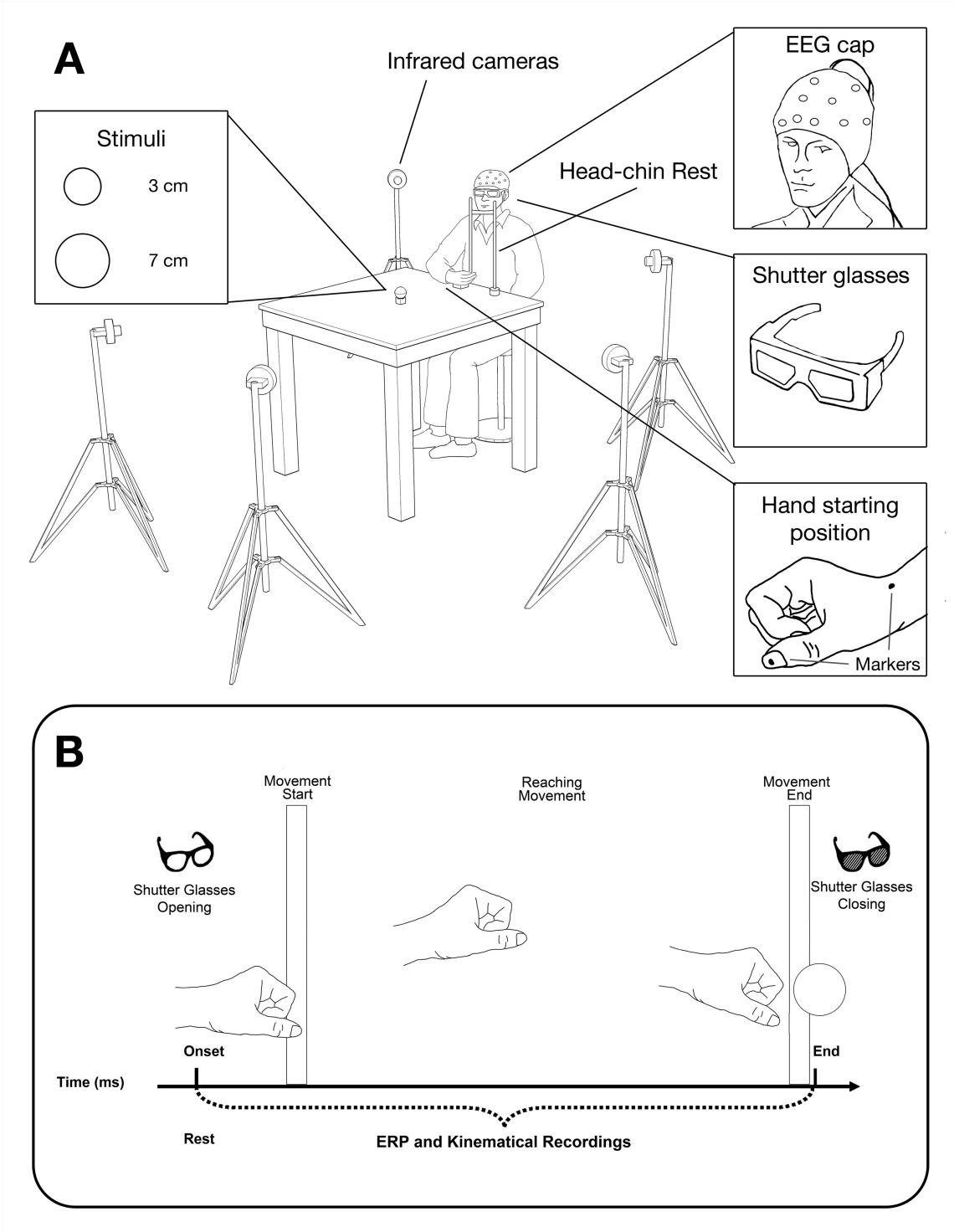

Figure 4.1. Panel (A) represents the Experimental set-up. Panel (B) represents the timeline of events, within which ERP and kinematical data were recorded.

4.2.4 Kinematical recording and data processing

Kinematical recording and data processing were the same as for the experiment reported in Chapter 3. Reaching was assessed by analysing the trajectory and the velocity profiles of the wrist marker. Reaction time was defined as the time interval between the opening of the crystal liquid lenses and the release of the start button upon which the hand was resting. Movement duration was calculated as the time between movement onset (defined as the time at which the button press was released) and the end of the action (defined as the time when the reaching hand touched the target). The dependent variables were (i) reaction time; (ii) movement duration, (iii) time and amplitude of peak velocity of the wrist marker, (iv) the time from peak velocity to the end of the movement (deceleration time), (v) time and amplitude of the maximum height of the wrist trajectory, and (vi) the trajectory length.

4.2.5 Electrophysiological recording and data processing

Electroencephalography recording and data processing were the same as the experiment reported in Chapter 3.

4.3 Data analysis

Mean values for reaction time, movement duration and each kinematical measure were entered within analysis of variance (ANOVA) with object size (small, large) as a within-subjects factor. ERP components were analyzed by means of separate repeated measure ANOVAs (see Results section). The alpha level of significance was fixed at 0.05. Before running the analyses, I checked for all the main assumptions behind this statistical parametric model (i.e., normality and sphericity). Kolmogorov-Smirnov test revealed that the normality assumption was satisfied. In all ANOVAs, Mauchly test showed that the sphericity assumption was not violated. The effect

size of ANOVA results was quantified by means of partial eta-square values (η^2_p). Post-hoc comparisons of ANOVA were corrected by Bonferroni method. Correlation analyses by means of Pearson's *r* coefficient were performed between kinematical and ERP measures. Namely, mean peak and latency values (the maximum ERP amplitude value measured in a specific time window and its corresponding point in time) of P300 and N400 components, and mean amplitude within the 400-800 time window, at relevant sites, were considered.

4.4. Results

4..4.1. Reaction time

Results obtained on reaction time suggest that participants reacted faster to execute a reaching movement towards a large (479 ± 86 ms) than a small (492 ± 97.25 ms) object. However such difference only approached significance ($P > 0.053$).

4.4.2. Kinematics

The manipulation of object size determined significant effects on reaching kinematics (Figure 4.2.). Movement duration was longer for the small than for the large object (1183 ± 243 vs 1099 ± 230 ms; $F_{1,21} = 233.60$, $P < 0.0001$; $\eta^2_p = 0.75$). Object size significantly modified the amplitude of peak velocity ($F_{1,21} = 9.76$, $P < 0.001$; $\eta^2_p = 0.68$; Figure 4.2. Panel A). The peak velocity was higher for the larger than the smaller object (1054 ± 114 vs 1001 ± 116 mm/s; Figure 4.2. Panel A). The time of peak velocity occurred earlier for the small than for the large object (420 ± 31 vs 431 ± 35 ms; $F_{1,21} = 11.12$, $P < 0.05$; $\eta^2_p = 0.62$; Figure 4.2. Panel A). Deceleration time was longer for the smaller than for the larger object (763 ± 43 vs 668 ± 58 ms; $F_{1,21} = 51.12$, $P < 0.0001$; $\eta^2_p = 0.80$; Figure 4.2. Panel A). In terms of spatial trajectories, the point at which the wrist trajectory reached its maximum

distance from the working surface was higher for the large (115 ± 11 mm) than for the smaller (108 ± 10 mm) object ($F_{1,21} = 10.96$, $P < 0.003$; $\eta^2_p = 0.76$; Figure 4.2. Panel B). The total length of the trajectory was longer for the smaller than for the larger object (322 ± 19 vs 303 ± 15 mm; $F_{1,21} = 11.75$, $P < 0.001$; $\eta^2_p = 0.69$).

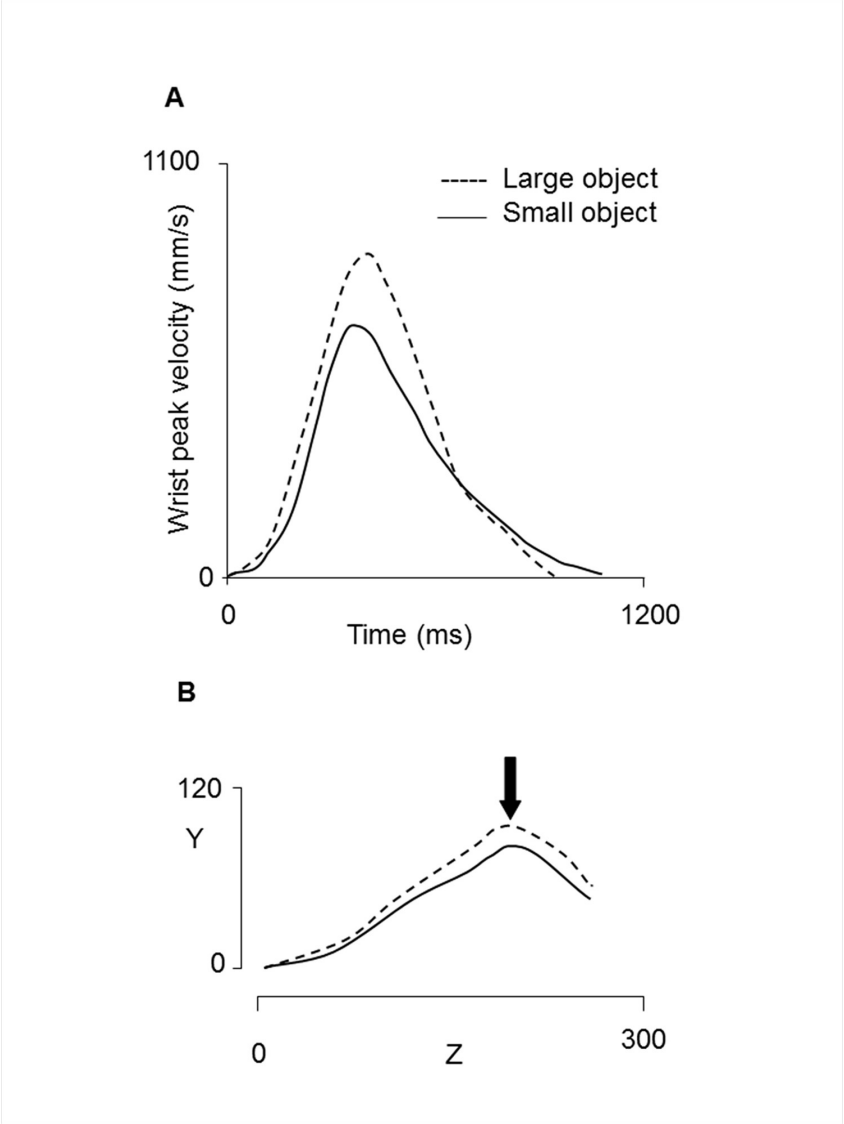

Figure 4.2. Panel (A) represents the velocity profile for a representative subject. Panel (B) depicts representative examples of trajectories of the reaching component on the sagittal plane for the small and large object conditions. Values on the axis are in millimeters (mm). Axis z = sagittal axis; axis y = vertical axis. The arrow indicates the point of maximum trajectory height.

4.4.3. Evoked Related Potentials

Figure 4.3. depicts grand-average waveforms locked to the time at which the shutter glasses opened (i.e., object appearance), in the two object conditions. ERPs were characterized by an early negative peak at around 100 ms (N100), more marked at parietal and central electrode sites, which showed similar amplitude and latency for both the small and the large object. Then, differences in amplitude between the two object conditions became evident. Specifically, a positive peak at around 300 ms (P300), maximally expressed at parietal electrode sites, showed higher amplitude for the large compared to the small object. Subsequently, a negative electrical activity, peaking at around 400 ms at central and frontal electrode sites, and sustained for a time-window lasting from 400 to 800 ms, showed higher amplitude for the small compared to the large object. The polarity, the temporal trend and the scalp distribution for such component suggested that this was likely linked to the motor component of action planning and to premotor areas, therefore I termed this component as motor-related N400 (m-N400; De Sanctis et al., 2013). From 800 to about 1200 ms after object visual availability, a slow ERP deflection from negative to positive values at all electrode sites was found. The following sustained positivity from 1200 to 1800 ms was similarly large for the two conditions and distributed over central and frontal sites.

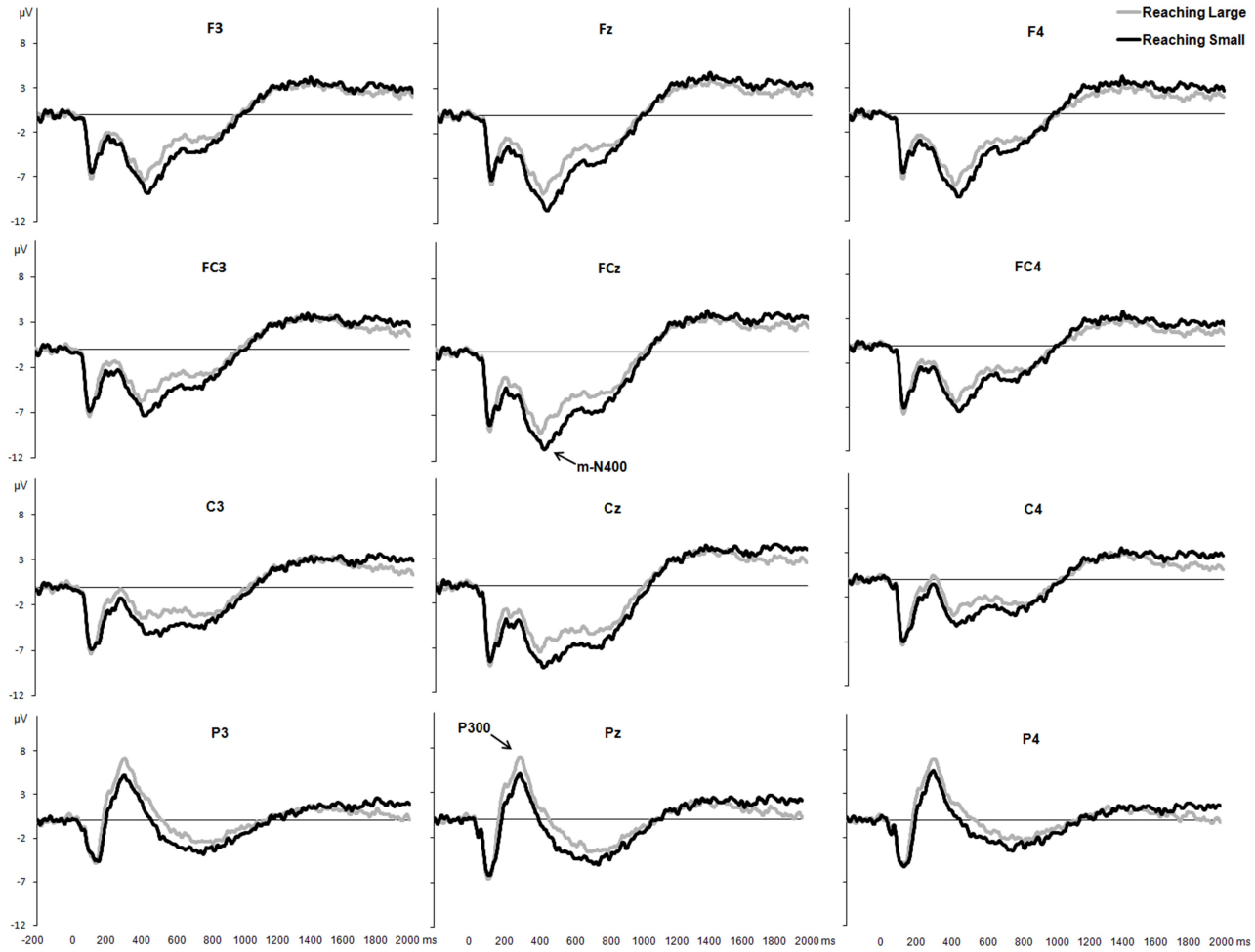

Figure 4.3. The plot depicts grand-average ERP waveforms locked to the time at which the shutter glasses opened (i.e., object appearance), for Reaching Small and Reaching Large conditions.

P300: The amplitude and the latency of this component were analyzed by means of a 2 (object size: small, large) × 3 (electrode position: left, midline, right) repeated-measure ANOVA. The analysis revealed a main effect of object size ($F_{1,21} = 25.38$, $p < 0.001$; $\eta^2_p = 0.55$), namely a higher P300 amplitude for the large than for the small object was found. No difference in peak latency between reaching conditions was present. Rather, P300 latency was significantly affected by electrode position ($F_{2,20} = 4.53$, $p = 0.017$; $\eta^2_p = 0.18$). Post-hoc comparisons revealed that P300 peak reached maximal amplitude earlier in the left site (P3) compared to the midline (Pz) and right (P4) ones ($p = 0.017$ and $p = 0.023$, respectively).

No significant differences between Pz and P4 were detected. The scalp map in Figure 4.4., showing the topography of the differential amplitude (Reaching Small – Reaching Large), confirms that within the 300-350 ms time window ERPs were larger for the large compared to the small object.

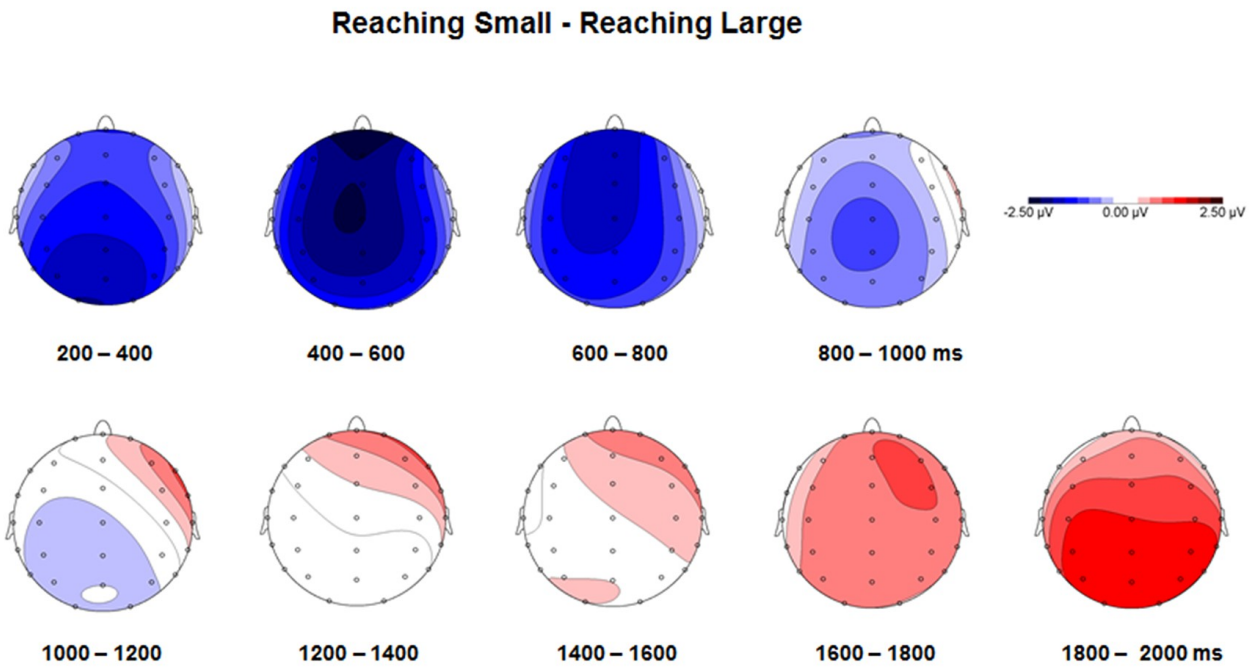

Figure 4.4. The scalp maps show the topography of the differential ERP amplitude between Reaching Small and Reaching Large conditions, from 200 to 2000 ms.

M-N400: Amplitude and latency of the negative ERP deflection peaking at around 400 ms (m-N400) were analyzed by means of a 2 (object size: small, large) × 3 (anterior-posterior electrode position: frontal, fronto-central, and central) × 3 (left-right electrode position: left, midline, right) repeated-measure ANOVA. This analysis yielded a main effect of object size ($F_{1,21} = 13.18$, $p = 0.002$; $\eta^2_p = 0.41$), namely the m-N400 peak was found to reach higher (more negative) amplitudes when participants were required to reach the small compared to the large object. A main effect of anterior-posterior electrode position was found ($F_{2,20} =$

25.33, $p < 0.001$; $\eta^2_p = 0.57$). Post-hoc comparisons revealed that, for both conditions, m-N400 amplitude was higher at frontal compared to fronto-central ($p = 0.002$) and central ($p < 0.001$) sites, and at fronto-central compared to central sites ($p < 0.001$). Furthermore, a main effect of left-right electrode position ($F_{2,20} = 38.99$, $p < 0.001$; $\eta^2_p = 0.67$) showed that, for both reaching conditions, m-N400 amplitude was higher at midline compared to left ($P < 0.001$) and right ($p < 0.001$) sites. The post-hoc analysis of the anterior-posterior × left-right electrode position interaction ($F_{4,18} = 27.67$, $p < 0.001$; $\eta^2_p = 0.59$) revealed that for both conditions at left and right sites m-N400 amplitude increased progressively from central to frontal areas ($p < 0.003$), whereas at midline sites was wider distributed along the anterior-posterior direction (only at FCz the amplitude was higher compared to Cz, $p = 0.004$).

Neither object size nor electrode position effect was found on peak latency. In summary, the m-N400 showed higher amplitude for the small than for the large object at all considered electrode sites. Specifically, the maximum peak value was reached at FCz (Small object: MAmpl= -13.51 ± 4.09 μV, MLat= 410.15 ± 54.85 ms; Large object: MAmpl= -11.29 ± 3.73 μV, MLat= 409.96 ± 53.83 ms). The differential scalp distribution for the m-N400 component depicted in Figure 4.4. clearly shows that in this time window ERP are higher and more negative for the small object condition at frontal and central areas.

400-800 ms: As shown in Figure 4.4., a sustained potential was observed from 400 to 800 ms at frontal, fronto-central, central, and parietal electrode sites (F3, Fz, F4, FC3, FCz, FC4, C3, Cz, C4, P3, Pz, P4). Mean ERP amplitude in this time window was analyzed. Similarly to m-N400 results, the 2 (object size) × 4 (anterior-posterior electrode position) × 3 (left-right electrode position) ANOVA revealed that such potential reached overall higher

(more negative) mean ERP amplitude for the small compared to the large object, in all frontal, fronto-central and central electrode sites (main effect of object size: $F_{1,21} = 10.63$, $p = 0.004$; $\eta^2_p = .35$). A significant main effect of anterior-posterior electrode position ($F_{2,20} = 42.68$, $p < 0.001$; $\eta^2_p = 0.68$) revealed that, for both reaching conditions, the mean amplitude were progressively larger from parietal to frontal areas (all $p < 0.009$), whereas it did not differ between frontal and fronto-central sites. As for the m-N400, a significant main effect of left-right electrode position ($F_{2,20} = 37.03$, $p < 0.001$; $\eta^2_p = 0.65$) showed that mean ERP amplitude within the 400-800 time-window was maximal at midline compared to both left and right sites ($p < 0.001$). The post-hoc analysis of the anterior-posterior × left-right electrode position interaction ($F_{4,18} = 27.67$, $p < 0.001$; $\eta^2_p = 0.59$) revealed that for the both reaching conditions such sustained negativity at right sites was progressively larger from parietal to frontal sites, whereas at left sites no differences were found between frontal and fronto-central sites, and at midline electrodes no differences were found between frontal, fronto-central and central sites. This result reflects an equal distribution of such component at Fz, FCz and Cz electrodes. The maximum mean values of this sustained activity were found at FCz (Small object: MAmpl= -7.58 ± 2.78 μV; Large object: MAmpl= -5.85 ± 3.57 μV).

4.4. Correlations between kinematic and ERP measures

Mean amplitude and latency of P300 were averaged across P3, Pz and P4 electrodes; mean amplitude and latency of m-N400 was considered where such component was maximally expressed (i.e. at FCz). These values were correlated with reaction time, movement time, and the time of peak velocity (Figure 4.5., Panel A). A positive correlation was found between movement time and m-N400 latency for both the small and the large objects (Small object: $r = 0.59$, $p = 0.005$; Large object: $r = 0.45$, $p = 0.039$). Figure 4.5. Panel B

illustrates individual mean individual latency values of the m-N400 component and individual movement times for the two conditions.

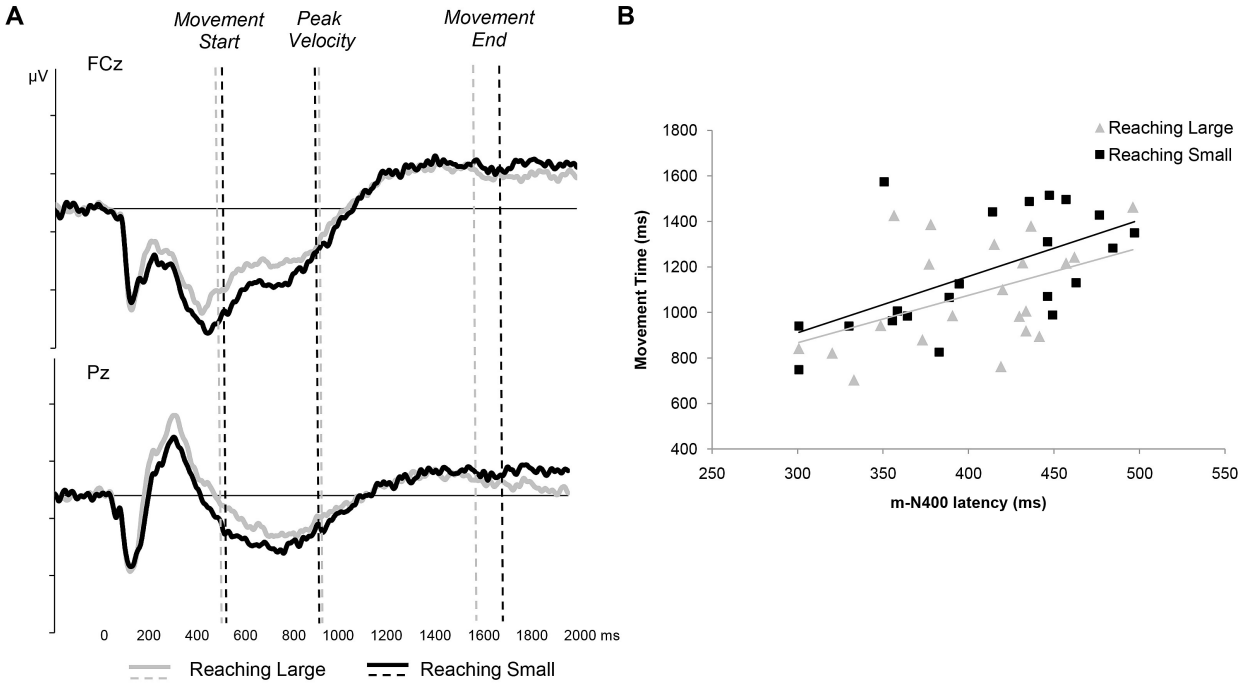

Figure 4.5. Panel (A) depicts the timeline of events (Movement Start, Peak Velocity, and Movement End) together with the ERP grand-average waveforms at representative sites (FCz and Pz). Panel (B) represents the correlation between individual movement time and individual m-N400 latency in Reaching Small and Reaching Large conditions.

4.5. Discussion

The aim of the present study was to investigate kinematics and ERP activity during reaching movements performed towards either a large or a small object. Differently from previous studies I did not investigate ERPs evoked by a cue anticipating specific object's intrinsic features, but by the target object itself. Such approach may allow to examine how information about an object's geometric properties is transformed into specific motor programs more directly. Overall the results indicate that object size determines a modulation in timing and amplitude of specific kinematic landmarks and ERP components during reaching movements. In particular, the novelty of the present study resides in the fact that 1) the modulation of parietal activity to object size

precedes the beginning of the movement and 2) fronto-parietal areas are modulated by object size although this property does not need to be integrated in the motor act.

Before I discuss how our results fit with previous studies, it is worth clarifying that previous experiments in humans have employed a variety of tasks to investigate the behavioural and the neural correlates of reaching. These tasks include reach-to-touch (Cavina-Pratesi et al., 2010; Levy et al., 2007; Pellijeff et al., 2006), pointing (Astafiev et al., 2003; Connolly et al., 2000, 2003; DeSouza et al., 2000; Fernandez-Ruiz et al., 2007; Hagler et al., 2007), and joystick manipulation (Grefkes et al., 2004). These tasks differ widely in the extent of arm movement, purpose and cortical recruitment (Culham et al., 2006; Culham & Valyear, 2006; Filimon et al., 2009). Furthermore, these tasks also differ in terms of initial hand posture, a factor which has the ability to influence the unfolding of reaching movements (Kritikos et al., 1998). Therefore, I cannot exclude that adopting a different task might have brought to different outcomes.

Consistent with previous reports, arm trajectories changed their shape when targets of different size were used, and that this effect was chiefly due to modifications in the deceleration phase (MacKenzie et al., 1987; Gentilucci et al., 1991; Castiello, 2001). Fitt's law (1954) was found to apply given that movement time increased as a function of task difficulty. Movement time was longer and maximum velocity was lower for smaller objects requiring a greater level of accuracy. Altogether these findings indicate that the size of the object had the ability to influence selectively the execution of a reaching movement. This is an important aspect of the present study because in order to ascertain the effects that such differential processing might have on ERPs, it is necessary to demonstrate that the participants' movement show differential kinematic signatures depending on reach conditions.

For an efficient reaching movement the brain must integrate information about the selected arm with information about the selected target. The general consensus is that this integrative action is accomplished through interactions between posterior parietal and premotor areas of the brain in

both monkeys (Kalaska et al., 1997; Wise et al., 1997; Caminiti et al., 1998) and humans (Grafton et al., 1996; Thoenissen et al., 2002; Astafiev et al., 2003; Connolly et al., 2003; Medendorp et al., 2003, 2005; Beurze et al., 2007; Culham et al., 2006; Gallivan et al., 2011; Bozzacchi et al., 2012; Konen et al., 2013). Our EEG recording corroborate these findings revealing that the planning and execution of reaching movements evolves across several cortical areas within the fronto-parietal network following a specific timing (Weinrich et al., 1984; Kalaska & Crammond, 1992; Glover et al., 2012).

Differences in amplitude between the small and the large object conditions become evident over parietal sites at around 300 ms (P300), during the planning phase of the movement. This activity reflects the involvement of parietal areas in the planning of reaching movements (Culham et al., 2006; Beurze et al. 2007, 2009; Gallivan et al., 2011; Konen et al., 2013). These areas include part of either the classic parietal reach region identified in the macaque (Andersen & Buneo, 2002; Bhattacharyya et al., 2009) and area V6A (e.g. Fattori et al., 2005; Bosco et al., 2010) or theirs putative human homologue, the superior parieto-occipital cortex (SPOC) region (Cavina-Pratesi et al., 2010; Connolly et al., 2003; Gallivan et al., 2009).

The P300 peak amplitude was higher for the large than for the small object condition. This finding might indicate the greater amount of visuo-spatial information to be extracted from larger objects, reflecting parietal activity that in both humans and macaques appears to serve a variety of visuomotor and attention-related functions. For instance, it might be concerned with the encoding 3D visual features of objects for action (Gallivan et al., 2011; Fattori et al., 2012) and the integration of both target and effector-specific information for movements (Beurze et al. 2009). In this respect, attention research indicates that the focus of attention can be modulated depending on the size of the area over which focal attention is allocated (Castiello & Umiltà, 1990, 1992). Furthermore, this finding is also in line with recent fMRI research showing that parietal areas, such as the AIP are involved in integrating information about 3D real objects, such

as the object size and the grasp-relevant dimension (Monaco et al., 2013). In addition, it agrees with neurophysiological findings showing that neurons in area V6A are influenced by spatial attention. The general suggestion is that this area, primarily involved in visuo-motor transformation for reaching, may form a neural basis for coupling attention to the preparation of reaching movements (Galletti et al., 2010). Overall, this particular finding might provide additional evidence for the integration of visuomotor and attention-related processes during movement planning (Baldauf & Deubel, 2010; Gallivan et al., 2011; Konen et al., 2013).

Altogether the results concerned with parietal activity fit with neurophysiological findings suggesting that areas of the dorsomedial pathway are sensitive to intrinsic features of target objects such as shape (Fattori et al., 2010, 2012).

In terms of frontal regions I found a negative electrical activity, peaking at around 400 ms following object appearance (m-N400), which was evident over central and frontal electrode sites. The spatio-temporal characteristics of the m-N400 might be assimilated to an index of motor planning and it is strongly influenced by motor variables. The polarity, the timing and the scalp distribution suggest that such component reflects motor planning and that it is linked to premotor activity (Shibasaki & Hallett, 2006).

In the frontal cortex of monkeys premotor dorsal (PMd) and premotor ventral (PMv) neurons are shown to be involved in different aspects of reaching movements (Calton et al. 2002; Hoshi & Tanji 2000, 2002, 2004a, b, c, 2006; Hoshi et al. 2005). Similarly, in humans electrophysiological (Naranjo et al. 2007), neuroimaging (Beurze et al., 2007; Grol et al., 2007; Glover et al. 2012) and neuropsychological (Heilman & Gonzalez Rothi, 1993) evidence indicate that premotor cortices are central to the process of reach planning. Our findings are in agreement with these views, by showing that premotor cortices are activated during reaching preparation. Importantly, the m-N400 peak had a later onset and a wider fronto-central distribution for the

small than for the large object. A result demonstrating that premotor activity during reach planning is not only concerned with reach direction or the integration of target location with information about the selected effector (Batista & Andersen 2010; Buneo et al., 2002; Calton et al., 2002; Hoshi & Tanji 2000, 2002, 2004a, b, c, 2006; Kertzman et al., 1997; Medendorp et al., 2005), but also with intrinsic features of objects.

A point worth noting is that the difference in amplitude for the small than the large objects remained significant up to 800 ms. This suggests that the size-dependent modulation of premotor activity noticed during reach planning spreads into the execution phase of the action, implying that before the action can begin, the motor programme has yet to be fully formulated and that kinematic planning might be fully fledged during the online control phase of the movement. In this respect our behavioural results might support this view. Whereas for reaction time there was a (non-significant) tendency to be longer for the small than the large object, the time to peak velocity occurred significantly earlier for the small than for the large object. This indicates that planning continues to be influential and optimized early in the movement. Such a gradual crossover between planning and control systems has the benefit of allowing for smooth rather than jerky corrections (Wolpert & Ghahramani, 2000; Glover, 2004). The differences between the small and the large object may reflect the need for additional sensory-motor control mechanisms for the more accurate condition (i.e., small object). In this respect, the present and previous psychophysical studies demonstrated that as object size decreased, subjects had longer movement times, slower speeds, and more asymmetrical hand-speed profiles (Berthier et al., 1996; Gentilucci et al., 1991).

Altogether the above mentioned findings suggest that both preparatory and execution activity along the frontoparietal circuit underlying reaching are modulated by object size. This result can be explained in terms of the intimate relationship between reaching and grasping components during prehension movements (Jeannerod, 1984). It is known that grasping in humans and

macaques activates parietal and premotor areas which overlap with reach-related activations (Tanné-Gariépy et al., 2002; Culham et al., 2003; Castiello, 2005; Davare et al., 2006; Fattori et al., 2009, 2010, 2012; Raos et al., 2004). Therefore it might be conceivable that the neural network which controls proximal movements in reaching-to-grasp has information about object size given that the two components should act in concert in order to determine the timing of hand preshaping during reaching. But why should the proximal neural channel be sensitive to object size during reaching alone given that the distal program remains unmodified for small and large objects? In our opinion, it would be difficult to conceive how the reaching channel could act without extracting information regarding object size. For the mere fact that it occupies space, an object must have a size, and locate it entails necessarily information about its dimension. In this respect, our findings might provide a novel demonstration that the reaching and grasping phases are represented by overlapping parietofrontal circuits, suggesting a lack of strict functional segregation between parietofrontal circuits for grasping and reaching in monkeys (e.g., Fattori et al., 2010) and humans (Filimon et al., 2009, 2010; Grol et al., 2007).

As a final issue, I found that for both the large and the small objects the individual mean latency for the premotor m-N400 component significantly correlated with the individual mean for movement time. According to behavioural evidence, reaching movements are characterized by a ballistic and a feedback-based phase. The ballistic phase is a product of a feedforward system that defines the initial state of the limb and the goal. The feedback phase is used at the end of this movement to achieve and accurate contact with the object. An alternative possibility is that the second phase is controlled, as it is the first one, by a feedforward system which takes into account the object size and accordingly sets its duration. This might indicate that an estimate of movement time, possibly performed at the level of premotor areas, might serve to plan the amount of on-line control required during the final part of the movement.

4.6. Conclusion

The present study demonstrates that the use of converging techniques with different characteristics might allow to better understand how the human brain controls the reaching function. In particular, it presents the timing of activation of the cortical regions engaged for the planning and execution of a human reach, starting from the early coding of the intrinsic features of the object to the motor plan that leads to the actualization of the movements. Although these findings confirm previous evidence concerned with reach planning and execution in general, they add to previous literature demonstrating that in humans the neural network underlying reaching movements is modulated by object size.

5. SIMULTANEOUS RECORDING OF EEG AND FMRI SIGNALS DURING REACH TO GRASP MOVEMENT[3]

The overarching aim of the experimental work presented in this chapter was ambitious. That is, to co-register EEG and fMRI signals in order to identify spatial and temporal characteristics of both the dorsolateral circuit (AIP-PMv), traditionally considered to be involved in grasping, and the dorsomedial circuit (SPL-PMd), the putative reaching circuit, to be involved in grasping in humans (Grol et al., 2007; Filimon, 2010; Gallivan et al., 2011a; Konen et al., 2013). Furthermore I was interested in understanding how these circuits were modulated by the intrinsic features of objects. In particular, via the 'size' manipulation, I wanted to shed further light on whether reaching and grasping were represented by overlapping parieto-frontal circuits or whether these circuits were functionally segregated. Although the distinction between cortical regions involved in the grasping and reaching discussed in the ensuing pages might serve to delineate the dorsolateral and dorsomedial networks, because of the limited time and a variety of technical problems concerned with co-registration techniques I am not in the position to present the results concerned with co-registration, conjunction and multivoxel pattern analyses (MVPA) which would have helped to clarify the issues at stake in my thesis. This work, however, is in progress and I am striving to identify and apply the most appropriate analysis procedures to finalize my experimentation.

3 Begliomini, C., De Sanctis T., Marangon, M., Tarantino, V., Sartori, L., Diego Miotto, D., Motta, R., Stramare, R., Castiello, U. (2013). The neural circuits underlying reaching and grasping movements: from planning to execution. *Frontiers in Human Neuroscience, under review.*

5.1. Introduction

Prehension requires the integration of visual and somatosensory information into a coordinated motor plan for transporting the arm to a target while shaping the hand to match the target geometry. The different components of the behavior are well timed so that finger enclosure occurs at the proper moment (Jeannerod, 1984). Kinematic studies have established the close interrelationship of transport and hand shaping (Gentilluci et al., 1991; Jakobson & Goodale, 1992; Chieffi & Gentilucci, 1993; Smeets & Brenner, 1998).

In neural terms, a prominent hypothesis is that these two components are controlled by independent frontoparietal systems, a dorsomedial network for reaching and a dorsolateral network for grasping (Jeannerod 1988; Jeannerod et al., 1995). Consistent with this hypothesis, neurophysiological studies in macaque monkeys have revealed a dorsolateral circuit, connecting AIP to the rostral part of PMv (area F5), and a dorsomedial circuit consisting of the medial posterior parietal area V6A (Fattori et al., 2001, 2005), the PRR (Andersen & Buneo, 2002; Buneo et al., 2002; Connolly et al., 2003) and the PMd (area F2; Hoshi & Tanji, 2004 b). Human neuroimaging studies go in the same direction (for review see Filimon, 2010). They showed the involvement of the anterior portion of the human AIP in grasping behavior and they proposed human homologues of both the ventral and dorsal premotor cortices during grasping (Grol, et al., 2007). Whereas, reaching activates the medial intraparietal and the superior parieto-occipital cortex (Konen et al., 2013).

Recent neurophysiological and neuroimaging evidence has questioned such dichotomic view suggesting that the dorsolateral and dorsomedial networks are not simply independent networks for reaching and grasping. For example, reaching-related neurons in macaque area V6A (Fattori et al., 2001; Galletti et al., 1999) are sensitive not only to the direction of a reach (Fattori et al., 2004) but also to the orientation of a target (Fattori et al., 2009), the hand shape necessary to grasp different targets (Fattori et al., 2010), and the target shapes themselves (Fattori et al.,

2012). The proposal is that the relative contributions of the dorsomedial and dorsolateral networks during prehension may reflect different requirements of specific movements in terms of planning (Glover et al., 2012; Konen et al., 2013), online control (Grol et al., 2007; Glover et al., 2012), or the integration of perceptual information (Verhagen et al., 2008).

The question of where reach and grasp are controlled in humans motivated the following experiment. Images of blood level oxygen dependent (BOLD) and ERPs were acquired to define activity during visually guided movements of the right arm. The tasks were designed to examine three issues: (1) to localize movement related activity during reach and grasp or reach towards different sized objects; (2) to identify differences of BOLD and ERPs responses during reaching with grasp and reaching; such a difference might identify overlapping areas that are recruited for these two movements; and (3) to perform the simultaneous recording of blood flow and EEG responses in cerebral cortex as to better understand the time course descriptions of hemodynamic activity during reaching and reach to grasp.

5.2. Material and methods

5.2.1. Participants

Twenty three volunteers (9 men, 14 women, range 20-31 years old, SD 2.71) participated in the study. All participants fulfilled the inclusion criteria suggested by the Italian Society of Medical Radiology (appendix VIa), none had a history of neurological, major medical, or psychiatric disorders. They were all right-handed according to the Edinburgh Handedness Inventory (Oldfield, 1971, appendix VIb). Experimental procedures and scanning protocols were approved by the University of Padua Ethics Committee and conducted in accordance with the Declaration of Helsinki (Sixth revision, 2008). All participants gave their informed written consent (appendix VIc) to participate in the study.

None of the participants experienced discomfort during simultaneous EEG-fMRI acquisition.

5.2.2 Apparatus and procedures

Experimental stimuli were administered by means of a motorized circular rotating table (ABRAM; http://www.ab-acus.com/products.html, Figure 5.1.), for the presentation of 3D stimuli in MRI environment. Experimental stimuli consisted of two wooden spheres of different dimensions (a small wooden sphere of 3 cm diameter and a large wooden sphere of 7 cm diameter).

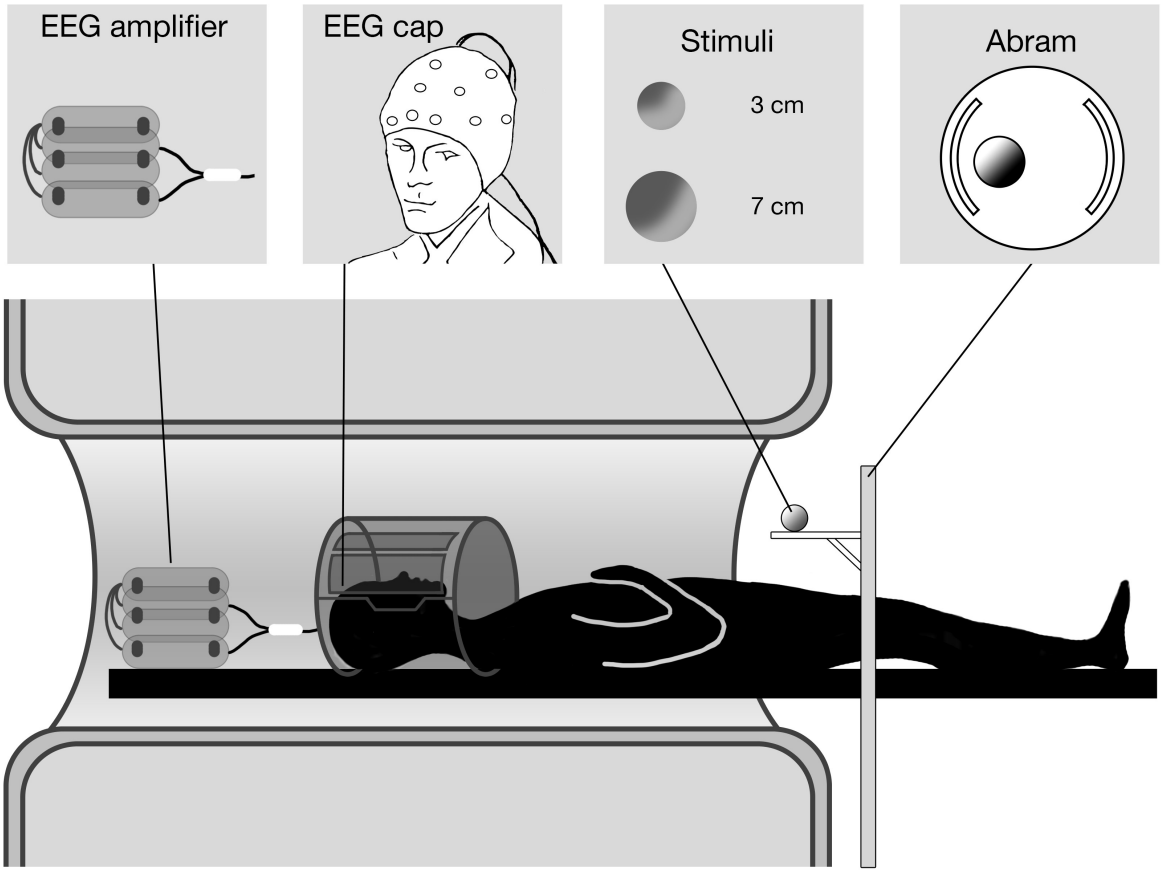

Figure 5.1. Experimental setup: BrainAmp MR Plus electroencephalography recording system and ABRAM stimulus administrator.

Participants were requested to perform two different kinds of movement: (i) reach the stimulus and grasp it; (ii) reach the stimulus with the hand in a fist posture (see methods section in Chapter 4). All participants naturally adopted a PG to grasp the small stimulus and a WHG to grasp the large stimulus. During movement execution, participants were requested to maintain the eyes on the stimulus. To facilitate direct viewing of the stimulus the head was tilted (10-15°) by means of foam cushions. Given that participants performed the actions with the right hand, another MRI compatible cushion was placed under the upper right arm, in order to minimize discomfort during the movement.

Trial structure was the following: (i) a sound delivered through MR-compatible headphones indicated the type of movement to perform. A single tone indicated a reach to grasp movement (duration 300 ms; frequency 1600 Hz). A double pulse tone indicated a reaching only movement (each pulse lasted 70 ms with a frequency of 400 Hz). The interval between the two pulses was of 60 ms (the total duration of the tone was 200 ms); (ii) following a 2 s delay a 'go' signal was presented (i.e., whistle; duration 200 ms; frequency 440 Hz). Participants were requested to wait for the 'go' signal to begin the movement indicated by the acoustic cue previously presented. Participants were trained as to familiarize with the acoustic instructions during a training session before scanning. They were requested to perform the movement at a natural speed and to avoid blinking during the presentation of the acoustic signals announcing the type of movement to perform.

5.2.3. Experimental Design

The entire experiment consisted of 4 runs of 45 trials each. Stimulus size (small, large) was randomized across runs and movement type (grasping, reaching) was randomized within runs. Therefore the design (factorial 2x2) included 4 experimental conditions: reach to

grasp towards a small stimulus (GS), reach to grasp towards a large stimulus (GL), reaching only towards a small stimulus (RS), reaching only towards a large stimulus (RL). The 4 experimental conditions were administered in 4 experimental runs: since stimulus size was randomized across runs, for each run 2 movements had to be performed, either grasping or reaching (see Figure 5.2.). A mixed design was adopted, grouping trials belonging to the same type (grasping or reaching) in short sequences, ranging from x to y trials of the same type, in order to minimize task predictability and avoid frequent changes in task request, which may result in task-switching related activity. Variable Inter Stimulus Interval (ISI) was considered, including durations from 3 to 6 seconds according to a long exponential probability distribution (Dale, 1999; Hagberg et al., 2001). ISI duration was independently randomized within each experimental run. Considering the complexity of the experimental procedures, scanning run duration was minimized and short breaks between runs were planned, in order to avoid participants' fatigue.

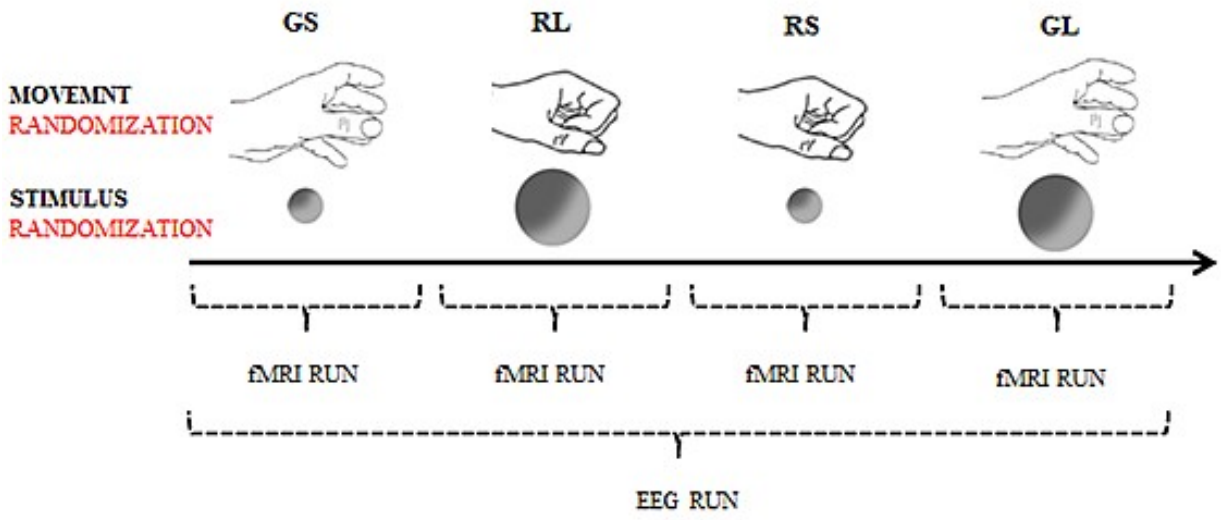

Figure 5.2. Schematic representation of the experimental design.

5.3. Recording and data processing

5.3.1. EEG Data Acquisition

The EEG was acquired by means of a 32-channels MR compatible system (BrainAmp MR Plus, Brain Products GmbH, Munich, Germany) equipped with a MR compatible cap system (BrainCap MR, Brain Products GmbH, Munich, Germany), according to the 10–20 International System (AEEGS, 1991). Thirty-three EEG electrodes were placed on the scalp, including the reference electrode positioned at FCz and the ground electrode placed at position AFz. Moreover one external electrode was applied to the subjects back in order to acquire the electrocardiogram (ECG) reading. The resolution and dynamic range of the EEG acquisition system were 100 nV and 3.2 mV, respectively. Impedance of all electrodes was kept below 5kΩ. The montage included the following scalp positions: Fp1,Fpz, Fp2, F7, F3, Fz, F4, F8, FC3, FCz, FC4, T3, C3, Cz, C4, FT7, FT8, T3, T8, T5, CP3, CPz, CP4, P3, Pz, P4, T6, TP7,TP8, O1, O2. The ground electrode was placed in CPz. The EEG signal were digitized at a sampling rate of 250 Hz (16 bit AD converter), and high-pass filtered at 0.15 Hz. Data were recorded on a laptop computer through Brain Recorder v1.04 software (Brain Products, Munich, Germany) at a sampling rate of 5 kHz with a band-pass filter of 0.016 to 250 Hz. Event timings and reaction times were calculated off-line using event timings acquired by Brain Recorder v1.04 software (BrainProducts) at this higher frequency sampling.

5.3.2 fMRI Data Acquisition

The experiment was carried out on a whole body 1.5 T scanner (Siemens Avanto) equipped with a standard Siemens 8 channels coil. Functional images were acquired with a gradient-echo, echo-planar (EPI) T2*-weighted sequence in order to measure blood oxygenation level-dependent (BOLD) contrast throughout the whole brain (37 contiguous axial slices

acquired with descending interleaved sequence, 56×64 voxels, 3.5×3.5×4.0 mm resolution, FOV=196×224 mm, flip angle= 90°, TE=49 ms). Volumes were acquired continuously for each run with a repetition time (TR) of 3 s; 102 volumes were collected in each single scanning run, resulting in functional runs of 5 minutes and 25 seconds duration (21 minutes and 40 seconds of acquisition time in all). High-resolution T1-weighted image were acquired for each subject (3D MP-RAGE, 176 axial slices, no interslice gap, data matrix 256×256, 1 mm isotropic voxels, TR=1900 ms, TE=2.91 ms, flip angle=15°).

5.4. Data Analysis

5.4.1. EEG Data Preprocessing

EEG data were preprocessed using Brain Vision Analyser software, version 2.01 (BrainProducts, Munich, Germany). Before preprocessing, the first TTL pulse of each EPI session was removed as it occurred at a different point in the gradient artifact template. After this, gradient correction was applied using the average artifact subtraction (AAS) method (Allen et al., 2000). Templates of the artifact for each channel were created with a sliding average of 21 volumes. Data were then downsampled to 250 Hz and filtered by a low-pass 30-Hz cut-off, using Infinite Impulse Response module. R-peaks were then detected in the electrocardiogram channel and removed using the average artifact subtraction method (Allen et al., 1998). A semiautomatic procedure was used in order to identify R peaks (40 Hz) correlation factor of 0.7 with the R-peak template was used; all R-peaks were individually checked. A high-pass filter of 0.02 Hz and a notch filter of 50 Hz were further applied to continuous EEG signal. The data were then transferred to EEGLAB software (Delorme & Makeig, 2004) for further analyses. The residual ballistocardiogram (BCG) artifacts were removed by optimal basis set algorithm implemented in the FMRIB 1.2 toolbox (Niazy et al., 2005). This algorithm performs a principal component analysis

(PCA) on EEG data based on the R-peaks. The first three PCs were selected and subtracted from the data. BCG residuals and eye movement, were further removed using independent component analysis (ICA) (Debener et al., 2007; Jung et al., 2000). The ICA was applied to segmented signal. Specifically, epochs were extracted locked to the cue sound, from -500 ms to 2500 ms. Artifact-related components were carefully selected by visual inspection, and excluded in the ICA back-projection procedure. A final visual inspection of single trials was performed before the averaging procedure, in order to reject significant EEG deflection (mainly exceeding 100 μV). A total of 18 participants were considered for statistical analyses.

Epochs were extracted separately for each of the two type of object stimuli (small, large) and two type of movement (reach to grasp, reaching only) time-locked at cue signal, go signal and execution time.

5.4.2. fMRI Data Preprocessing

Data preprocessing and analysis were performed using SPM8 (Statistical Parametric Mapping, Wellcome Institute of Cognitive Neurology, London, UK) implemented in MATLAB 7.5.0 environment (MathWorks, Natick, MA, USA). For each participant, the first two volumes of each fMRI run were discarded because of the non-equilibrium state of the magnetization in order to allow for stabilization. ArtRepair toolbox (ArtRepair software Package, for SPM, http://www.fil.ion.ucl.ac.uk/spm/ext/#ArtRepair) was adopted in order to correct for possible images corruption due to signal spikes induced by head motion. Motion correction was carried out by realigning and unwarping data. Structural images were segmented in all their components (white matter, gray matter and cerebrospinal fluid) and subsequently gray matter was co-registered with all the functional images. Structural and functional images were then normalized adopting the template provided by the

Montréal Neurological Institute (MNI) implemented in SPM8. Finally, functional images were spatially smoothed using a 7 × 7 × 8-mm full-width-at half-maximum (FWHM) Gaussian Kernel. At the end Artrepair toolbox was applied in order to identify and correct large scan-to-scan head motion, which may result in large global intensity changes.

5.4.3. EEG Data Analysis

Based on visual inspection of grand average waveforms and amplitude scalp maps, the following time-windows were separately compared between the two object size conditions: 700-1350 ms, 1350-2000 ms. Mean amplitude was calculated in such time windows and compared between object size and electrode position. In order to examine the topographical distribution of ERPs in these time windows, a 3 × 3 electrode array was considered into an ANOVA model (F3, Fz, F4, C3, Cz, C4, P3, Pz, P4). In summary, a 2 × 3 × 3 ANOVA was performed, which include the following factors: object size (small, large), anterior-posterior electrode position (frontal, central and parietal sites) and the left-right electrode position. Difference related to object size emerged in the second time window (1350-2000 ms).

5.4.4. fMRI Data Analysis

Data analysis was conducted by adopting a Finite Impulse Response (FIR) model (Henson, 2003), in order to fit the measured BOLD response and enhance task features.

A post-stimulus time window of 10 seconds length was considered, starting from cue onset, and divided into 10 time bins of 1 second each. Time bin width was lower than the TR used during data acquisition (3 seconds) because I attempted to specifically target a stimulus time interval. In addition, it has also been shown that it is possible to sample the

impulse response at post-stimulus intervals shorter than TR by jittering event onsets with respect to scan onsets (Josephs et al., 1997; Schilbach et al., 2008). In this study inter stimulus interval varied from 3 to 6 seconds and had a jittered distribution.

Image analyses were carried out after high-pass filtering (154 seconds) to remove subject-specific, low-frequency signal drifts and global intensity scaling. Following the estimation of a GLM for each single participant, effects for each experimental condition were tested by applying appropriate linear contrasts to the parameter estimates for each single participant, resulting in a t-statistic for each voxel (SPM_t). Images for each experimental regressor/condition (4 conditions x 10 time bins; 40 in all) were entered in a second level random effect analysis (RFX) allowing for inference to the general population, with time bin (1 to 10) and type of movement (grasping small, GS; grasping large, GL; reaching small, RS; reaching large, RL) as factors. Violations of data sphericity were accounted for by modeling non-dependence across levels for the variable type of movement (GS, GL, RS, RL), and dependence across levels for the variable time bin. Unequal variance was assumed for both stimulus size and time bin (1 to 10).

5.5. Results

5.5.1. EEG Data

The Figures (Figure 5.3., Figure 5.4.) depicts grand-average waveforms locked to the time at which the CUE signal was delivered to participant, in the two object conditions. ERPs were characterized by (1) an early complex (N1-P1-N2), related to the sound and more evident in Cz; (2) a slow negative component (CNV), evident at fronto-central sites. The amplitude of the N1-P1-N2 complex varied according to the sound intensity; namely it was higher for the higher frequency sound (i.e., the grasping small cue signal) and lower for the

lower frequency sound (i.e., the grasping large signal). Then, the ERP signal shows a sustained negative variation (CNV) which appears larger for the small object condition, regardless movement type, and lasts until the GO signal sound (at 2000 ms after the CUE onset). This component was related to motor requirements and was considered for statistical analyses.

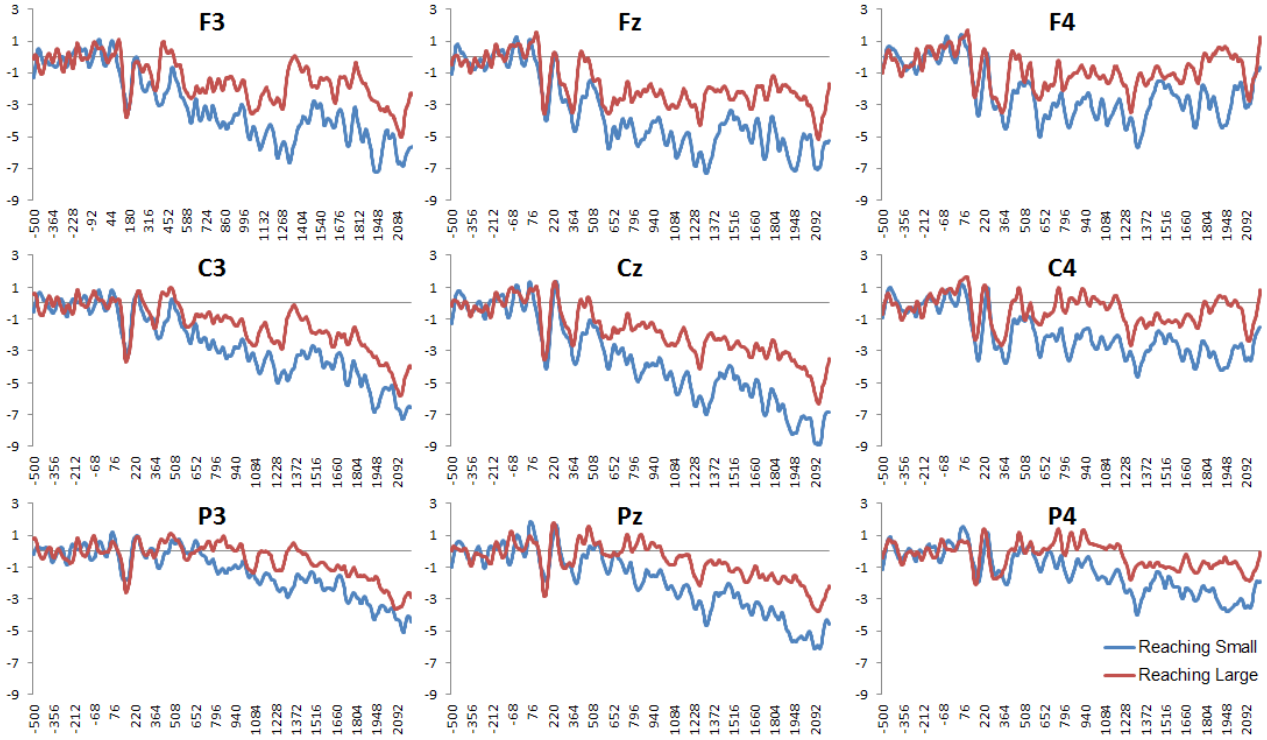

Figure 5.3. The plot depicts grand-average ERP waveforms locked to the time between the cue and go sounds, for RS and RL conditions.

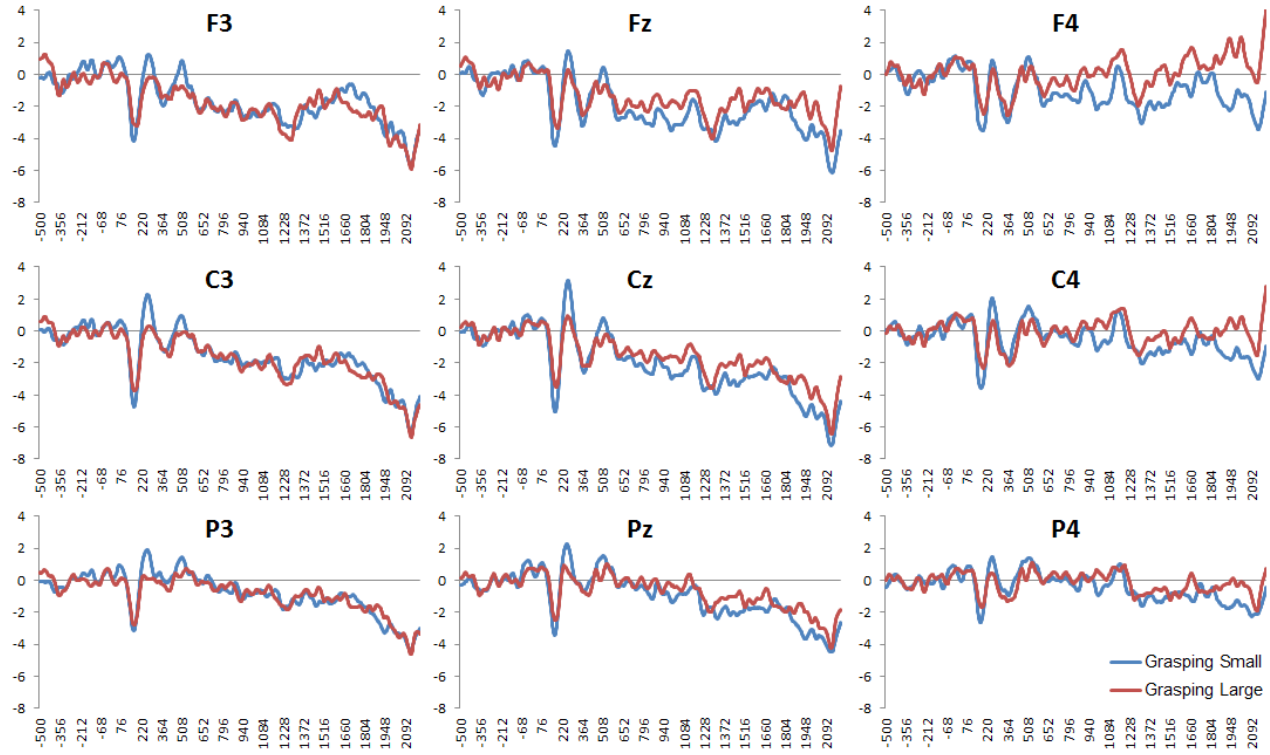

Figure 5.4. The plot depicts grand-average ERP waveforms locked to the time between the cue and go sounds, for GS and GL conditions.

Reaching

Similarly for the grasping condition, in the reaching condition a CNV developed after the processing of the signal to prepare the movement (cue sound) until the signal to start the movement (go signal). As shown in Figure 5.5, the CNV was expressed at fronto-central electrode position, mainly in the left sites, and overall was larger for the reaching small compared to the reaching large condition.

Reaching (700-1350 ms): The ANOVA revealed a main effect of the object size emerged ($F_{1,17} = 10.38$, $p = 0.005$). Furthermore, a main effect of anterior-posterior ($F_{2,16} = 14.32$, $p < 0.001$) and left-right ($F_{2,16} = 13.01$, $p < 0.001$) electrode position was found.

Reaching (1350-2000 ms):A significant main effect of object size emerged in this time windows, namely the CNV reached more negative values for the small compared to the large object size ($F_{1,17} = 9.94$, $p = 0.006$). From a topographical point of view, the CNV showed maximal values in central ($F_{2,16} = 3.70$, $p = 0.36$) and midline ($F_{2,16} = 15.28$, $p < 0.001$) electrode sites (Figure 5.5.).

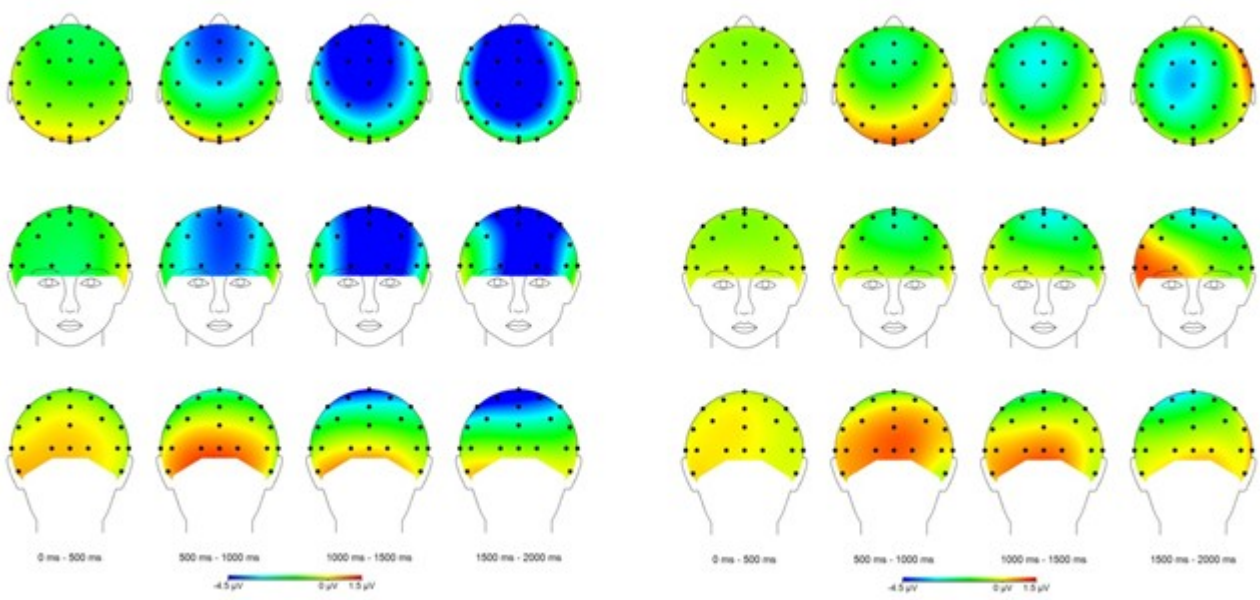

Figure 5.5. The scalp maps represent the topographical distribution of ERP amplitude in the RS (left panel) and RL (right panel) conditions.

Grasping

*Grasping (700-1350 ms):*As shown in Figure 5.6. the CNV is expressed at fronto-central electrode position, mainly in the left sites, in both object size conditions. The ANOVA revealed main effects of electrode position, both along the anterior-posterior ($F_{1,17} = 10.71$, $p < 0.001$) and left-right axis ($F_{2,16} = 12.29$, $p < 0.001$). The post-hoc analysis confirms that the CNV was larger at frontal and central sites compared to parietal sites (all ps < .004), and at left and midline sites compared to right sites (all ps < .004). The differences in CNV amplitude between the two object size conditions did not result statistically significantly.

Grasping (1350-2000 ms) :The ANOVA yielded a main effect of the left- right electrode position ($F_{2,16} = 12.85$, $p < 0.001$), and significant object size × left- right electrode position ($F_{2,16} = 3.86$, $p = 0.032$), anterior-posterior × left- right electrode position ($F_{4,14} = 6.06$, $p < 0.001$), and object size × left-right electrode position × left- right electrode position ($F_{4,14} = 4.06$, $p = 0.005$). The post-hoc analysis showed that generally the CNV was higher (more negative) in frontal and central sites compared to parietal sites. The three-way interaction revealed that the CNV in the grasping small condition has a broader distribution, which include right sites, compared to the grasping large condition. Indeed, the CNV was higher in the small compared to the large object condition in right frontal site (F4, p= 0.039). This effect reflects the broader topographical distribution of the CNV in frontal sites in the planning phase of the grasping movement of a small object (Figure 5.6.).

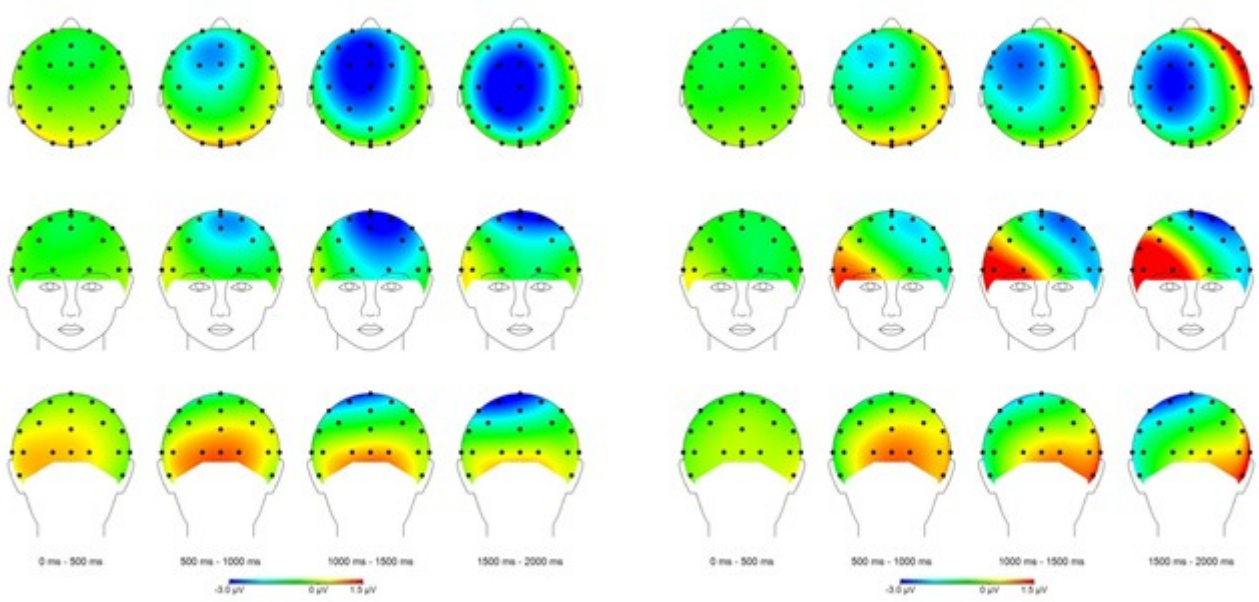

Figure 5.6. The scalp maps represent the topographical distribution of ERP amplitude in the GS (left panel) and GL (right panel) conditions.

In summary, in the grasping condition ERPs showed differences related to object size in the sustained negative component during the second part of the planning phase; in the reaching condition differences related to object size emerged in the negative component during the all durations of the planning phase (starting at around 700 ms after the cue sound until the go signal). Overall, grasp to reach and reaching movements toward a small object elicited a higher CNV amplitude compared to grasp to reach and reaching movements toward a large object. In both conditions, the CNV first was localized in midline fronto-central sites, then it shifted toward the left sites. This passage is compatible with a passage of the electrical signal from premotor to motor cortices.

5.5.2. fMRI Data

The aim of the study was a complete monitoring of all action stages, spanning from planning to execution. In order to identify the contribution of specific brain areas in these processes and their temporal evolution, I considered a time window of 10 seconds duration,

divided in 10 time bins of 1 second each. For each of these time bins, I focused on differences of activation patterns observed between reaching only (RS, RL) and reach to grasp (GS, GL) conditions. In order to clearly localize the neural substrates underlining the proposed reach to grasp or reaching only tasks, analysis was conducted by adopting a searching mask built by several regions of interest, on the basis of available literature (for review see Castiello & Begliomini, 2008), suggesting a primary distinction between planning and execution-related areas. According to this distinction, the dorsolateral region of the prefrontal cortex (Rizzzolatti & Luppino, 2001) and the anterior cingulate area (Matelli et al., 1991) would be mainly involved in movement planning, while the primary motor (Glover, 2005; Tunik et al., 2005; Rice et al., 2006) and premotor cortices (Culham et al., 2003; Frey et al., 2005; Begliomini et al., 2007b), as well as the parietal cortex (Binkofski et al., 1998; Culham et al., 2006; Begliomini et al., 2007a) would play a substantial role in action execution. The toolbox WFU PickAtlas (Wake Forest University, www.ansir.wfubmc.edu) was adopted to build the mask involving all the mentioned areas.

For consistency with previous experimental chapters, analysis for reaching and grasping have been performed separately and will be therefore presented in different sections

Reaching

In order to capture differences of activation patterns associated with the two reaching conditions (RS; RL) for each single time point, planned contrasts (t-tests, one-tailed) were performed within each single bin (Table 5.1.). Results were FDR corrected for multiple comparisons ($k \geq 10$).

T-tests did not reveal any significant difference between RS and RL for the considered areas in time bins 1 to 3.

Time bin 4: in *time bin 4* RL was associated with a significantly stronger activity than RS within the right inferior parietal lobule (IPL) (BA 40) and the right angular gyrus (AG, BA 39). The same pattern was evident in the left superior frontal gyrus (SFG, BA 10) and in the right Cuneus (Cu, BA 7) and Precuneus (PreCu, BA 31).

The opposite pattern (RS > RL) did not reveal any significant effect.

Time bin 5: In *time bin 5* the right SFG (BA 6) revealed significantly stronger activity for RL in respect to RS. The opposite contrast (RS > RL) underlined significant differences within the left Precentral Frontal Gyri (PFG) and Middle Frontal Gyri (MFG) (BA 4 and 6), as well as the left SMA (BA 32).

Time bin 6: *in time bin 6* the contrast RL > RS revealed significant differences within the right SFG (encompassing BA 9 and 10) and Middle (BA 8) Gyri, as well as the right SMA (BA 32). In addition also the right AG (BA 39) and Precuneus (BA 31) resulted as significantly more activated by RL rather than RS. Concerning the left hemisphere, significant effects for the contrast RL>RS were circumscribed to several regions of the frontal lobe, namely the Superior (BA 9), MeFG (BA 10) and MFG (BA 9). The opposite comparison, RS>RL, revealed significant activity only within the left Precentral (PreCg, BA 4) and MFG (BA 6).

Tine bin 7: *in time bin 7*, the contrast RL > RS did not reveal any significant result. The contrast RS > RL was associated with significant increase of activity within s the MFG (BA 6) and the PreCg (BA 4).

No significant results were observed for time bins 8 to 10 (see Figure 5.7.).

Table 5.1. List of significant activations associated with the contrast RL > RS and RS > RL for each single time bin. Results are obtained by means of the random-effects analysis performed on 18 participants included in the study and are circumscribed to the anatomical mask built on the basis of Castiello and Begliomini (2008). Coordinates are in MNI space. *p* values are corrected for multiple comparisons (FDR .05). BA: Brodmann area; *k* = number of the activated voxels (cluster size: ≥ 10)

Region	BA	H	k	MNI Coordinates			t	p	effect
				x	y	z			
TIME BIN 4									
Inferior Parietal Lobule	**40**	**Right**	32	**55**	**-60**	**38**	**5.03**	**.001**	**RL > RS**
Angular gyrus	39	Right		48	-70	30	4.11	.006	RL > RS
Superior Frontal Gyrus	**10**	**Left**	12	**-8**	**56**	**2**	**4.39**	**.003**	**RL > RS**
Cuneus	**7**	**Right**	12	**6**	**-77**	**30**	**3.89**	**.008**	**RL > RS**
Precuneus	**31**	**Right**		**6**	**-70**	**26**	**3.60**	**.015**	RL > RS
TIME BIN 5									
Superior Frontal Gyrus	**6**	**Right**	10	**6**	**25**	**62**	**4.21**	**.023**	**RL > RS**
Middle Frontal Gyrus	**6**	**Left**	**34**	**-26**	**-11**	**58**	**6.26**	**.000**	**RS > RL**
Precentral Gyrus	6	Left		-40	-7	50	4.05	.005	RS > RL
Supplementary Motor Area	**32**	**Left**	**10**	**-8**	**-4**	**50**	**4.06**	**.005**	**RS > RL**
TIME BIN 6									
Superior Frontal Gyrus	**9**	**Right**	**20**	**6**	**56**	**30**	**4.97**	**.001**	**RL > RS**
Medial Frontal Gyrus	**10**	**Left**	**47**	**-8**	**53**	**5**	**4.76**	**.001**	**RL > RS**
Superior Frontal Gyrus	10	Left		-33	56	2	3.52	.012	RL > RS
Middle Frontal Gyrus	**9**	**Left**	**34**	**-29**	**35**	**42**	**4.62**	**.002**	**RL > RS**
Superior Frontal Gyrus	9	Left		-22	46	38	4.18	.003	RL > RS
Supplementary Motor Area	**32**	**Right**	**21**	**3**	**46**	**2**	**4.49**	**.002**	**RL > RS**
Superior Frontal Gyrus	10	Right		6	63	2	3.52	.012	RL > RS
Angular Gyrus	**39**	**Right**	**19**	**55**	**-60**	**34**	**4.34**	**.002**	**RL > RS**
Superior Frontal Gyrus	**8**	**Right**	**22**	**17**	**28**	**54**	**3.99**	**.005**	**RL > RS**
Middle Frontal Gyrus	8	Right		20	28	46	3.77	.007	RL > RS
Precuneus	**31**	**Right**	**18**	**3**	**-63**	**22**	**3.50**	**.013**	**RL > RS**
Precentral Gyrus	**4**	**Left**	**25**	**-36**	**-25**	**62**	**4.76**	**.002**	**RS > RL**
Middle Frontal Gyrus	6	Left		-33	-4	62	4.67	.002	RS > RL
TIME BIN 7									
Middle Frontal Gyrus	**6**	**Left**	**55**	**-33**	**-4**	**62**	**5.00**	**.001**	**RS > RL**
Precentral Gyrus	4	Left		-36	-25	62	4.87	.001	RS > RL
Middle Frontal Gyrus	6	Left		-26	-14	66	4.44	.002	RS > RL

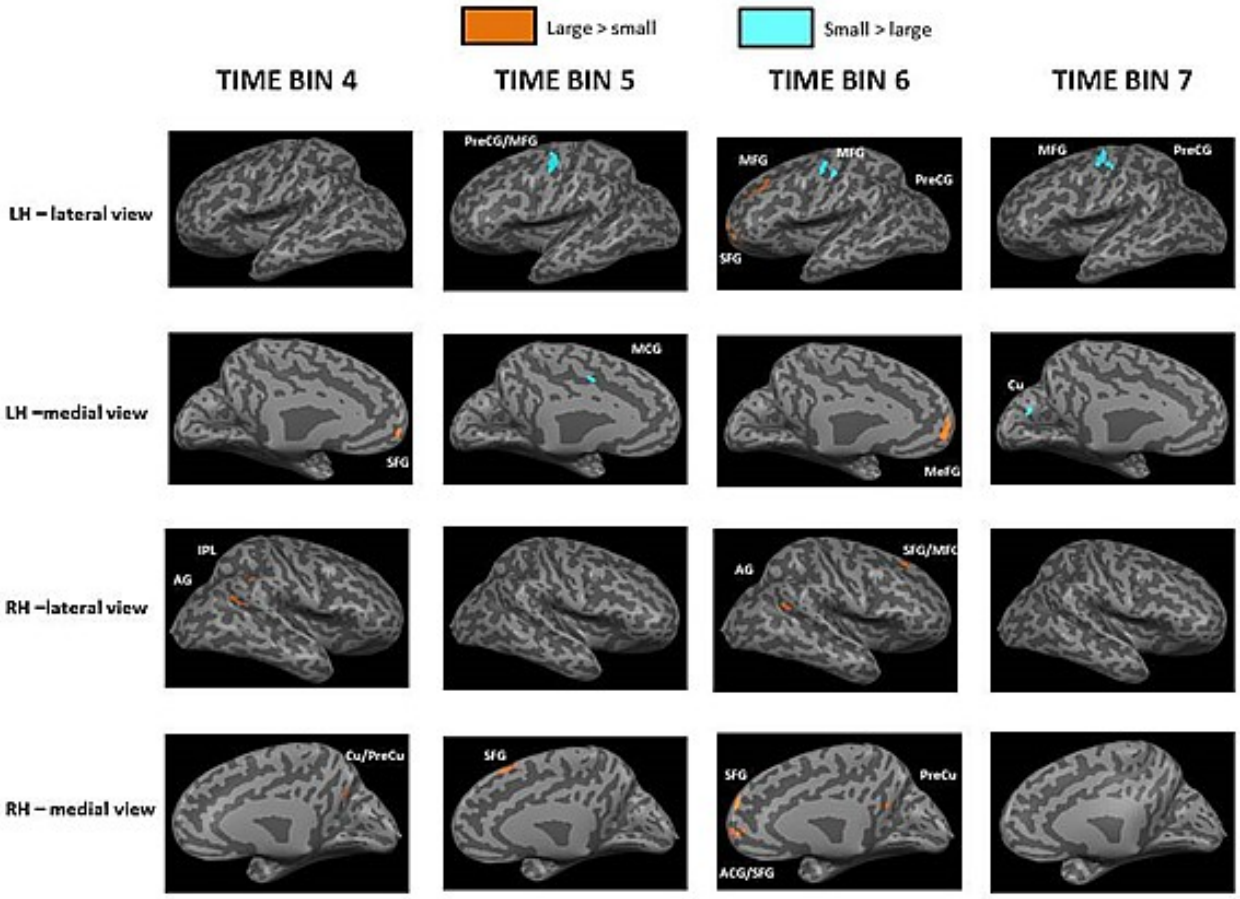

Figure 5.7. Localization of brain activations detected in both hemisphere for the contrasts RL > RS and RS > RL for each single time bin. Only time bins with significant results are reported. Results are obtained by means of the random-effects analysis performed on 18 participants included in the study and are circumscribed to the anatomical mask built on the basis of Castiello and Begliomini (2008). Statistical parametric maps (*t* statistics - $p<.05$ FDR-corrected) are imported in the software package Brain Voyager QX by means of the Matlab toolbox NeuroElf(http://neuroelf.net/). The resulting .vmp images have been transformed into Talairach space and the overlaid on a mesh template provided by Brain Voyager QX. The mesh has been inflated in order to better visualize sulci activations. Activations are reported in Table 5.1. Both medial and lateral views of both hemispheres are shown. Results are reported in Table 5.1. (LH: left hemisphere; RH: right hemisphere; SMA: Supplementary Motor Area; AG: Angular Gyrus; Cu: Cuneus; IPL: Inferior Parietal Lobule; MeFG: Medial Frontal Gyrus; MFG: Middle Frontal Gyrus; PreCg: Precentral Gyrus; PreCu: Precuneus; SFG: Superior Frontal Gyrus)

Grasping

Concerning grasping, data analysis followed the same approach as the one adopted for reaching (Table 5.2.). T-tests did not reveal any significant result for time bins 1 to 5.

Time bin 6: in *time bin 6,* the contrast GL>GS did not reveal any significant effects. The opposite comparison, GS>GL, led to significant effects confined to the left hemisphere, within the MFG (BA 6), the IPL and the Supramarginal Gyrus (SMG, BA 40). Furthermore, GS was associated to a significantly stronger activity in respect to GL also in the left SMA (BA 32).

Time bin 7: *in time bin 7*, the contrast GL>GS did not reveal any significant effects. The opposite comparison, GS > GL, underlined significant differences in several regions of the left, hemisphere, precisely the MFG (BA 6), the PreCg (BA 4 and 6) and the IPL (BA 40).

No differences in activity for time bins 8 to 10 were noticed (see Figure 5.8.).

Table 5.2. List of significant activations associated with the contrast GL > GS and GS > GL for each single time bin. Results are obtained by means of the random-effects analysis performed on 18 participants included in the study and are circumscribed to the anatomical mask built on the basis of Castiello and Begliomini (2008). Coordinates are in MNI space. *p* values are corrected for multiple comparisons (FDR .05). BA: Brodmann area*; k* = number of the activated voxels (cluster size: ≥ 10).

Region	BA	H	k	MNI Coordinates			t	p	Effect
				x	y	z			
TIME BIN 6									
Middle Frontal Gyrus	**6**	**Left**	**30**	**-29**	**-7**	**54**	**5.55**	**.000**	**GS > GL**
Inferior Parietal Lobule	**40**	**Left**	**10**	**-36**	**-39**	**46**	**5.03**	**.000**	**GS > GL**
Supramarginal Gyrus	40	Left		-43	-46	38	3.69	.009	GS > GL
Inferior Parietal Lobule	**40**	**Left**	**31**	**-61**	**-32**	**34**	**4.99**	**.000**	**GS > GL**
Supramarginal Gyrus	40	Left		-54	-46	30	4.41	.001	GS > GL
Supplementary Motor Area	**32**	**Left**	**12**	**-5**	**4**	**50**	**4.63**	**.001**	**GS > GL**
TIME BIN 7									
Middle frontal Gyrus	**6**	**Left**	**37**	**-29**	**-7**	**58**	**5.83**	**.000**	**GS > GL**
Precentral Gyrus	**6**	**Left**		**-29**	**-18**	**70**	**4.08**	**.007**	**GS > GL**
Precentral Gyrus	**4**	**Left**		**-33**	**-25**	**54**	**3.30**	**.033**	GS > GL
Inferior Parietal Lobule	**40**	**Left**	**15**	**-54**	**-28**	**34**	**4.93**	**.000**	**GS > GL**
Inferior Parietal Lobule	**40**	**Left**		**-61**	**-32**	**30**	**3.75**	**.014**	GS > GL

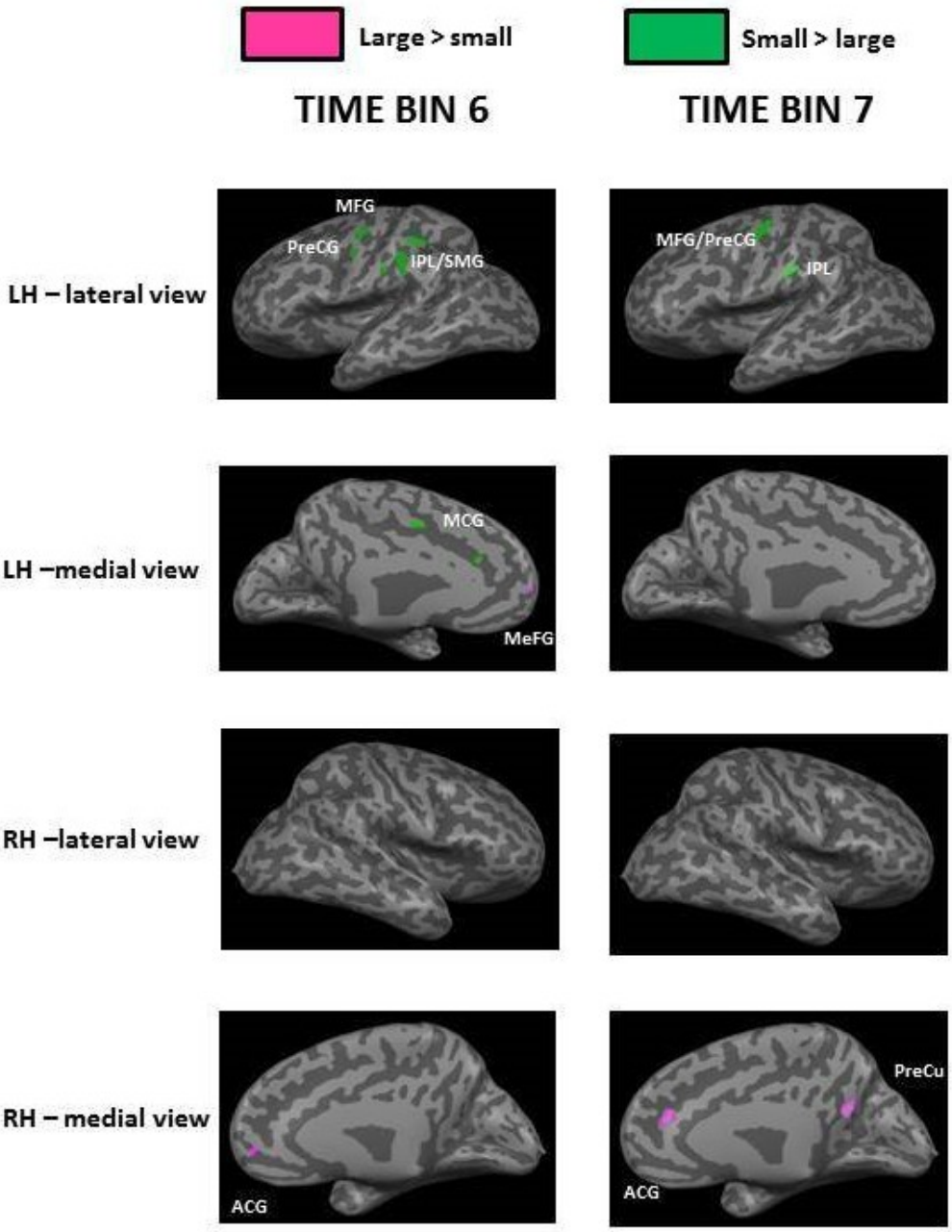

Figure 5.8. Localization of brain activations detected in both hemisphere for the contrasts GL > GS and GS > GL for each single time bin. Only time bins with significant results are reported. Results are obtained by means of the random-effects analysis performed on 18 participants included in the study and are circumscribed to the anatomical mask built on the basis of Castiello and Begliomini (2008). Statistical parametric maps (*t* statistics - $p<.05$ FDR-corrected) are imported in the software package Brain Voyager QX by means of the Matlab toolbox NeuroElf (http://neuroelf.net/). The resulting vmp image has been transformed into Talairach space and the overlaid on a mesh template provided by Brain Voyager QX. The mesh has been inflated in order to better visualize sulci activations. Activations are reported in Table 5.1. LH: left hemisphere; RH: right hemisphere. Both medial and lateral views of both hemispheres are shown. Results are reported in table 5.2. (SMA: Supplementary Motor Area; IPL: Inferior Parietal Lobule; MFG: Middle Frontal Gyrus; PreCg: Precentral Gyrus; SMG: Supramarginal Gyrus)

5.6. Discussion

Human neuroimaging has revealed similarities between human and macaque cortical organization for hand movements (Grefkes & Fink, 2005), it appears that in humans, the areas involved in different hand movements are not functionally specialized, isolated cortical regions. Rather, there are highly distributed, overlapping parieto-frontal networks with gradients in preference for one movement compared to another. The debate on this issue, however, remains vivid. Here I have attempted to shed further light on this question by identifying reach- and grasp-related areas and how such networks were modulated by object size.

Summarized in Figure 5.9. all the results for RS, RL, GS and GL during significant time bins. In line with the previous experimental chapters results will be discussed for reaching and grasping separately.

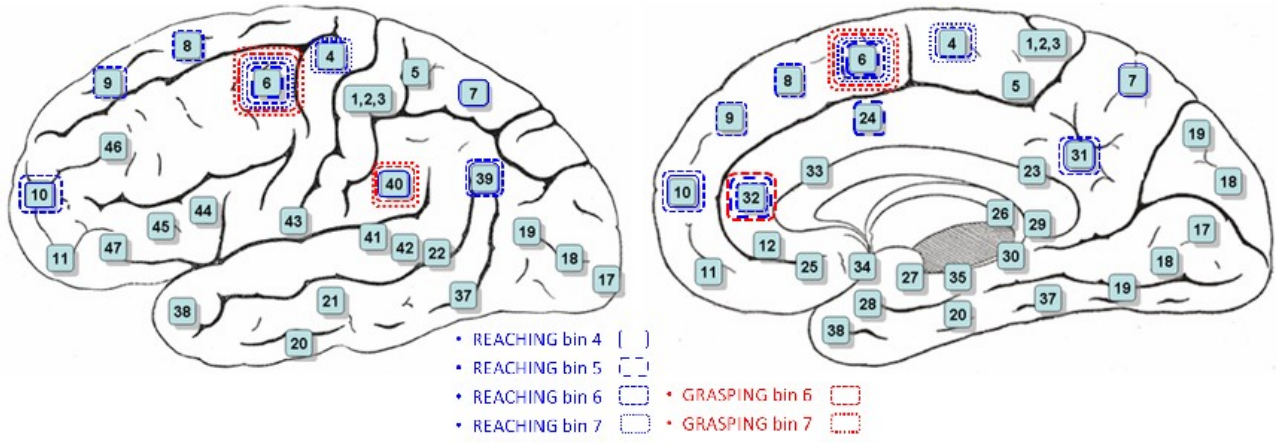

Figure 5.9. Brodmann areas activated relatively to the RL, RS, GL and GS conditions during significant time bins.

Reaching

As far as action planning is concerned, ERPs data show an early differential bilateral activity between the small and the large stimulus at the level of frontal areas, involving premotor activity (Time Bin 2). Differences in amplitude related to object size emerged in the negative component

(CNV) at all durations of the planning phase (starting at around 700 ms after the cue sound until the go signal). This finding is in line with previous evidence suggesting that the modulation of CNV amplitude by specific variables is likely to reflect the activation of planning processes preceding movement onset (Bares et al., 2007; Prescott, 1986; Rohrbaugh & Gaillard, 1983; Zaepffel & Brochier, 2012). The CNV effects reported here might suggest that the planning of reaching movements, depending on object size, generates sufficient and/or appropriate neuronal activity to evoke differential effects at the scalp level. Overall, these findings might reflect processes occurring at the level of premotor areas, which integrate intrinsic features of the target and the effector selected for the response (Beurze et al., 2007; Hoshi & Tanji, 2000, 2006). This interpretation implies that the modulation of CNV amplitude represents the combination of high- and low-level motor planning processes.

In terms of BOLD signal, the present findings indicate an early (Time Bin 4) parieto-occipital activity confined to the right hemisphere, which seems related to initial analysis of stimulus features. In particular, activity concerned with parieto-occipital areas appears to be significantly stronger when the object to be reached is larger rather than small. This kind of activation is likely to reflect activity concerned with the amount of visual information related to the object, and it might be seen as the initial step of the transformation leading from representation of objects to movement (Gallivan et al., 2011a). Here I extend these findings demonstrating that this process takes into account object size and that object metric properties such as size, seems to be processed at parieto- occipital level. This idea is supported by neurophysiological evidence suggesting that parieto-occipital neurons are sensitive to intrinsic features of objects such as size and shape (Fattori et al., 2009, 2010). Furthermore, it should be noted that a similar kind of activity has been associated to the ability to predict upcoming reach movements in both humans (Gallivan et al., 2011b) and macaques (Fattori et al., 2009). In this respect, the present findings offer new insights into the detailed movement information contained in human preparatory brain

activity and advance our present understanding of sensorimotor planning processes through a description of the parietal activity according to objects features they can predict.

At the level of the PMd, differential activity between the small and the large stimulus at Time Bin 5 do emerge. As previously noticed in the monkeys, PMd neurons seems to be involved in different aspects of reaching movements (Calton et al., 2002; Hoshi & Tanji, 2000, 2002, 2004a, b, c, 2005, 2006; Hoshi et al., 2005). Similarly, neuroimaging evidence in humans indicates that the PMd is central to the process of reach planning (Beurze et al., 2007; Grol et al., 2007; Gallivan et al., 2011a, b; Glover et al., 2012). Our findings are in agreement with these views, by showing that the PMd is activated during reaching preparation. In particular, activity at the level of the left premotor areas increases for the small than for the large stimulus. This might signify that the hemisphere responsible for movement execution needs to take into account the level of accuracy dictated by the stimulus. A result demonstrating that premotor activity during reach planning is not only concerned with reach direction or the integration of target location with information about the selected effector (Batista & Andersen, 2001; Buneo et al., 2002; Calton et al., 2002; Hoshi & Tanji 2000, 2002, 2004, 2006; Kertzman et al., 1997; Medendorp et al., 2005), but also with intrinsic features of objects such as size.

A similar pattern of activity as that detected for the PMd, was also revealed for the left SMA, suggesting a greater level of somatosensory activity for movement execution towards the small stimulus. In this respect, various other studies in humans (Gallivan et al., 2011; Beurze, 2006, 2009) and in the monkey (Cisek et al., 2003; Shen & Alexander, 1997; Snyder et al., 2000), reported reach-planning activity in this region. Though, it should be said that in these investigations the object size manipulation was not considered. In this respect, the present findings provide a novel addition to available literature.

At Time Bin 6, when presumably the action is about to start, a network of frontal areas (i.e.,

superior and middle frontal gyri) shows an increase of activity for the large than for the small stimulus. This might due to inhibitory mechanisms put in place to halt the instinct to grasp rather than reach the larger object. It is known that the coupling between parieto-frontal networks underlying reaching movements increases during reaching to grasp toward large objects, but not toward small objects (Grol et al., 2007). And it might be possible that these two actions share pre-specified motor plan (Chieffi & Gentilucci, 1993). Therefore, it might well be that one of these two actions needs to be inhibited depending on task demands.

Finally, at Time Bin 7, during movement execution, only the primary motor cortex and the dorsal premotor cortex activity within the left hemisphere resulted as significantly activated by the contrast RS > RL. These results confirm the important role of the PMd in the on-line control of reaching movements. Specifically, the proposal here is that the PMd involvement during goal-directed actions might be highly correlated with the accuracy requirement of the on-going movement (Gomez et al., 2000). Here I suggest that the PMd has the role of keeping in memory the motor representation of the object and combining it with visual information as to continuously update the configuration and orientation of the hand as it approaches the object to be reached. In this view, the PMd involvement during goal-directed actions appears to be highly correlated with the accuracy requirement of the on-going movement (Raos et al., 2004).

Grasping

Previous human neuroimaging studies showed the involvement of the anterior portion of the human AIP in grasping behaviour (see Culham, 2006; Castiello & Begliomini, 2008; Filimon, 2010) and they proposed human homologues of both the PMv and PMd during grasping (e.g., Begliomini et al., 2008). Furthermore, a differential level of activity in these areas depending on grasp type has been reported (Begliomini et al., 2008).

With this in mind, here I found significant differences depending on object size (and the type of grasp adopted) in the amplitude of the CNV at Time Bin 2 and in the extent of BOLD signal at Time Bins 6 and 7 for AIP and the PMd.

In particular, I found that at Time Bin 2, during the planning phase, the CNV showed a broader topographical distribution in frontal sites (at the level of the PMd) for grasping movement towards a small object than for grasping movements towards a large object. In this respect, previous evidence suggests that CNV originates from multiple cortical generators, including premotor areas (Bareš et al., 2007; Hamano et al., 1997, Lamarche et al., 1995). These areas are known to be major components of the reach to grasp networks (Jeannerod et al., 1995) and are activated in relation to movement planning (Baumann et al., 2009; Deiber et al., 1996; Hoshi & Tanji, 2006; Riehle & Requin, 1995; Shima et al., 1996). Therefore, it might well be that in the present study the CNV generators are differentially activated during the planning of reach to grasp movements depending on the hand shape/object size ensemble.

A consistent result across fMRI studies is the activation of a grasp-specific region within the AIP which has been proposed as the putative homologue of the macaque area AIP (Begliomini et al., 2007; Binkofski et al., 1998; Culham et al., 2003; Culham 2004; Culham et al., 2004; Frey et al., 2005). Specifically, the focus of activation was located at the junction of the AIP with the postcentral sulcus within the left hemisphere of subjects performing a grasping action with the right hand. Here, previous findings concerned with AIP activity were fully confirmed.

In terms of the ventral premotor cortex, only a paucity of studies have demonstrated brain activity related to this area during a reach to grasp movement (e.g., Ehrsson, 2000, 2002). These essentially null findings, which contrast with the strong involvement of PMv for grasping movements in macaques (e.g. Rizzolatti et al., 1988), could be due to several possibilities. For one, there may be interspecies differences in the organization of the PMv. The development of a

motor speech area in humans may have changed the location of the human functional homologue of monkey area F5 (Amunts et al., 2001). For another, it is customary to isolate grasping related activations by subtracting activations obtained during the reaching-only tasks from the reach to grasp tasks. As such both the reaching and the grasping tasks require specific motor goals that usually trigger premotor activations. Consequently the lack of activations within the ventral premotor cortex in previous literature and in the current study may be due to the above factors.

With respect to the PMd, a variety of neurophysiological and neuroimaging studies provide some evidence of bilateral PMd activity presiding the control of visually guided hand-grasping actions. Raos and others (2004) demonstrated that within area F2 a distal forelimb field does exist. This study provides compelling evidence that in the distal forelimb representation of area F2 there are neurons which are selective for the type of prehension required for grasping the object as those previously described in area F5 (Murata et al., 1997; Rizzolatti et al., 1988). In humans the contribution of the dorsal premotor cortex has been revealed in a series of recent studies (Begliomini et al., 2008; Gallivan et al., 2011a,b; Grol et al., 2007). These findings suggest that the increase of activity within the dorsal premotor cortex for specific grasp types seems to provide the evidence that, in humans as in monkeys (Raos et al., 2004), this area is involved in the control of grasping movements. In particular, PMd activity seems to play a crucial role in monitoring the configuration of fingers during planning and execution of grasping actions. Importantly, one study shows a greater level of activation for precision than whole hand grip movements (Begliomini et al., 2008). My findings are in line with these observations. I show that significant activity in PMd (at the adopted significance threshold) was greater for a small stimulus grasped with a precision grip than a large stimulus grasped with the whole hand. Therefore the difference in activation between the small and the large stimulus may reflect the need for additional sensory-motor control mechanisms for precision grip movements. In humans,

evidence from developmental, psychophysical and neuropsychological studies seems to suggest that precision grip is characterised by a greater degree of complexity. Firstly, the ability to perform independent finger movements and grasp with the precision grip is not present when voluntary grasping emerges (e.g., Gordon, 1994). Secondly, consistent results within the adult reach to grasp behavioral literature indicate that the performance of a precision grip movement is characterized by the need for additional time. This allows the use of feedback in order to meet the more precise requirements for grasping a small object and allows for the independent use of the index finger and thumb.

Finally, as reported for the reaching action, differential activity for the small than for the large stimulus was evident at the level of the SMA. This observation is in line with recent evidence suggesting that this area is involved in the on-line control of grasping actions (Glover et al., 2012).

5.7. Conclusion

In conclusion, I here identified brain activity related to how object size modulates the pre-movement planning and online control of reaching and grasping in humans using functional MRI. For reaching, differences related to pre-movement planning were observed in the SPOC, the PMd, the SMA and the superior and middle frontal gyri. In contrast, differential activity depending on object size related to online control actions was confined to the PMd. For grasping, object size modulated activity within the PMd during the planning phase and the PMd and the SMA during the execution phase of the action.

6. CONCLUDING REMARKS

It has been suggested that, when we reach and grasp an object, the brain needs to extract visuospatial information about the spatial location of the object relative to the subject (extrinsic features), as well as information about its size, shape, and orientation (intrinsic features) (Arbib, 1981). Kinematic data show that varying object size affects the maximum hand aperture, whereas varying object distance affects the kinematic profile of the reaching limb (Jeannerod, 1984). These findings have led to the suggestion that manual prehension is controlled through two visuomotor channels: a reach component, transporting the hand toward the object, and a grasp component, preshaping the fingers according to the size and the center of mass of the object (Jeannerod, 1988). This functional organization appears to have a physiological counterpart in two anatomically segregated parieto-frontal circuits: a dorsolateral circuit, consisting of an anterior intraparietal (AIP) area connected to the rostral part of the ventral premotor cortex (PMv; area F5), and a dorsomedial circuit, consisting of the an- terior portion of the occipito-parietal sulcus (area V6A) and the caudal dorsal premotor cortex (PMd; area F2) (Tanne-Gariepy et al., 2002; Galletti et al., 2003). The dorsolateral circuit has been linked to the grasping component of prehension (Jeannerod et al., 1995). In contrast, the dorsomedial circuit has been linked to the reaching component (Burnod et al., 1999). Area V6A in macaques contains reaching cells (Fattori et al., 2001, 2005) and visuomotor neurons coding object position in space (Galletti et al., 1999).

A number of human neuroimaging studies have attempted to identify a human homolog of the dorsolateral and the dorsomedial circuit (Hinkley et al., 2009; Grol et al., 2007; Culham et al.,

2003; Stark & Zohary, 2008; Binkofski et al., 1999; for reviews, see Castiello 2005; Culham et al., 2006; Culham & Valyear 2006; Filimon, 2010; Gallivan et al., 2011). The main idea stemming from these studies is that in the human, grasping and reaching are not as distinct as proposed in the macaque, in which a ventral parietofrontal pathway for grasping and a dorsal parieto-frontal pathway for reaching have been proposed (Matelli & Luppino, 2001). In fact, recent evidence in macaques shows the dorsal pathway is involved in the control of both reaching and grasping (Fattori et al., 2009, 2010). Widespread PPC activations for grasping have been found using the ^{14}C-deoxyglucose method in macaques, corrobo- rating human results (Evangeliou and others 2009). In humans, both the dorsolateral circuit (AIP-PMv), traditionally considered to be involved in grasping, and the dorsomedial circuit (SPL-PMd), the putative reaching circuit, are involved in grasping in humans (Grol et al., 2007; Gallivan et al., 2011; Konen et al., 2013). Nevertheless whether reaching and grasping are represented by overlapping parietofrontal circuits, suggesting a lack of strict functional segregation between parietofrontal circuits for grasping and reaching in humans is still under debate.

Along these lines the overarching aim of the present thesis was to identify the network of interconnected structures in the parietal and frontal lobes for the planning and the control of reaching and reach to grasp movements. And to investigate how these circuits were modulated by object size. To this endeavour, I used converging techniques with different characteristics that might allow to better understand how the human brain controls the reaching and the grasping functions.

In the first two experiments I combined kinematic and event-related potential techniques to explicitly test how activity within human grasping-related brain areas is modulated in time. I hypothesized that the ERP analysis may reveal the time course of activation of the differential cortical areas related to the planning, initiation and on-line control of reaching and grasping

movements and how such activity varies depending on the accuracy dictated by the stimuli. Kinematic analysis provides an objective standard for parsing hand movements into distinct stages and for determining their temporal occurrence.

Another aspect that depicts the novelty of my approach is that differently from previous studies I did not investigate ERPs evoked by a cue signaling specific object's intrinsic features, but by the target stimulus itself. Such approach has allowed me to examine how information about an object's geometric properties is transformed into specific motor programs more directly.

In the experiment reported in Chapter 3 participants were asked to reach towards either a small or a large object while kinematical and EEG signals were recorded. Behavioral results showed that the precision requirements were taken into account and the kinematics of reaching was modulated depending on object size. Similarly, reaching-related neural activity at the level of the posterior parietal and premotor cortices was modulated by the level of accuracy determined by object size. The central advance of these findings is that, for the first time, it has been shown that in humans object size is engaged in the neural computations for reach planning and execution, consistent with the results from physiological studies in nonhuman primates.

In the experiment reported in Chapter 4 participants were asked to reach towards and grasp either a small stimulus using a precision grip (i.e., the opposition of index finger and thumb) or a large stimulus using a whole hand grasp (i.e., the flexion of all digits around the stimulus). Results revealed a time course of activation starting at the level of parietal regions and continuing at the level of premotor regions. More specifically, they show that activity within these regions was tuned for specific grasps well before movement onset and this early tuning was carried over - as evidenced by kinematic analysis - during the preshaping period of the task.

Altogether, these findings add to the current debate about the nature of the sensorimotor transformations underlying reach to grasp movement providing a strict link between the

kinematical unfolding of this action and neural activity.

In the final experimental chapter (Chapter 5) I co-registered EEG and fMRI signals in order to identify spatial and temporal characteristics of both the dorsolateral circuit and the dorsomedial circuit to be involved in reaching and grasping respectively. Although I provide only a subset of data concerned with EEG and fMRI data separately, some interesting results did emerge. First, I found a distinction in terms of movement planning depending on object features for reaching and grasping. Whereas for reaching parieto-occipital areas were activated during the planning phase, for grasping these areas did not show differential activity depending on object size. Rather, for both movements it was at the level of movement execution that similar brain areas (PMd and SMA) seem to be sensitive to the level of accuracy dictated by the stimulus. This aspect may add a further level of complexity to the notion that separate visuomotor regions subserve basic mechanisms of planning versus on-line control, an argument that so far has been controversial. The additional co-registration analyses I am planning to perform will allow me to provide more definite insights on this issue. Nevertheless, I believe that by investigating the complexity of hand movements by means of converging techniques with different characteristics has allowed to gain further understanding of how stimulus features are processed by the neural networks underlying the control of hand actions.

REFERENCES

Aguirre, G.K., Zarahn, E. & D'esposito, M. (1998). The variability of human, BOLD hemodynamic responses. *Neuroimage, 8*, 360-369.

Allen, G.I. & Tsukahara, N. (1974). Cerebrocerebellar communication systems. *Physiological Review, 54*, 957-1006.

Andersen, R.A. & Buneo, C.A. (2002). Intentional maps in posterior parietal cortex. *Annual Review of Neuroscience, 25,* 189-220.

Andersson, J., Ashburner, J. & Friston, K.J. (2001). A global estimator unbiased by local changes. *NeuroImage, 13*, 1193-1206.

Andrews, P. (1987). Aspects of hominoid phylogeny. In Patterson, C. (Eds.). Molecules and Morphology in Evolution: *Conflict or Compromise* (pp. 23-54). New York: Cambridge University Press.

Ashburner, J. & Friston, K.J. (1997). The role of registration and spatial normalization in detecting activations in functional imaging. *Clinical MRI, 7*, 26-28.

Ashburner, J. & Friston, K.J. (1999). Nonlinear spatial normalization using basis functions. *Human Brain Mapping, 7*, 254-266.

Astafiev, S.V., Shulman, G.L., Stanley, C.M., Snyder, A.Z., Van Essen, D.C. & Corbetta, M. (2003). Functional organization of human intraparietal and frontal cortex for attending, looking, and pointing. *Journal of Neuroscience, 23*, 4689-4699.

Astafiev, S.V., Stanley, C.M., Shulman, G.L. & Corbetta M. (2004). Extrastriate body area in human occipital cortex responds to the performance of motor actions. *Nature Neuroscience, 7*, 542-8.

Babiloni, F., Mattia, D., Babiloni, C., Astolfi, L., Salinari, S., Basilisco, A., ... & Cincotti, F. (2004). Multimodal integration of EEG, MEG and fMRI data for the solution of the neuroimage puzzle. *Magnetic resonance imaging, 22*, 1471-1476.

Baldauf, D. & Deubel, H. (2010). Attentional landscapes in reaching and grasping. *Vision Research, 50*, 999-1013.

Bareš, M., Nestrašil, I., & Rektor, I. (2007). The effect of response type (motor output versus mental counting) on the intracerebral distribution of the slow cortical potentials in an externally cued (CNV) paradigm. *Brain research bulletin*, *71*, 428-435.

Batista, A.P. & Andersen, R.A. (2001). The parietal reach region codes the next planned movement in a sequential reach task. *Journal Neurophysiology, 85*, 539-544.

Battaglia-Mayer, A., Caminiti, R., Lacquaniti, F., & Zago, M. (2003). Multiple levels of representation of reaching in the parieto-frontal network. *Cerebral Cortex, 13*, 1009-1022.

Battaglia-Mayer, A., Ferraina, S., Mitsuda, T., Marconi, B., Genovesio, A., Onorati, P., Lacquaniti, F. & Caminiti, R. (2000). Early coding of reaching in the parieto-occipital cortex. *Journal of Neurophysiology, 83*, 2374-2391.

Battaglini, P. P., Muzur, A., Galletti, C., Skrap, M., Brovelli, A., & Fattori, P. (2002). Effects of lesions to area V6A in monkeys. Experim*ental Brain Research, 144*, 419-422.

Baumann, M. A., Fluet, M. C., & Scherberger, H. (2009). Contextspecific grasp movement representation in the macaque anterior intraparietal area. *Journal of Neuroscience, 29*, 6436–6448.

Begliomini, C., Caria, A., Grodd, W., & Castiello, U. (2007b). Comparing natural and constrained movements: new insights into the visuomotor control of grasping. *PLoS One, 2(10)*, e1108.

Begliomini, C., Nelini, C., Caria, A., Grodd, W., & Castiello, U. (2008). Cortical activations in humans grasp-related areas depend on hand used and handedness. *PloS one, 3*, e3388.

Begliomini, C., Wall, M. B., Smith, A. T., & Castiello, U. (2007a). Differential cortical activity for precision and whole-hand visually guided grasping in humans. European Journal of *Neuroscience, 25*, 1245-1252.

Bennett, K. M., & Castiello, U. (Eds.). (1994). *Insights into the reach to grasp movement* (Vol. 105). Elsevier.

Berger, H. (1929). Über das elektrenkephalogramm des menschen. *European Archives of Psychiatry and Clinical Neuroscience, 87*, 527-570.

Berkeley, G. (1910). A new theory of vision (1709). *Principles o-Human Knowledge, 1710*,

1733-34.

Berndt, I., Franz, V.H., Bulthoff, H.H. & Wascher, E. (2002). Effects of pointing direction and direction predictability on event-related lateralizations of the EEG. *Human Movement Science, 21*, 387-410.

Berthier, N. E., Clifton, R. K., Gullapalli, V., McCall, D. D., & Robin, D. J. (1996). Visual information and object size in the control of reaching. *Journal of Motor Behavior, 28*, 187-197.

Berthier, N.E., Clifton, R.K., McCall, D.D. & Robin, D.J. (1999). Proximodistal structure of early reaching in human infants. *Experimental Brain Research, 127*, 259-269.

Beurze, S.M., de Lange, F.P., Toni, I. & Medendorp, W.P. (2007). Integration of target and effector information in the human brain during reach planning. *Journal of Neurophysiology, 97*, 88-199.

Beurze, S.M., de Lange, F.P., Toni, I. & Medendorp, W.P. (2009). Spatial and effector processing in the human parietofrontal network for reaches and saccades. *Journal of Neurophysiology*, *101*, 3053-3062.

Bhattacharyya, R., Musallam, S. & Andersen, R.A. (2009). Parietal reach region encodes reach depth using retinal disparity and vergence angle signals. *Journal of Neurophysiology, 102*, 805-816.

Binkofski, F. & Buccino, G. (2006). The role of ventral premotor cortex in action execution and action understanding. *Journal of Physiology Paris, 99*, 396-405.

Binkofski, F., Buccino, G., Posse, S., Seitz, R.J., Rizzolatti, G. & Freund H.(1999). A frontoparietal circuit for object manipulation in man: evidence from an fMRI-Study. *European Journal of Neuroscience, 11*, 3276-3286.

Binkofski, F., Butler, A., Buccino, G., Heide, W., Fink, G., Freund, H.J. & Seitz, R.J. (2003). Mirror apraxia affects the peripersonal mirror space. A combined lesion and cerebral activation study. *Experimental Brain Research, 153*, 210-219.

Binkofski, F., Dohle, C., Posse, S., Stephan, K. M., Hefter, H., Seitz, R. J., & Freund, H. J. (1998). Human anterior intraparietal area subserves prehension A combined lesion and

functional MRI activation study. *Neurology, 50*, 1253-1259.

Bloch, F., Hansen, W.W. & Packard, M. (1946). The nuclear induction experiment. *Physical Review, 70,* 474-485.

Blume, W.T. & Oliver, L.M. (1996). Noninvasive electroencephalography in supplementary sensorimotor area epilepsy. *Advances in Neurology, 70*, 309-317.

Bonfiglioli, C., De Berti, G., Nichelli, P., Nicoletti, R. & Castiello U. (1998). Kinematic analysis of the reach to grasp movement in Parkinson's and Huntington's disease subjects. *Neuropsychologia, 36*, 1203-1208.

Bonini, L., Rozzi, S., Serventi, F. U., Simone, L., Ferrari, P. F., & Fogassi, L. (2010). Ventral premotor and inferior parietal cortices make distinct contribution to action organization and intention understanding. *Cerebral Cortex, 20*, 1372-1385.

Bonini, L., Serventi, F. U., Bruni, S., Maranesi, M., Bimbi, M., Simone, L., & Fogassi, L. (2012). Selectivity for grip type and action goal in macaque inferior parietal and ventral premotor grasping neurons. *Journal of Neurophysiology, 108,* 1607-1619.

Bonini, L., Serventi, F. U., Simone, L., Rozzi, S., Ferrari, P. F., & Fogassi, L. (2011). Grasping neurons of monkey parietal and premotor cortices encode action goals at distinct levels of abstraction during complex action sequences. *The Journal of Neuroscience, 31*, 5876-5886.

Bootsma, R.J., Marteniuk, R.G., Mackenzie, C.L. & Zaal, F.T.J. (1994). The speed-accuracy trade off in manual prehension: effects of movement amplitude, object size and object width on kinematic characteristics. *Experimental Brain Research, 98*, 535-541.

Bosco, A., Breveglieri, R., Chinellato, E., Galletti, C. & Fattori, P. (2010). Reaching activity in the medial posterior parietal cortex of monkeys is modulated by visual feedback. *Journal of Neuroscience, 30*, 14773-14785.

Bozzacchi, C., Giusti, M.A., Pitzalis, S., Spinelli, D. & Di Russo, F. (2012). Awareness affects motor planning for goal-oriented actions. *Biological Psychology, 89*, 503-514.

Brammer, M.J. (2002) Head Motion and its Correction In: Jezzard, P. Matthews, P. & Smith, S.M. *Functional MRI: an introduction to methods*. (pp. 243-250). Oxford: University Press.

Broca, P. (1861). Perte de la parole. Ramolissement chronique et desctruction partielle du lobe antérieur gauche du cerveau. *Bulletin de la Société d'Anthropologie, 11*, 235-238.

Brochier, T., & Umiltà, M. A. (2007). Cortical control of grasp in non-human primates. *Current Opinion in Neurobiology, 17*, 637-643.

Brochier, T., Spinks, R. L., Umilta, M. A., & Lemon, R. N. (2004). Patterns of muscle activity underlying object-specific grasp by the macaque monkey. *Journal of Neurophysiology, 92*, 1770-1782.

Brodmann, K. (1903). Beiträge zur histologischen Lokalisation der Grosshirnrinde. 1. Mitteilung: die Regio rolandica. *Journal of Psychological Neurology, 2*, 79-107.

Brouwer, A.M., Georgiou, I., Glover, S., Castiello, U. (2006). Adjusting reach to lift movements to sudden visible changes in target's weight. *Experimental Brain Research, 173*, 629-636.

Buneo, C.A. & Andersen, R.A. (2006). The posterior parietal cortex: Sensorimotor interface for the planning and online control of visually guided movements. *Neuropsychologia, 44*, 2594-2606.

Buneo, C.A., Jarvis, M.R., Batista, A.P., & Andersen, R.A. (2002). Direct visuomotor transformations for reaching. *Nature, 416*, 632-636.

Burton, H. & Carlson, M. (1986). Second somatic sensory cortical area (SII) in a prosimian primate, Galago crassicaudatus. *Journal of Computational Neurology, 247*, 200-220.

Calton, J.L., Dickinson, A.R. & Snyder, L.H. (2002). Non-spatial, motor-specific activation in posterior parietal cortex. *Nature Neuroscience, 5*, 580-588.

Caminiti, R., Ferraina, S. & Mayer, A.B (1998). Visuomotor transformations: early cortical mechanisms of reaching. *Current Opinion in Neurobiology, 8*, 753-761.

Caplan, D., Alpert, N., Waters, G. & Olivieri, A. (2000). Activation of Broca´s areas by syntactic processing under conditions of concurrent articulation. *Human Brain Mapping, 9*, 65-71.

Castiello U. (2005) The neuroscience of grasping. *Nature Review Neuroscience, 6*, 726-736.

Castiello, U., & Umiltà, C. (1990). Size of the attentional focus and efficiency of processing. *Acta psychologica*, *73*, 195-209

Castiello, U., & Umiltà, C. (1992). Splitting focal attention. *Journal of Experimental Psychology: Human Perception and Performance*, *18*, 837.

Castiello, U. (1996). Grasping a fruit: selection for action. *Journal of Experimental Psychology: Human Perception and Performance, 22*, 582-603.

Castiello, U. (2001). The effects of abrupt onset of 2-D and 3-D distractors on prehension movements. *Perception & psychophysics*, *63*, 1014-1025.

Castiello, U. (2005). The neuroscience of grasping. *Nature Neuroscience Reviews, 6,* 726-736.

Castiello, U., & Begliomini, C. (2008). The cortical control of visually guided grasping. *The Neuroscientist, 14*, 157-170.

Castiello, U., Bennet, K.M., Stelmach, G.E. (1993). Reach to grasp: the neural response to perturbation of object size. *Experimental Brain Research, 94*, 163-178.

Castiello, U., Bennett, K.M., Egan, G.F., Tochon-Danguy, H.J., Kritikos, A. & Dunai, J. (1999). Human inferior parietal cortex 'programs' the action class of grasping. *Cognitive Systems Research, 1*, 89-97.

Cavina-Pratesi, C., Goodale, M. A., & Culham, J. C. (2007). FMRI reveals a dissociation between grasping and perceiving the size of real 3D objects. *PLoS One, 2*, e424.

Cavina-Pratesi, C., Monaco, S., Fattori, P., Galletti, C., McAdam, T.D., Quinlan, D.J., Goodale, M.A., & Culham, J.C. (2010). fMRI reveals the neural substrates of arm transport and grip formation in reach to grasp actions in humans. *The Journal of Neuroscience, 30*, 10306-10323.

Cavina-Pratesi, C., Monaco, S., Fattori, P., Galletti, C., McAdam, T.D., Quinlan, D.J., Goodale, M.A., & Culham, J.C. (2010). fMRI reveals the neural substrates of arm transport and grip formation in reach to grasp actions in humans. *The Journal of Neuroscience, 30*, 10306-10323.

Chao, L.L.& Martin, A. (2000). Representation of manipulable man-made objects in the dorsal stream. *Neuroimage, 12*, 478-484.

Chapman, H., Gavrilescu, M., Wang, H., Kean, M., Egan, G. & Castiello U. (2002). Posterior parietal cortex control of reach to grasp movements in humans. *European Journal of*

Neuroscience, 15, 2037-2042.

Chieffi, S., & Gentilucci, M. (1993). Coordination between the transport and the grasp components during prehension movements. *Experimental Brain Research, 94*, 471-477.

Choi, H. J., Zilles, K., Mohlberg, H., Schleicher, A., Fink, G. R., Armstrong, E., & Amunts, K. (2006). Cytoarchitectonic identification and probabilistic mapping of two distinct areas within the anterior ventral bank of the human intraparietal sulcus. *Journal of Comparative Neurology*, *495*, 53-69.

Chouinard, P.A. & Paus, T. (2006). The primary motor and premotor areas of the human cerebral cortex. *The Neuroscientist, 12*,143-152.

Christel, M.I. & Billard, A. (2002). Comparison between macaques' and humans' kinematics of prehension: the role of morphological differences and control mechanisms. *Behavioral Brain Research, 131*, 169–184.

Clower, D.M., Dum, R.P. & Strick, P.L. (2005). Basal ganglia and cerebellar inputs to 'AIP'. *Cerebral Cortex, 15*, 913-920.

Connolly, J. D., Andersen, R. A., & Goodale, M. A. (2003). FMRI evidence for a parietal reach region'in the human brain. *Experimental Brain Research, 153*, 140-145.

Connolly, J.D., Goodale, M.A., DeSouza, J.F., Menon, R.S., & Vilis, T. (2000). A comparison of frontoparietal fMRI activation during anti-saccades and anti-pointing. *Journal of Neurophysiology, 84*, 1645–1655.

Cook, A.M., Meng, M.Q., Gu, J.J.& Howery, K.(2002). Development of a robotic device for facilitating learning by children who have severe disabilities. *IEEE Transaction in Neural System Rehabilitation Engineering, 10*,178-87.

Creem-Regehr, S.H, & Lee, J.N. (2005). Neural representations of graspable objects: are tools special? *Cognitive Brain Research, 22*, 457-469.

Crossman, A.R. (2000). Functional anatomy of movement disorders. *Journal of Anatomy, 196*, 519-525.

Culham, J. C., & Valyear, K. F. (2006). Human parietal cortex in action. *Current opinion in neurobiology, 16*, 205-212.

Culham, J. C., Danckert, S. L., De Souza, J. F., Gati, J. S., Menon, R. S., & Goodale, M. A. (2003). Visually guided grasping produces fMRI activation in dorsal but not ventral stream brain areas. *Experimental Brain Research, 153*, 180-189.

Culham, J.C. & Kanwisher N.G. (2001). Neuroimaging of cognitive functions in human parietal cortex. *Current Opinion in Neurobiology, 11*, 157-163.

Culham, J. C. (2003). Human brain imaging reveals a parietal area specialized for grasping. *Attention and performance XX: functional neuroimaging of human cognition. Oxford University Press, Oxford*.

Culham, J.C., Cavina-Pratesi, C. & Singhal A. (2006). The role of parietal cortex in visuomotor control: What have we learned from neuroimaging? *Neuropsychologia, 44*, 2668-2684.

Culham, J.C., Danckert, S.L., DeSouza, J.F., Gati, J.S., Menon, R.S. & Goodale, M.A. (2003). Visually guided grasping produces fMRI activation in dorsal but not ventral stream brain areas. *Experimental Brain Research, 153*, 180–189.

Da Silva, F. L. (2010). EEG: origin and measurement. In *EEG-fMRI* (pp. 19-38). Springer Berlin Heidelberg.

Dale, A.M. & Buckner, R.L. (1999). Selective averaging of rapidly presented individual trials using fMRI. *Human Brain Mapping, 5*, 329-340.

Davare, M., Andres, M., Clerget, E., Thonnard, J. L., & Olivier, E. (2007). Temporal dissociation between hand shaping and grip force scaling in the anterior intraparietal area. *The Journal of Neuroscience, 27*, 3974-3980.

Davare, M., Andres, M., Cosnard, G., Thonnard, J. L., & Olivier, E. (2006). Dissociating the role of ventral and dorsal premotor cortex in precision grasping.*The Journal of Neuroscience, 26*, 2260-2268.

Davare, M., Kraskov, A., Rothwell, J. C., & Lemon, R. N. (2011). Interactions between areas of the cortical grasping network. *Current Opinion in Neurobiology,21*, 565-570.

Davare, M., Montague, K., Olivier, E., Rothwell, J. C., & Lemon, R. N. (2009). Ventral premotor to primary motor cortical interactions during object-driven grasp in humans. *Cortex, 45*, 1050-1057.

De Sanctis, T., Tarantino, V., Straulino, E., Begliomini, C. & Castiello, U. (2013). Co-Registering Kinematics and Evoked Related Potentials during Visually Guided reach to grasp Movements. *PloS One, 8*, e65508.

Debener, S., Ullsperger, M., Siegel, M., & Engel, A. K. (2006). Single-trial EEG–fMRI reveals the dynamics of cognitive function. *Trends in Cognitive Sciences, 10*, 558-563.

Decety, J. (1994). Brain areas responsible for the generation and control of reaching and grasping. Anatomy with Positron Emission Tomography (PET). In: Bennett,K.M.B & Castiello U. (Eds) *Insights into the Reach to Grasp Movement* (pp.109-126). Amsterdam: Elsevier Science.

Decety, J., Kawashima, R., Gulyás, B. & Roland, P.E. (1992). Preparation for reaching: a PET study of the participating structures in the human brain. *Neuroreport, 3*, 761-764.

Deiber, M. P., Ibanez, V., Sadato, N., & Hallett, M. (1996). Cerebral structure participating in motor preparation in humans: A positron tomography study. *Journal of Neurophysiology, 75*, 233–247.

Delorme, A., & Makeig, S. (2004). EEGLAB: an open source toolbox for analysis of single-trial EEG dynamics including independent component analysis. *Journal of Neuroscience Methods, 134*, 9-21.

Desmurget, M., Epstein, C.M., Turner, R.S., Prablanc, C., Alexander, G.E. & Grafton, S.T. (1999). Role of the posterior parietal cortex in updating reaching movements to a visual target. *Nature Neuroscience, 2*, 563-567.

DeSouza, J.F., Dukelow, S.P., Gati, J.S., Menon, R.S., Andersen, R.A. & Vilis T. (2000). Eye position signal modulates a human parietal pointing region during memory guided movements. *The Journal of Neuroscience 20*, 5835–5840.

Donaldson, D.I.& Buckner, R.L. (1999). Trying versus succeeding: event-related designs dissociate memory processes. *Neuron, 22*, 412-414.

Doyon, J., Penhune, V. & Ungerleider, L.G. (2003). Distinct contribution of the cortico-striatal and cortico-cerebellar systems to motor skill learning. *Neuropsychologia, 41*, 252-262.

Dum, R.P. & Strick, P.L. (1991). The origin of corticospinal projections from the premotor areas

in the frontal lobe. *Journal of Neuroscience, 11*, 667-689.

Easthough. D., Edwards, M.G. (2007). Movement kinematics in prehension are affected by grapingobjects of different mass. *Experimental Brain Research, 176*, 193-198.

Ehrsson, H. H., Fagergren, A., Jonsson, T., Westling, G., Johansson, R. S., & Forssberg, H. (2000b). Cortical activity in precision-versus power-grip tasks: an fMRI study. *Journal of Neurophysiology, 83*, 528-536.

Ehrsson, H. H., Kuhtz-Buschbeck, J. P., & Forssberg, H. (2002). Brain regions controlling nonsynergistic versus synergistic movement of the digits: a functional magnetic resonance imaging study. *The Journal of neuroscience,22*, 5074-5080.

Ehrsson, H.H., Fagergren, A., Johnsson, T., Westling, G., Johansson, R.S. & Forssberg, H. (2000a). Simultaneous movements of upper and lower limbs are coordinated by motor representations that are shared by both limbs: a PET Study. *European Journal of Neuroscience, 12*, 3385-3398.

Ehrsson, H.H., Fagergren, E. & Forssberg, H. (2001). Differential fronto-parietal activation depending on force used in a precision grip task: an fMRI Study. *Journal of Neurophysiology, 85*, 2613–2623.

Fagg, A.H. & Arbib, M.A. (1998). Modelling parietal-premotor interactions in primate control of grasping. *Neural Networks, 11*, 1277–1303.

Faillenot, I., Toni, I., Decety, J., Gregoire, M. C., & Jeannerod, M. (1997). Visual pathways for object-oriented action and object recognition: functional anatomy with PET. Cerebral Cort*ex, 7*, 77-85.

Fattori, P., Breveglieri, R., Marzocchi, N., Filippini, D., Bosco, A. & Galletti, C. (2009). Hand orientation during reach to grasp movements modulates neuronal activity in the medial posterior parietal area V6A. *The Journal of Neuroscience, 29*, 1928-1936.

Fattori, P., Breveglieri, R., Raos, V., Bosco, A. & Galletti, C. (2012). Vision for action in the macaque medial posterior parietal cortex. *The Journal of Neuroscience, 32*, 3221-34.

Fattori, P., Gamberini, M., Kutz, D. F., & Galletti, C. (2001). 'Arm-reaching'neurons in the parietal area V6A of the macaque monkey. *European Journal of Neuroscience, 13*, 2309-

2313.

Fattori, P., Kutz, D.F., Breveglieri, R., Marzocchi, N. & Galletti, C. (2005). Spatial tuning of reaching activity in the medial parieto-occipital cortex (area V6A) of macaque monkey. *European Journal of Neuroscience*, 22, 956-972.

Fattori, P., Raos, V., Breveglieri, R., Bosco, A., Marzocchi, N., & Galletti, C. (2010). The dorsomedial pathway is not just for reaching: grasping neurons in the medial parieto-occipital cortex of the macaque monkey. *The Journal of Neuroscience, 30*, 342-349.

Faugier–Grimaud, S., Frenois, C. & Stein, D.G. (1978). Effects of posterior parietal lesions on visually guided behaviour in monkeys. *Neuropsychologia, 16,* 151–168.

Fernandez-Ruiz, J., Goltz, H.C., DeSouza, J.F., Vilis, T. & Crawford, J.D. (2007). Human parietal "reach region" primarily encodes intrinsic visual direction, not extrinsic movement direction, in a visual motor dissociation task. *Cerebral Cortex, 17*, 2283–2292.

Filimon, F. (2010). Human cortical control of hand movements: parietofrontal networks for reaching, grasping, and pointing. *The Neuroscientist, 16*, 388-407.

Filimon, F., Nelson, J.D., Huang, R.S. & Sereno, M.I. (2009). Multiple parietal reach regions in humans: cortical representations for visual and proprioceptive feedback during on-line reaching. *The Journal of Neuroscience, 29*, 2961-2971.

Fitts, P. M. (1954). The information capacity of the human motor system in controlling the amplitude of movement. *Journal of Experimental Psychology, 47*, 381.

Flatters, I. J., Otten, L., Witvliet, A., Henson, B., Holt, R. J., Culmer, P., ... & Mon-Williams, M. (2012). Predicting the effect of surface texture on the qualitative form of prehension. *PloS one, 7*, e32770.

Fogassi, L., Gallese, V., Buccino, G., Craighero, L., Fadiga, L. & Rizzolatti, G. (2001). Cortical mechanism for the visual guidance of hand grasping movements in the monkey: a reversible inactivation study. *Brain, 124*, 571–586.

Forssberg, H., Kinoshita, H., Eliasson, A.C., Johansson, R.S., Westling, G. & Gordon, A.M. (1992). Development of human precision grip. II. Anticipatory control of isometric forces targeted for object's weight. *Experimental Brain Research, 90*, 393-398.

Frey, S.H., Vinton D., Norlund, R. & Grafton, S.T. (2005). Cortical topography of human anterior intraparietal cortex active during visually guided grasping. *Cognitive Brain Research, 23*, 397–405.

Friston, K.J., Fletcher, P., Josephs, O., Holmes, A., Rugg, M.D. & Turner, R. (1998). Eventrelated fMRI: characterizing differential responses. *Neuroimage, 7*, 30-40.

Friston, K.J., Glaser, K., Mechelli, A., Turner, R. & Price, C. (2003). Hamodynamic Modelling In: Frackowiak, R.S.J., Friston, K.J., Frith, C.D., Dolan, R.J., Price, C.J., Zeki, S., Ashburner,J. & Penny, W. (Eds). *Human Brain Function*. (pp. 823-842). San Diego: Elsevier Academic Press.

Friston, K.J., Holmes, A.P., Poline, J.B., Grasby, P.J., Williams, S.C.R., Frackowiak, R.S.J., Turner, R. (1995). Analysis of fmri time series revisited. *Neuroimage, 2*, 45–53.

Friston, K.J., Holmes, A.P., Worsley, K.J., Poline, J.B., Frith, C.& Frackowiak, R.S.J. (1995b). Statistical Parametric Maps in Functional Imaging: A General Linear Approach. *Human Brain Mapping, 2*, 189-210.

Friston, K.J., Mechelli, A., Turner, R. & Price, C.J. (2000). Nonlinear responses in fMRI: the Balloon model, Volterra kernels, and other hemodynamics. *Neuroimage, 12*, 466-477.

Friston, K.J., Tononi, G., Reeke, G.N. Jr, Sporns, O. & Edelman, G.M. (1994). Value-dependent selection in the brain: simulation in a synthetic neural model. *Neuroscience, 59*, 229-243.

Friston, K.J.,. Ashburner, J., Frith, C., Poline, J.B., Heather, J.D. & Frackowiak, R.S.J. (1995a). Spatial Registration and Normalization of Images. *Human Brain Mapping, 3*, 165-189.

Friston, K.J.; Williams, S., Howard, R., Frackowiak, R.S.J. & Turner, R. (1996). Movementrelated effects in fMRI time series. *Magnetic Resonance in Medicine, 35*, 289-291.

Gail, A., Andersen, R. A. (2006). Neural dynamics in monkey parietal reach re-gion reflect context-specific sensorimotor transformations. *The Journal of Neuroscience, 26*, 9376–9384.

Gaillard, A. W. K. (1977). The late CNV wave: preparation versus expectancy. *Psychophysiology, 14*, 563-568.

Gallese, V., Murata, A., Kaseda, M., Nikim N. & Sakata, H. (1994). Deficit of hand preshaping after muscimol injection in monkey parietal cortex. *Neuroreport, 5*, 1525-1529.

Galletti, C., Breveglieri, R., Lappe, M., Bosco, A., Ciavarro, M., & Fattori, P. (2010). Covert shift of attention modulates the ongoing neural activity in a reaching area of the macaque dorsomedial visual stream. *PloS one*, *5*, e15078..

Galletti, C., Fattori, P., Battaglini, P.P., Shipp, S. & Zeki S. (1996). Functional demarcation of a border between areas V6 and V6A in the superior parietal gyrus of the macaque monkey. *European Journal of Neuroscience, 8*, 30-52.

Galletti, C., Fattori, P., Kutz, D.F. & Battaglini, P.P. (1997). Arm movement-related neurons in the visual area V6A of the macaque superior parietal lobule of special interest. *European Journal of Neuroscience, 9*, 410–413.

Galletti, C., Kutz, D. F., Gamberini, M., Breveglieri, R., & Fattori, P. (2003). Role of the medial parieto-occipital cortex in the control of reaching and grasping movements. *Experimental Brain Research, 153*, 158-170.

Gallivan, J. P., McLean, D. A., Valyear, K. F., Pettypiece, C. E., & Culham, J. C. (2011). Decoding action intentions from preparatory brain activity in human parieto-frontal networks. *The Journal of Neuroscience, 31*, 9599-9610.

Gallivan, J.P., Cavina-Pratesi, C. & Culham, J. (2009). Is that within reach? fMRI reveals that the human superior parieto-occipital cortex encodes objects reachable by the hand. *The Journal of Neuroscience, 29*, 4381-4391.

Gallivan, J.P., McLean, D.A., Valyear, K.F., Pettypiece, C E. & Culham, J.C. (2011). Decoding action intentions from preparatory brain activity in human parieto-frontal networks. *The Journal of Neuroscience, 31*, 9599-9610.

Gardner, E. P., Babu, K. S., Ghosh, S., Sherwood, A., & Chen, J. (2007b). Neurophysiology of prehension. III. Representation of object features in posterior parietal cortex of the macaque monkey. *Journal of Neurophysiology, 98*, 3708-3730.

Gardner, E. P., Babu, K. S., Reitzen, S. D., Ghosh, S., Brown, A. S., Chen, J., ... & Ro, J. Y. (2007a). Neurophysiology of prehension. I. Posterior parietal cortex and object-oriented hand behaviors. *Journal of Neurophysiology, 97*, 387-406.

Gardner, E. P., Ro, J. Y., Babu, K. S., & Ghosh, S. (2007c). Neurophysiology of prehension. II. Response diversity in primary somatosensory (SI) and motor (MI) cortices. *Journal of Neurophysiology, 97*, 1656-1670.

Gardner, E.P., Debowy, D.J., Ro, J.Y., Ghosh, S. & Srinivasa, B. (2002). Sensory monitoring of prehension in the parietal lobe: a Study using digital video. *Behavioral Brain Research, 135*, 213–224.

Gentilucci, M., Castiello, U., Corradini, M. L., Scarpa, M., Umiltá, C.A., & Rizzolatti, G. (1991). Influence of different types of grasping on the transport component of prehension movements. *Neuropsychologia, 29*, 361-378.

Geyer, S., Ledberg, A., Schleicher, A., Kinomura, S., Schormann, T., Bürgel, U., Klingberg, T., Larsson, J., Zilles, K. & Roland, P.E. (1996). Two different areas within the primary motor cortex of man. *Nature, 382*, 805-807.

Gibson, A.R., Horn, K.M. & Van Kan, P.L.E. (1994). Grasping cerebellar function. In: Bennett, K.M.B & Castiello U. (Eds), *Insights into the Reach to Grasp Movement*. (pp 129-150) Amsterdam: Elsevier Science.

Glover , S., Miall, R.C. & Rushworth, M.F.S. (2005). Parietal rTMS selectively disrupts the initiation of on-line adjustments to a perturbation of object size. *Journal of Cognitive Neuroscience, 17*, 124–136.

Glover, S. (2003). Optic ataxia as a deficit specific to the on-line control of actions. *Neuroscience & Biobehavioral Reviews*, *27*, 447-456.

Glover, S. (2004). Separate visual representations in the planning and control of action. *Behavioral and Brain Sciences, 27*, 3–78.

Glover, S. (2004). Separate visual representations in the planning and control of action. *Behavioral and Brain Sciences*, *27*, 3-24.

Glover, S., Wall, M. B., & Smith, A. T. (2012). Distinct cortical networks support the planning and online control of reaching-to-grasp in humans. *European Journal of Neuroscience, 35*, 909-915.

Godschalk M, Lemon RN, Nijs HG, Kuypers HG (1981). Behaviour of neurons in monkey peri-

arcuate and precentral cortex before and during visually guided arm and hand movements. *Experimental Brain Research 44*, 113-116.

Goodale, M.A. & Milner, A.D. (1992). Separate visual pathways for perception and action. *Trends in Neurosciences, 15*, 20-25.

Gordon AM, Forssberg H, Iwasaki N (1994). Formation and lateralization of internal representations underlying motor commands during precision grip. *Neuropsychologia 32*, 555-568.

Gordon, A.M., Forssberg, H., Johansson, R.S. & Wresting, G. (1991). Visual size cues in the programming of manipulative forces during precision grip. *Experimental Brain Research, 83*, 477-482.

Gorniak, S.L., Zatsiorsky, V.M., Latash, M.L. (2010). Manipulation of fragile object. *Experimental Brain Research, 202*, 413-430.

Grafton ST (2010). The cognitive neuroscience of prehension: recent developments. *Experimental Brain Research 204*, 475–491.

Grafton ST, Fagg H, Woods RP, Arbib M (1996). Functional anatomy of pointing and grasping in humans. *Cereb Cortex 6*, 226–237.

Grafton, S.T. (2010). The cognitive neuroscience of prehension: recent developments. *Experimental Brain Research, 204*, 475-491.

Grafton, S.T., Arbib, M.A., Fadiga, L. & Rizzolatti G. (1996). Localization of grasp representations in humans by positron emission tomography. *Experimental Brain Research, 112*, 103-111.

Grafton, S.T., Fagg, A.H. & Arbib, M.A. (1998). Dorsal premotor cortex and conditional movement selection: A PET functional mapping Study. *Journal of Neurophysiology, 79*, 1092-1097.

Grafton, S.T., Fagg, A.H., Woods R.P. & Arbib M.A. (1996). Functional anatomy of pointing and grasping in humans. *Cerebral Cortex, 6*, 226-237.

Graziano, M.S., Taylor, C.S., Moore, T. & Cooke, D.F. (2002). The cortical control of movement revisited. *Neuron, 36,* 349-62.

Grefkes, C. & Fink, G.R. (2005). The functional organization of the intraparietal sulcus in humans and monkeys. *Journal of Anatomy, 207*, 3-17.

Grefkes, C., Ritzl, A., Zilles, K. & Fink, G.R. (2004). Human medial intraparietal cortex subserves visuomotor coordinate transformation. *Neuroimage, 23*, 1494-506.

Gregoriou G G, Savaki HE (2003). When vision guides movement: a functional imaging study of the monkey brain. *NeuroImage 19*, 959–967.

Grèzes, J., Armony, L., Rowe, J. & Passingham, R.E. (2003). Activations related to 'mirror' and 'canonical' neurons in the human brain: an fMRI Study. *Neuroimage, 18*, 928–937.

Grèzes, J., Fonlupt, P., Berthenthal, B., Delon-Martin, C., Segerbath, C. & Decety, J. (2001). Does perception of biological motion rely on specific brain regions? Neuroimage, *13*, 775-85.

Grill-Spector, K. & Malach, R. (2004). The human visual cortex. *Annual Review of Neuroscience, 27*, 649-67.

Grol, M.J., Majdandzic, J., Stephan, K.E., Verhagen, L., Dijkerman, H.C., Bekkering, H., Verstraten, F.A.J. & Toni, I. (2007). Parieto-frontal connectivity during visually guided grasping. *The Journal of Neuroscience, 27*, 11877-11887.

Grosskopf, A. & Kuhtz-Buschbeck, J.P. (2006). Grasping with the left and right hand: a kinematic Study. *Experimental Brain Research, 168*, 230-40.

Grubb, R.L., Raichle, M.E., Eichling, J.O. & Ter-Pogossian, M.M. (1974). The effects of changes in PaCO2 on cerebral blood volume, blood flow, and vascular mean transit time. *Stroke, 5*, 630-639.

Hagberg, G.E., Zito, G., Patria, F. & Sanes, J.N. (2001). Improved detection of event-related functional MRI signals using probability functions. *Neuroimage, 14*, 1193-1205.

Hagler, D. J. Jr, Riecke, L., & Sereno M. I. (2007). Parietal and superior frontal visuospatial maps activated by pointing and saccades. *Neuroimage, 35*, 1562–1577.

Haines, R.W. (1955). The anatomy of the hand of certain insectivores. *Proceedings of the Zoological Society of London, 125*, 761-777.

Hamano, T., Lu ¨ ders, H. O., Ikeda, A., Collura, T. F., Comair, Y. G., & Shibasaki, H. (1997). The cortical generators of the contingent negative variation in humans: A study with subdural electrodes. *Electroencephalography and Clinical Neurophysiology, 104*, 257–268.

Hari, R., Karhu, J., Hamalainen, M., Knuutila, J., Salonen, O., Sams, M.& Vilkman, V. (1993). Functional organization of the human first and second somatosensory cortices: a neuromagnetic study. *European Journal of Neuroscience, 5*, 724 34.

Hazeltine, E. (2001). Ipsilateral sensorimotor regions and motor sequence learning. Trends in *Cognitive Sciences, 5*, 281-282.

Hazeltine, E., Bunge, S.A., Scanlon, M.D. & Gabrieli, J.D. (2003). Material-dependent and material-independent selection processes in the frontal and parietal lobes: an event-related fMRI investigation of response competition. *Neuropsychologia, 41*, 1208-1217.

Heeger, D. J. & Ress, D. (2002). What does fMRI tell us about neuronal activity? Nature Reviews *Neuroscience, 3*, 142-151.

Heeger, D.J., Huk, A.C., Geisler, W.S.& Albrecht, D.G. (2000). Spikes versus BOLD: what does neuroimaging tell us about neuronal activity? *Nature Neuroscience, 3*, 631-633.

Heilman, K. M., & Gonzalez Rothi, L. J. (1993). Apraxia. In Heilman, K. M. & Valenstein, E. (eds.), *Clinical Neuropsychology*. Oxford University Press, New York, pp. 141–150.

Henson, R.N.A., Rugg, M.D. & Friston, K.J. (2001). The choice of basis functions in eventrelated fMRI. *Neuroimage, 13*, 127.

Hepp-Reymond, M.C., Huesler, E.J. & Maier, M.A. (1996). Precision grip in humans: temporal and spatial synergies. In: Wing, A.M., Haggard, P. & Flanagan, J.R. (Eds). *Hand and Brain: the Neurophysiology and Psychology of Hand Movements* (pp. 37-62). San Diego: Academic press.

Holsapple, J.W., Preston, J.B. & Strick, P.L. (1991). The origin of thalamic inputs to the "hand" representation in the primary motor cortex. *The Journal of Neuroscience, 11*, 2644-54.

Hoshi, E. & Tanji, J. (2000). Integration of target and body-part information in the premotor cortex when planning action. *Nature, 408*, 466-470.

Hoshi, E. & Tanji, J. (2002). Contrasting neuronal activity in the dorsal and ventral premotor

areas during preparation to reach. *Jorunal of Neurophysiology, 87*, 1123-1128.

Hoshi, E. & Tanji, J. (2004a). Functional specialization in dorsal and ventral premotor areas. *Progress in Brain Research, 143*, 507-511.

Hoshi, E. & Tanji, J. (2004b). Differential roles of neuronal activity in the supplementary and presupplementary motor areas: from information retrieval to motor planning and execution. *Journal of Neurophysiology, 92*, 3482-3499.

Hoshi, E. & Tanji, J. (2004c). Area-selective neuronal activity in the dorsolateral prefrontal cortex for information retrieval and action planning. *Journal of Neurophysiology, 91*, 2707-2722.

Hoshi, E. & Tanji, J. (2006). Differential involvement of neurons in the dorsal and ventral premotor cortex during processing of visual signals for action planning. *Journal of Neurophysiology*, *95*, 3596-3616.

Hoshi, E., & Tanji, J. (2002). Contrasting neuronal activity in the dorsal and ventral premotor areas during preparation to reach. *Journal of Neurophysiology*, *87*, 1123-1128.

Hoshi, E., Sawamura, H. & Tanji, J. (2005). Neurons in the rostral cingulate motor area monitor multiple phases of visuomotor behavior with modest parametric selectivity. *Journal of Neurophysiology, 94*, 640-656.

Huettel, S. A., Song, A. W., & McCarthy, G. (2004). *Functional magnetic resonance imaging* (Vol. 1). Sunderland: Sinauer Associates.

Hyvärinen, A. (2013). Independent component analysis: recent advances. *Philosophical Transactions of the Royal Society A: Mathematical, Physical and Engineering Sciences*, 371(1984).

Hyvärinen, A., Hurri, J., & Hoyer, P. O. (2009). Independent component analysis. In *Natural Image Statistics* (pp. 151-175). Springer London.

Hyvärinen, A., Karhunen, J., & Oja, E. (2001). What is Independent Component Analysis? *Independent Component Analysis*, 145-164.

Iacoboni, M. (1999). Modulation of motor and premotor activity during imitation of targetdirected actions. *Cerebral Cortex, 12*, 847-855.

Jakobson, L.S. & Goodale, M.A. (1991). Factors affecting higher-order movement planning: a kinematic analysis on human prehension. *Experimental Brain Research, 86*, 199-208.

James, T.W., Culham, J.C., Humphreys, G.K., Milner, A.D. & Goodale, M.A. (2003). Ventral occipital lesions impair object recognition but not object-directed grasping: an fMRI Study. *Brain, 126*, 2463–2475.

Jeannerod M (1981). Intersegmental coordination during reaching at natural visual objects. In: Long J, Baddley A, editors. *Attention and Performances IX*. Hillsdale, NJ: Erlbaum; pp153–168.

Jeannerod, M. (1984). The timing of natural prehension movements. *Journal of Motor Behaviour, 16*, 235-254.

Jeannerod, M. (1986). Mechanisms of visuomotor coordination: a Study in normal and braindamaged subjects. *Neuropsychologia, 24*, 41–78.

Jeannerod, M., Arbib, A., Rizzolatti, G. & Sakata, H. (1995). Grasping objects: the cortical mechanisms of visuomotor transformation. *Trends in Neuroscience, 18*, 314–320.

Jenkinson, M. (2002). Registration, Brain Atlases and Cortical Flattening. In: Jezzard, P. Matthews, P.M. & Smith, S.M.: *Functional MRI: an introduction to methods*. (pp. 271-294). Oxford: Oxford University Press.

Jezzard, P & Clare (2002). Principles of Nuclear Magnetic Resonance and MRI. In : Jezzard, P. Matthews, P.M. & Smith, S.M.: *Functional MRI: an introduction to methods*. (pp. 67-92) Oxford: Oxford University Press.

Johansson, R.S. (1998). Sensory input and the control of grip. In G.R. Block & J.A. Goode (Eds), Novartis Foundation Symposia: Vol. 219. *Sensory Guidance of Movement* (pp. 45-63). New York: John Wiley.

Johnson, P.B., Ferraina, S., Bianchi, L. & Caminiti, R. (1996). Cortical networks for visual reaching: physiological and anatomical organization of frontal and parietal lobe arm regions. *Cerebral Cortex, 6*, 102-119.

Jorge, J., Van Der Zwaag, W., & Figueiredo, P. (2013). EEG-fMRI integration for the study of human brain function. *NeuroImage*.

Josephs, O., Turner, R. & Friston, K.J. (1997). Event-related fMRI. *Human Brain Mapping, 5*, 243-248.

Jung TP, Makeig S, Westerfield M, Townsend J, Courchesne E, et al (2000). Removal of eye activity artifacts from visual event-related potentials in normal and clinical subjects. *Clinical Neurophysiology, 111*, 1745-1758.

Jung, T.P., Humphries, C., Lee, T.W., McKeown, M.J., Iragui, V. & Sejnowski, T.J. (2000). Removing electroencephalographic artifacts by blind source separation. *Psychophysiology, 37*, 163-78.

Jung, T.P., Makeig, S., Humphries, C., Lee, T.W., McKeown, M.J., Iragui, V. & Sejnowski, T.J. (2000). Removing electroencephalographic artifacts by blind source separation. *Psychophysiology, 37*, 163-78.

Jutten, C., & Herault, J. (1991). Blind separation of sources, part I: An adaptive algorithm based on neuromimetic architecture. *Signal processing, 24*, 1-10.

Kalaska, J.F. & Crammond, D.J. (1992). Cerebral cortical mechanisms of reaching movements. *Science, 255*, 1517-1523.

Kalaska, J.F., Scott, S.H., Cisek, P. & Sergio, L.E. (1997). Cortical control of reaching movements. *Current Opinion in Neurobiology, 7*, 849-859.

Kawashima, R., Satoh, K., Itoh, H., Ono, S., Furumoto, S., Gotoh, R., Koyama, M., Yoshioka, S., Takahashi, T., Takahashi, K., Yanagisawa, T. & Fukuda, H. (1996). Functional anatomy of GO/NO-GO discrimination and response selection-a PET study in man. *Brain Research, 728*, 79-89.

Kertzman, C., Schwarz, U., Zeffiro, T.A. & Hallett M. (1997). The role of posterior parietal cortex in visually guided reaching movements in humans. *Experimental Brain Research, 114*, 170-83.

Kiebel, S. & Holmes, A. (2003). The general linear model. In: Frackowiak, R.S.J., Friston, K.J.,Frith, C.D., Dolan, R.J., Price, C.J., Zeki, S., Ashburner, J. & Penny, W. (Eds). *Human Brain Function.* (pp. 725-750) San Diego: Elsevier Academic Press.

Kok A (1986). Effects of degradation of visual stimulation on components on the event-related

potential (ERP) in go/nogo reaction tasks. *Biological Psychology 23*, 21-38.

Konen, C. S., Mruczek, R. E., Montoya, J. L., & Kastner, S. (2013). Functional organization of human posterior parietal cortex: grasping-and reaching-related activations relative to topographically organized cortex. *Journal of Neurophysiology, 109*, 2897-2908.

Kourtis D, Sebanz N, Knoblich G (2012). EEG correlates of Fitts's law during preparation for action. *Psychological Research 76*, 514-524.

Kritikos, A., Jackson, G.M., Jackson, S.R. (1998). The influence of initial hand posture on the expression of prehension parameters. *Experimental Brain Research*, *119*, 9-16.

Króliczak G, Cavina-Pratesi C, Goodman D, Culham JC (2007). What does the brain do when you fake it? An FMRI study of pantomimed and real grasping. *Journal of Neurophysiology 97*, 2410–2422.

Kuhtz-Buschbeck, J. P., Stolze, H., Boczek-Funcke, A., Jöhnk, K., Heinrichs, H., & Illert, M. (1998a). Kinematic analysis of prehension movements in children. *Behavioral Brain Research, 93*, 131–141.

Kuhtz-Buschbeck, J. P., Stolze, H., Jöhnk, K., Boczek-Funcke, A., & Illert, M. (1998b). Development of prehension movements in children: A kinematic study. *Experimental Brain Research, 122*, 424–432.

Kwong, K.K., Belliveau, J.W., Chesler, D.A., Goldberg, I.E., Weisskoff, R.M., Poncelet, B.P., Kennedy, D. N., Hoppel, B.E., Cohen, M.S., Turner, R. et al. (1992). Dynamic magnetic resonance imaging of human brain activity during primary sensory stimulation. *Proceedings of the National Academy of Science, 89*, 5675-5679.

Lacourse, M.G., Orr, E.L., Cramer, S.C. & Cohen, M.J. (2005). Brain activation during execution and motor imagery of novel and skilled sequential hand movements. *Neuroimage 27*, 505-519.

Lamarche, M., Louvel, J., Buser, P., & Rektor, I. (1995). Intracerebral recordings of slow potentials in a contingent negative variation paradigm: An exploration in epileptic patients. *Electroencephalography and Clinical Neurophysiology, 95*, 268–276.

Lang, C.E. & Schieber, M.H. (2004). Reduced muscle selectivity during individuated finger

movements in humans after damage to the motor cortex or corticospinal tract. Journal of. *Neurophysiology, 91*, 1722–1733.

Lawrence, D.G. & Hopkins, D.A. (1976). The development of motor control in the rhesus monkey: evidence concerning the role of corticomotoneuronal connections. *Brain, 99*, 235–254.

Lemieux, L., Salek-Haddadi, A., Josephs, O., Allen, P., Toms, N., Scott, C., ... & Fish, D. R. (2001). Event-related fMRI with simultaneous and continuous EEG: description of the method and initial case report. *Neuroimage, 14*, 780-787.

Lemon, R. N., Nijs, H. G. T., & Kuypers, H. G. J. M. (1981). Behaviour of neurons in monkey peri-arcuate and precentral cortex before and during visually guided arm and hand movements. *Experimental Brain Research, 44*, 113-116.

Leuthold H, Jentzsch I (2009). Planning of rapid aiming movements and the contingent negative variation: are movement duration and extent specified independently*? Psychophysiology 46,* 539-550.

Leuthold, H., Sommer, W., & Ulrich, R. (2004). Preparing for action: Inferences from CNV and LRP. *Journal of Psychophysiology, 18*, 77-88.

Levy, I., Schluppeck, D., Heeger, D.J., Glimcher, P.W. (2007). Specificity of human cortical areas for reaches and saccades. *The Journal of Neuroscience, 27*, 4687–4696.

Liu, T.T. (2004). Efficiency, power and entropy in event-related fMRI with multiple trial types: Part II: Design of experiments. *Neuroimage, 21*, 401-413.

Logothetis, N.K. & Wandell, B.A. (2004). Interpreting the BOLD signal. *Annual Review of Physiology, 66*, 735-769.

Loveless NE, Sanford AJ (1974). Slow potential correlates of preparatory set. *Biological Psychology 1*, 303-314.

Luck, S. J. (2005). An introduction to the event-related potential technique (*Cognitive Neuroscience*). The MIT Press Cambridge.

Luck, S. J., & Girelli, M. (1998). Electrophysiological approaches to the study of selective attention in the human brain. *The Attentive Brain*, 71-94.

Luppino, G., Calzavara, R., Rozzi,S. & Matelli, M. (2001). Projections from the superior temporal sulcus to the agranular frontal cortex in the macaque. *European Journal of Neuroscience, 14*, 1035-1040.

Luppino, G., Murata, A., Covoni, P. & Matelli, M. (1999). Largely segregated parietofrontal connections linking rostral intraparietal cortex (areas AIP and VIP) and the ventral premotor cortex (areas F5 and F4). *Experimental Brain Research,128*, 181–187.

Luppino, G., Rozzi, S., Calzavara, R.& Matelli, M. (2003). Prefrontal and agranular cingulate projections to the dorsal premotor areas F2 and F7 in the macaque monkey. *European Journal of Neuroscience, 17*, 559-78.

MacKenzie, C. L., Marteniuk, R. G., Dugas, C., Liske, D., & Eickmeier, B. (1987). Three-dimensional movement trajectories in Fitts' task: implications for control. *The Quarterly Journal of Experimental Psychology*, *39*, 629-647.

Malmivuo, J., & Plonsey, R. (1995). *Bioelectromagnetism: principles and applications of bioelectric and biomagnetic fields*. Oxford University Press.

Malonek, D.& Grinvald, A. (1996). Interactions between electrical activity and cortical microcirculation revealed by imaging spectroscopy: implications for functional brain mapping. *Science, 26*, 551-554.

Manthey, S., Schubotz, R.I.& von Cramon, D.Y. (2003). Premotor cortex in observing erroneous action: an fMRI Study. *Brain Research Cognitive Brain Research, 15*, 296-307.

Maranesi, M., Rodà, F., Bonini, L., Rozzi, S., Ferrari, P. F., Fogassi, L., & Coudé, G. (2012). Anatomo-functional organization of the ventral primary motor and premotor cortex in the macaque monkey. *European Journal of Neuroscience, 36*, 3376-3387.

Mari, M., Castiello, U., Marks, D., Marraffa, C. & Prior, M. (2003). The reach to grasp movement in children with autism spectrum disorder. *Philosophical Transactions of the Royal Society of London, 358*, 393-403.

Marteniuk, R.G., Leavitt, J.L., Mackenzie & C.L., Athenes, S. (1990). Functional relationship between grasp and transport components in prehension task. *Human Movement Science, 9*, 149-176.

Martin, R. D. (1990). *Primate origins and evolution: a phylogenetic reconstruction* (p. 804). Princeton: Princeton University Press.

Mascaro, M., Battaglia-Mayer, A., Nasi, L., Amit, D.J., & Caminiti, R. (2003). The eye and the hand: neural mechanisms and network models for oculomanual coordination in parietal cortex. *Cerebral Cortex, 13*, 1276-1286.

Mason, C.R., Hendrix, C.M.& Ebner, T.J. (2006). Purkinje cells signal hand shape and grasp force during reach to grasp in the monkey. *Journal of Neurophysiology, 95*, 144-158.

Mason, C.R., Theverapperuma, L.S., Hendrix, C.M. & Ebner, T.J. (2004). Monkey hand postural synergies during reach to grasp in absence of vision of the hand and object. *Journal of Neurophysiology, 91*, 2826-2837.

Matelli, M. & Luppino, G. (1996). Thalamic input to mesial and superior area 6 in the macaque monkey. *Journal of Computational Neurology, 372*, 59-87.

Matelli, M. & Luppino, G. (2001). Parietofrontal circuits for action and space perception in the macaque monkey. *Neuroimage,14*, 27–32.

Matelli, M., Luppino, G. & Rizzolatti, G. (1985). Patterns of cytochrome oxidase activity in the frontal agranular cortex of the macaque monkey. *Behavioral Brain Research,18*, 125–136.

Mattay, V.S., Callicott, J.H., Bertolino, A., Santha, A.K., Van Horn, J.D., Tallent, K.A., Frank, J.A. & Weinberger, D.R. (1998). Hemispheric control of motor function: a whole brain echo planar fMRI Study. *Psychiatry Research: Neuroimaging, 83*, 7-22.

McDowell, K., Jeka, J.J., Schöner, G. & Hatfield, B.D. (2002). Behavioral and electrocortical evidence of an interaction between probability and task metrics in movement preparation. *Experimental Brain Resesarch, 144*, 303-313.

Medendorp, W. P., Goltz, H. C., Crawford, J. D. & Vilis, T. (2005). Integration of target and effector information in human posterior parietal cortex for the planning of action. *Journal of Neurophysiology, 93*, 954-962.

Medendorp, W.P, Goltz, H.C., Vilis, T. &Crawford, J.D. (2003). Gaze-centered updating of visual space in human parietal cortex. *The Journal of Neuroscience, 23*, 6209-6214.

Meyer, G. (1987). Forms and spatial arrangement of neurons in the primary motor cortex of man.

Journal of Comparative Neurology, 262, 402-428.

Meyer, M., Friederici, A.D.& von Cramon, D.Y. (2000). Neurocognition of auditory sentence comprehension: event related fMRI reveals sensitivity to syntactic violations and task demands. *Cognitive Brain Research, 9*, 19-33.

Milner, A.D., Dijkerman, H.C., Pisella, L., McIntosh, R.D., Tilikete, C., Vighetto, A. & Rossetti,Y. (2001). Grasping the past. delay can improve visuomotor performance. *Current Biology, 11*, 1896-1901.

Mishkin M, Ungerleider LG. (1982). Contribution of striate inputs to the visuospatial functions of parieto-preoccipital cortex in monkeys. *Behavioral Brain Research, 6*, 57-77.

Moliner, J.L., Brenner, E., Smeets, J.B.J. (2007). Effects of texture and shape on perceived time to passage: knowing what influences judging when. *Perception&Psychophysics, 69*, 887-894.

Moll L, Kuypers HG (1977). Premotor cortical ablations in monkeys: contralateral changes in visually guided reaching behavior. *Science 198*, 317-319.

Monaco, S., Chen, Y., Medendorp, W. P., Crawford, J. D., Fiehler, K., & Henriques, D. Y. (2013). Functional magnetic resonance imaging adaptation reveals the cortical networks for processing grasp-relevant object properties. *Cerebral Cortex, 1, 1-15.*

Muir, R.B. & Lemon, R.N. (1983). Corticospinal neurons with a special role in precision grip. *Brain Research, 261*, 312–316.

Mulert, C., & Lemieux, L. (Eds.). (2010). EEG-fMRI: Physiological basis, technique, and applications. Springer.

Müller-Gethmann H, Rinkenauer G, Stahl J, Ulrich R (2000). Preparation of response force and movement direction: onset effects on the lateralized readiness potential. *Psychophysiology 37,* 507-514.

Mullinger, K., & Bowtell, R. (2011). Combining EEG and fMRI. In *Magnetic Resonance Neuroimaging* (pp. 303-326). Humana Press.

Murata, A., Fadiga, L., Fogassi, L., Gallese, V., Raos, V. & Rizzolatti G. (1997). Object representation in the ventral premotor cortex (area F5) of the monkey. *Journal of*

Neurophysiology, 78, 2226–2230.

Murata, A., Gallese, V., Luppino, G., Kaseda, M. & Sakata, H. (2000). Selectivity for the shape, size, and orientation of objects for grasping in neurons of monkey parietal area AIP. *Journal of. Neurophysiology, 83*, 2580–2601.

Napier, J. R. (1960). Studies of the hands of living primates. *Proceedings of the Zoological Society of London, 134*, 647-657.

Napier, J.R. (1961). Prehensility and opposability in the hands of primates. *Symposia of the. Zoologic Society, 5*, 115-132.

Naranjo, J.R., Brovelli, A., Longo, R., Budai, R., Kristeva, R. & Battaglini, P.P. (2007). EEG dynamics of the frontoparietal network during reaching preparation in humans. *Neuroimage, 34*, 1673-1682.

Niazy, R.K., Beckmann, C.F., Iannetti, G.D., Brady, J.M., Smith, S.M., 2005. Removal of FMRI environment artifacts from EEG data using optimal basis sets. *Neuroimage 28*, 720–737.

Nudo, R. J. & Masterton, R. B. (1986). Stimulation-induced [14C]2-deoxyglucose labeling of synaptic activity in the central auditory system. *Journal of Comparative Neurology, 245*, 553-565.

Nunez, P. L., & Silberstein, R. B. (2000). On the relationship of synaptic activity to macroscopic measurements: Does co-registration of EEG with fMRI make sense? *Brain Topography, 13*, 79-96.

Nunez, P. L., & Srinivasan, R. (2007). Electroencephalogram. *Scholarpedia, 2*, 1348.

Ogawa, S., Lee, T.M., Kay, A.R. & Tank, D.W. (1990). Brain magnetic Resonance imaging with contrast dependent on blood oxygenation. *Proceedings of the National Academy of Science,87*, 9868-9872.

Ogawa, S., Tank, D.W., Menon, R., Ellermann, J.M., Kim, S.G., Merkle, H. & Ugurbil, K. (1992). Intrinsic signal changes accompanying sensory stimulation: functional brain mappingwith magnetic resonance imaging. *Proceedings of the National Academy of Science, 89*, 5951-5955.

Oldfield, R.C. (1971). The assessment and analysis of handedness: the Edinburgh inventory.

Neuropsychologia, 9, 97-113.

Olivier E, Davare M, Andres M, Fadiga L (2007). Precision grasping in humans: from motor control to cognition. *Current Opinion in Neurobiology 17*, 644–648.

Passingham, R. E. (1987). Two cortical systems for directing movement. *Motor Areas of the Cerebral Cortex*, *132*.

Passingham, R.E. (1996). Functional specialization of the supplementary motor area in monkeys and humans. *Advances in Neurology, 70*, 105-116.

Passingham, R.E., Toni, I. & Rushworth, M.F. (2000). Specialisation within the prefrontal cortex: the ventral prefrontal cortex and associative learning. *Experimental Brain Research, 133*, 103-113.

Pellijeff, A., Bonilha, L., Morgan, P. S., McKenzie, K., & Jackson, S. R. (2006). Parietal updating of limb posture: an event-related fMRI study. *Neuropsychologia, 44*, 2685-2690.

Penny, W.D., Holmes, A.P., & Friston, K.J. (2003). Random effect analysis. In: Frackowiak, R.S.J., Friston, K.J., Frith, C.D., Dolan, R.J., Price, C.J., Zeki, S. Ashburner, J. & Penny, W.D. (Eds). *Human Brain Function.* (pp. 843-850). San Diego: Elsevier Academic Press.

Philips, C.G. (1985). *Movements of the hand. Liverpool*. University Press.

Picard, N. & Strick, P.L. (2001). Imaging the premotor areas. *Current Opinion in Neurobiology, 11*, 663-672.

Pisella, L., Grea, H., Tilikete, C., Vighetto, A., Desmurget, M., Rode, G., Boisson, D. & Rossetti, Y. (2000). An 'automatic pilot' for the hand in human posterior parietal cortex: toward reinterpreting optic ataxia. *Nature Neuroscience, 3*, 729-736.

Prablanc, C., Desmurget, M. & Grea, H. (2003). Neural control of on-line guidance of hand reaching movements. *Progress in Brain Research, 142*, 155-70.

Prado, J., Clavagnier, S., Otzenberger, H., Scheiber, C., Kennedy, H. & Perenin, M.T. (2005). Two cortical systems for reaching in central and peripheral vision. *Neuron, 48*, 849-858.

Prescoot, J. (1986). The effects of response parameters on CNV amplitude.*Biological psychology*, *22*, 107-135.

Ramnani, N., Behren, T.E.J., Penny, W. & Matthews, P.M. (2004). New approaches for exploring anatomical and functional connectivity in the human brain. *Biological Psychiatry, 56*, 613–619.

Raos V, Umiltá MA, Murata A, Fogassi L, Gallese V (2006). Functional properties of grasping-related neurons in the ventral premotor area F5 of the macaque monkey. *Journal of Neurophysiology, 95*, 709-729.

Raos, V., Umiltá, M. A., Gallese, V., & Fogassi, L. (2004). Functional properties of grasping-related neurons in the dorsal premotor area F2 of the macaque monkey. *Journal of Neurophysiology, 92*, 1990-2002.

Ress, D., Backus, B.T. & Heeger, D.J. (2000). Activity in primary visual cortex predicts performance in a visual detection task. *Nature Neuroscience, 3*, 940-945.

Rice, N.J., Tunik, E. & Grafton S.T. (2006). The anterior intraparietal sulcus mediates grasp execution, independent of requirement to update: new insights from transcranial magnetic stimulation. *Nature Neuroscience, 26*, 8176-8182.

Riehle, A., & Requin, J. (1995). Neuronal correlates of the specification of movement direction and force in four cortical areas of the monkey. *Behavioral Brain Research, 70*, 1–13.

Ritter, P., & Villringer, A. (2006). Simultaneous EEG–fMRI. *Neuroscience & Biobehavioral Reviews, 30*, 823-838.

Rizzolatti G, Camarda R, Fogassi L, Gentilucci M, Luppino G, et al. (1988). Functional organization of inferior area 6 in the macaque monkey. II. Area F5 and the control of distal movements. *Experimental Brain Research 71*, 491-507.

Rizzolatti, G & Luppino, G. (2001). The cortical motor system. *Neuron, 31*, 889–901.

Rizzolatti, G. & Arbib, M.A. (1998a). Language within our grasp. *Trends in Neurosciences, 21*,188-194.

Rizzolatti, G., Camarda, L., Fogassi, L., Gentilucci, M., Luppino, G. & Matelli, M. (1988). Functional organization of inferior area 6 in the macaque monkey. II. Area F5 and the control of distal movements. *Experimental. Brain Research, 71*, 491–507.

Rizzolatti, G., Fadiga, L., Matelli, M., Bettinardi, V., Paulesu, E., Perani, D. & Fazio, F.(1996).

Localization of grasp representations in humans by PET: 1. Observation versus execution. *Experimental Brain Research, 111*, 246-52.

Rizzolatti, G., Fogassi, L. & Gallese, V. (2002). Motor and cognitive functions of the ventral premotor cortex. *Current Opinion in Neurobiology, 12*, 149–154.

Rizzolatti, G., Luppino, G. & Matelli M. (1998b). The organisation of the cortical motor system:new concepts. *Electroencephalography and Clinical. Neurophysiology, 106*, 283–296.

Robertson, E.M. (2000). Neural features of the reach and grasp. *Motor Control, 4*, 117–120.

Rohrbaugh J, Gaillard AWK (1983). Sensory and motor aspects of the contingent negative variation. In Gaillard AWK, Ritter W, editors. *Tutorials in event-related potential research: Endogenous components,* pp. 269–310.

Rosa, M. J., Daunizeau, J., & Friston, K. J. (2010). EEG-fMRI integration: a critical review of biophysical modeling and data analysis approaches. *Journal of integrative neuroscience, 9*, 453-476.

Rose, M.D. (1992). Kinematics of the trapezium first metacarpal joint in extant anthropoids and Miocene hominoids. *Journal of Human Evolution, 22*, 255-266.

Rosenkranz, K., & Lemieux, L. (2010). Present and future of simultaneous EEG-fMRI. Magnetic Resonance Materials in Physics, *Biology and Medicine,23* , 309-316.

Roy, A.C., Paulignan, Y., Farnè, A., Jouffrais, C. & Boussaoud, D. (2000). Hand kinematics during reaching and grasping in the macaque monkey. *Behavioral Brain Research, 117*, 75–82.

Sanes, J.N. & Schieber, M.H. (2001). Orderly somatotopy in primary motor cortex: does it exist? *Neuroimage, 13*, 968–974.

Santello, M. & Soetching, J.F. (1998). Gradual molding of the hand to object contours. *Journal of Neurophysiology, 79*, 1307-1320.

Santello, M., Flanders, M. & Soetching, J.F. (2002). Patterns of hand motion during grasping and the influence of sensory guidance. *Journal of Neuroscience, 22*, 1426-1435.

Savelsbergh, G.J.P., Steenbergen, B. & van der Kamp, J. (1996). The role of fragility in the guidance for precision grip. *Human Movement Science, 15*, 115-127.

Schubotz, R,I, & von Cramon, D.Y. (2001). Interval and ordinal properties of sequences are associated with distinct premotor areas. *Cerebral Cortex, 11*, 210-222.

Schubotz, R.I. & von Cramon, D.Y. (2003). Functional-anatomical concepts of human premotor cortex: evidence from fMRI and PET studies. *Neuroimage, 20*, S120-131.

Schubotz, R.I. & von Cramon, Y. (2002). Dynamic patterns makes the premotor cortex interested in objects: influence of stimulus and task revealed by fMRI. *Cognitive Brain Research, 14*, 357-369.

Sereno, A.B. & Maunsell, J.H. (1998). Shape selectivity in primate lateral intraparietal cortex. *Nature, 395*, 500-503.

Sereno, M.I., Pitzalis, S., Martinez, A. (2001). Mapping of contralateral space in retinotopic coordinates by a parietal cortical area in humans. *Science, 294*, 1350-1354.

Shadmehr, R., & Wise, S.P. (2005). *Computational Neurobiology of Reaching and Pointing: A Foundation for Motor Learning.* MIT Press, Cambridge MA.

Shibasaki H, Hallett M (2006). What is the Bereitschaftspotential? *Clinical Neurophysiology, 17*, 2341-2356.

Shima, K., Mushiake, H., Saito, N., & Tanji, J. (1996). Role for cells in the presupplementary motor area in updating motor plans. *Proceedings of the National Academy of Sciences, 93*, 8694-8698.

Smeets, J.B.J. & Brenner, E. (1999). A new view on grasping. *Motor Control, 3*, 237-271.

Stern, J.T. & Susman, R.L. (1987). The locomotor anatomy of the Australopithecus afarensis. *American Journal of Physical Anthropology, 60*, 279-317.

Stone, JV (2004). *Independent Component Analysis: A Tutorial Introduction*, MIT Press, Boston

Tai, Y.F., Scherfler, C., Brooks, D.J., Sawamoto,N. & Castiello, U. (2004). The human premotor cortex is 'mirror' only for biological actions. *Current Biology, 14*, 117-120.

Taira, M., Mine, S., Georgopoulos, A.P., Murata, A. & Sakata, H. (1990). Parietal cortex neurons

of the monkey related to the visual guidance of hand movement. *Experimental Brain Research, 83*, 29-36.

Talairach J. & Tournoux P. (1988). Co-Planar Stereotaxic Atlas of the Human Brain Stuttgart, Germany: Thieme.

Tanné-Gariépy, J., Rouiller, E.M., & Boussaoud, D. (2002). Parietal inputs to dorsal versus ventral premotor areas in the macaque monkey: evidence for largely segregated visuomotor pathways. *Experimental Brain Research, 145*, 91-103.

Thoenissen, D., Zilles, K. & Toni, I. (2002). Differential involvement of parietal and precentral regions in movement preparation and motor intention. *The Journal of Neuroscience, 22*, 9024-9034.

Toni, I., Thoenissen, D. & Zilles, K. (2001). Movement preparation and motor intention. *Neuroimage, 14*, 110-117.

Tubiana, R. (1981). Architecture and function of the hand. In: R. T. Tubiana (Ed.). *The Hand*. Saunders (pp. 19-93). Philadelphia.

Tunik, E., Frey, S.H. & Grafton S.T. (2005). Virtual lesions of the anterior intraparietal area disrupt goal-dependent on-line adjustment of grasp. *Nature Neuroscience, 8*, 505-511.

Tunik, E., Houk, J. C., & Grafton, S. T. (2009). Basal ganglia contribution to the initiation of corrective submovements. *Neuroimage, 47*, 1757-1766.

Tunik, E., Rice, N. J., Hamilton, A., & Grafton, S. T. (2007). Beyond grasping: representation of action in human anterior intraparietal sulcus. *Neuroimage, 36*, T77-T86.

Uğurbil K, Toth L & Kim DS (2003). How accurate is magnetic resonance imaging of brain function? *Trends in Neurosciences, 26*, 108-114.

Ullsperger, M., & Debener, S. (2010). *Simultaneous EEG and fMRI: recording, analysis and application*. Oxford: Oxford University Press.

Umilta MA, Brochier T, Spinks RL, Lemon RN (2007). Simultaneous recording of macaque premotor and primary motor cortex neuronal populations reveals different functional contributions to visuomotor grasp. *Journal of Neurophysiology, 98*, 488-501.

Umilta, M.A. (2004). Frontal cortex: goal-relatedness and the cortical motor system. *Current Biology, 14*, 204-206.

Ungerleider, L.G. & Mishkin, M. (1982). Two cortical visual systems In:Ingle, D.J., Goodale, M.A. & Mansfield, R.J.W. (Eds), *Analysis of visual behaviour* (pp. 549 586). Cambridge, MA: The MIT Press.

Van de Kamp, Bongers, R.M., Zaal, F.T.J.M. (2009). Effects of changing object size during prehension. *Journal of Motor Behavior, 41*, 427-435.

Van de Kamp, C., Zaal, F.T.J.M. (2007). Prehension id really reaching and grasping. *Experimental Brain Research, 182*, 27-34.

Veltman, D. & Hutton, C. (2000). SPM99 Manual. Technical report. Wellcome Department of Imaging Neuroscience, London, UK.

Verhagen L, Dijkerman HC, Medendorp WP, Toni I (2012). Cortical dynamics of sensorimotor integration during grasp planning. *The Journal of Neuroscience, 32*, 4508-4519.

Walsh, V & Rushworth, M.F.S. (1999). A primer of magnetic stimulation as a tool for neuropsychology. *Neuropsychologia, 37*, 125–136.

Walter WG (1964). Slow potential waves in the human brain associated with the expectancy, attention and decision. *Arch für Psychiatr Nervenkr, 206*, 309-322.

Weinrich M, Wise SP (1982). The premotor cortex of the monkey. *The Journal of Neuroscience, 2*, 1329–1345.

Weinrich, M., Wise, S.P.& Mauritz, K.H. (1984). A neurophysiological study of the premotor cortex in the rhesus monkey. *Brain, 107*, 385-414.

Weir, P.L., Mackenzie, C.L., Marteniuk, R.G. & Cargoe, S.L. (1991a). Is object texture constraint on human prehension? *Journal of Motor Behavior, 23*, 205-210.

Weir, P.L., Mackenzie, C.L., Marteniuk, R.G., Cargoe, S.L. & Fraser, M.B. (1991b). The effects of object weight on the kinematics of prehension. *Journal of Motor Behavior, 23*, 192-204.

Welsh, T.N., Elliott, D. & Weeks, D.J. (1999). Hand deviations toward distractors. Evidence for response competition. *Experimental Brain Research, 127*, 207-212.

Wheaton, L. A., Shibasaki, H., & Hallett, M. (2005b). Temporal activation pattern of parietal and premotor areas related to praxis movements. *Clinical Neurophysiology, 116*, 1201-1212.

Wheaton, L. A., Yakota, S., & Hallett, M. (2005a). Posterior parietal negativity preceding self-paced praxis movements. *Experimental brain research, 163*, 535-539.

Winter, D. A. (1991). Biomechanics and Motor Control of Human Movement, 2nd edn. Wiley and Sons, Toronto. Wise, S.P., Boussaoud, D., Johnson, P.B. & Caminiti, R. (1997) Premotor and parietal cortex: Corticocortical connectivity and combinatorial computations. *Annual Review of Neuroscience, 20*, 25-42.

Wise, S.P., di Pellegrino, G. & Boussaoud, D. (1996). The premotor cortex and nonstandard sensorimotor mapping. *Canadian Journal of Physiological Pharmacology, 74*, 469-482.

Wolpert, D.M. & Ghahramani, Z. (2000). Computational principles of movement neuroscience. *Nature Neuroscience, 3*, 1212-1217.

Wolpert, D.M., Goodbody, S.J., & Husain, M. (1998). Maintaining internal representations: the role of the human superior parietal lobe. *Nature Neuroscience, 1*, 529-533.

Woodward, A.L. & Sommerville, J.A. (2000).Twelve-month-old infants interpret action in context. *Psychological Science, 11*, 73-77.

Worsley, K.J., Evans, A.C., Marrett, S. & Neelin, P. (1992). A three-dimensional statistical analysis for CBF activation studies in human brain. *Journal Cerebral of Blood Flow Metabolism, 12*, 900-918

Worsley, K.J., Marrett, S., Neelin, P., Vandal, A.C., Friston, K.J. & Evans, A.C. (1996). A unified statistical approach for determining significant voxels in images of cerebral activation. *Human Brain Mapping, 4*, 58-73.

Xiao J, Padoa-Schioppa C, Bizzi E (2006). Neuronal correlates of movement dynamics in the dorsal and ventral premotor area in the monkey. *Experimental Brain Research, 168*, 106-119.

Zaepffel, M., & Brochier, T. (2012). Planning of visually guided reach-to-grasp movements: Inference from reaction time and contingent negative variation (CNV). *Psychophysiology, 49*, 17-30.

Zilles, K., Schlaug, G., Matelli, M., Luppino, G., Schleicher, A., Qu, M., Dabringhaus, A., Seitz, R. & Roland, P.E. (1995). Mapping of human and macaque sensorimotor areas by integrating architectonic, transmitter receptor, MRI and PET data. *Journal of Anatomy, 187*, 515-537.

Zoia, S., Blason, L., D'Ottavio, G., Bulgheroni, M., Pezzetta, E., Scabra, A. & Castiello, U. (2007). Evidence of early development of action planning in the human foetus: a kinematic Study. *Experimental Brain Research, 176*, 217-226.

Zoia, S., Pezzetta, E., Blason, L., Scabar, A., Carrozzi, M., Bulgheroni, M., Castiello, U. (2006). A comparison of the reach to grasp movement between children and adults: a kinematic study. *Developmental Neuropsychology, 30*, 719-738.

APPENDICES

APPENDIX I:KINEMATIC ANALYSIS

A kinematic assessment will provide information on the relationship of parts of the body to each other. This is useful in measuring complex movements and it has provided the basis for understanding functional activities including hand grasping. Kinematic assessment uses anatomical terminology and a spatial reference system. For instance, the position of a hand joint would be described by a set of Y, X, Z coordinates that might represent the vertical, medial-lateral, and anterior-posterior components or directions, respectively (Winter, 1991).

1. Detected variables (sensors)

All measurement procedures ought not to alter the normal behavior of the system under investigation (Kelvin rule). Following such a rule, it makes sense for motion analysis techniques to be based on a photographic approach, specifically stereophotogrammetry, to allow both body sides and complete measurements.

Kinematic variables are sampled during time. The Shannon-Nyquist theorem states that an analog waveform signal, band limited, may be uniquely reconstructed, without error, from samples taken at equal time intervals. The sampling rate must be equal to, or greater than, twice the highest frequency component of the analog signal.

The frequency content of a movement such as grasping is below 10-Hz. (Allard et al., 1995). This is mainly due to the fact that the human body is not made of rigid links and the soft tissues act as a low-pass filter. Therefore the Shannon-Nyquist theorem gives a 20-Hz lower limit for data sampling. Knowledge regarding the frequency of a specific movement is a key point when planning data acquisition. This is because setting an inappropriate (e.g., too low) sampling

frequency brings to erroneous results (aliasing phenomena). In turn this suggests that high sampling frequencies may not be necessary when the field of application is clearly defined. High frequencies (e.g., more than 100Hz) are generally needed only for sport applications.

It is important to define some parameters linked to the position measurement in order to distinguish the performance between different systems (Ehara et al., 1997). They have been defined in different ways mainly because of technology changes. The following is a possible updated list of parameters and their definition: (i) Resolution, the minimum detectable movement of a marker; (ii) Precision, the standard deviation of random error of n samples; (iii) Accuracy, the standard deviation of the systematic error from n points equally distributed over the whole measuring volume. All the values obtained from both the resolution and the precision parameters have to be checked throughout that volume.

2. Video-Based Systems

A vast amount of qualitative information can be obtained from video recording. Human movement as a total pattern can be observed and re-observed. The relationship of all body parts to each other as well as the quality of the movement - whether it is fast or slow, uncoordinated or smooth - can be seen.

Quantitative data can be obtained by digitizing the video image and subjecting the data to computer processing and analysis. Digitization is the process whereby the image or parts of the image are converted to digital form so that the data can be manipulated by a computer. In order to be able to digitize film, it is helpful to place skin markers over major anatomical landmarks prior to filming. The process of digitizing can be undertaken either manually or by use of a computer software. This process involves viewing each frame (or field) of the video tape and identifying and storing the coordinates for each of the skin markers. This operation has to be

performed for each frame of the film. The data thus obtained can be called upon when calculations are required. Manual digitizing is reliable, accurate and human error is relatively small especially with experienced digitizers. Automatic digitization is also accurate and reliable, though it is necessary to undertake manual checks to ensure that the computer does not confuse two different markers when they cross in space. Direct measurements of an image on video tape taken from the video screen are subject to considerable error and should not be used as a method of quantifying human movement.

Computer aided analysis of video tape can give a wide range of information and most systems now allow the analysis of movement in more than one plane. The computer-analysis software makes possible to plot body coordinates (centre of gravity, etc.). Knowledge of the position of the centre of gravity is important when considering the efficiency of movement. For example smooth displacements of the centre of gravity tend to indicate a more efficient movement than those where the centre of gravity is subjected to extensive vertical displacement. The computer can also generate stick diagrams which are valuable as an initial qualitative analysis of the sequence of movement.

3. Optoelectronic techniques

Optoelectronic devices require markers to be placed on the body. The coordinates of these markers are tracked throughout the movement and calculations can then be made. Unlike other techniques such as video, these systems do not give a visual image of the subject, but simply a frame-by-frame representation of the position of each marker. From this, it is possible to produce computer-generated stick figures or graphs of the position of a joint showing motion range plotted against time. This gives good quantitative information but does not address the issue of quality of movement as there is no visual representation of the actual subject. Optoelectronic

systems can be subdivided in two main classes: that using active markers and that using passive markers.

3.1. Systems Using Passive Markers

Systems using passive markers rely on reflective markers (retro-reflective material on a plastic sphere) placed on the subject's skin. Some form of light, often infra-red, is transmitted towards the subject and the rays are reflected back off the markers to a series of 'cameras' that record the marker position. A sufficient number of 'cameras' needs to be placed around the subject so that each marker is visible to a minimum of two 'cameras'. Sampling frequency may vary from 50 to 250 Hz which enables the system to track the change in position of the markers and produces a reasonable record of the gross pattern of movement. The markers have no identity, leaving the system vulnerable if cross-over of markers occurs.

The accuracy of the system relies on human input to ensure that the computer accurately identifies which is for instance the wrist marker and which is the marker on the thumb, or it is dependent on a good quality computer software that is able to correctly process the incoming data. In order to avoid errors in the data processing then tracking procedures have to be used as to identify and track the markers trajectories. For the most advanced systems, these procedures are able to track the markers by starting from a model defined by the user and identifying the representative points almost in real time. The use of different filters (i.e., with different wavelengths) for the camera and different marker color could potentially simplify the tracking algorithm.

3.2. Systems using active markers

The more expensive systems use active skin markers. Markers have their own small power pack that enables them to actively transmit infra-red rays to a receiving system of several 'cameras'. Since each marker has its own transmitting signal, the receiver picks up not only the position and displacement of the marker but can identify which marker it has picked up. This gives the advantage of differentiating between markers and removes the potential source of error that can occur when two markers cross over each other. In other words, no post-collection marker identification is needed, as time sequencing between marker illumination and detector reception uniquely identifies each light emitting diodes (LED). Each marker is activated at a slightly different (in the order of microseconds) instant in time.

3.3. Potential errors in marker-based systems

Different kinds of errors can affect the measurement of marker-based systems (Cappozzo et al., 1996): (i) stereophotogrammetric errors (the manual definition of all markers), coming from various sources linked to the specific hardware and software equipment used (their value is in the range of 0.5-2 mm); (ii) skin movement artifacts, owing to relative movement occurring between the skin and the underlying bone during grasping (their value is in the range of 10-25 mm for the most critical representative points) (Fuller et al., 1997); (iii) markers re-positioning, owing to the difficulty of re-positioning of the markers on the same representative relative point (their value is in the range of 5-15 mm).

One of the basic problems working with markers systems is to obtain the three-dimensional (3D) coordinates in an absolute reference system. Some kind of mapping is needed to allow for a transformation from camera coordinates to 3D space. The identification of the parameters to reconstruct such model is called resection while its use

to compute 3D coordinates is called intersection.

For both the active and passive systems it is necessary to identify a reference point before measurement takes place. This enables the computer to calculate the absolute and relative positions of the markers in 3D. If only one marker is placed on an anatomical landmark of the body, the system can record the displacement of that landmark in 3D, giving the absolute and relative position. The application of two markers enables the system to calculate the distance between them relative to time. With three or more markers (a configuration classically used for reach to grasp movements), the angles at joints can be measured. Calculations of velocity and acceleration of limb segments can be performed on data from one or more markers.

APPENDIX II:SMART SYSTEM

The SMART system has been designed and developed for automatic and reliable analysis of body movement in various conditions and environments. It is based on real-time processing of the TV images to recognize multiple passive markers placed on the relevant point of the body and compute their coordinates. The fast processor for shape recognition (FPSR) constitutes the core of the SMART system (see Figure 1). It processes the TV image in real time and it uses a dedicated algorithm to recognize markers only if their shape matches a determined mask. The whole system has been designed to perform the following operations:

• To recognize the presence of markers

• To compute the X and Y coordinates of the markers centroids

• To perform the previous operations in real time

• To classify each marker on the basis of a suitable model of the body (system depending)

• To perform calibrating procedures, fitting techniques and 3D analysis by stereometric techniques when more cameras are used simultaneously

• to develop further data processing (i.e., a calculation of angular speed)

The fast processor for shape recognition (FPSR) performs cross- correlation processing on the incoming digitised TV signal, recognizes the markers and computes their coordinates. The FPSR unit is doubly connected to the interface to environment (ITE) because it not only receives the input data, but also provides the necessary signals for synchronization. The shape detecting algorithm, essentially based on a bidimensional cross correlation between the actual digitised image and the predetermined mask, is implemented by a parallel hardware structure allowing the

real time processing. The cross-correlated signal is compared to predetermined threshold value and the over- threshold point coordinates are considered as a probable marker component. Once the threshold detection has been performed, the centroid of the over threshold point is calculated. The points over the threshold form a cluster like that shown in Figure 1, left corner. The output from the FPSR are directly the "r" couples of horizontal and vertical coordinates of the "r" markers detected which are delivered to the central processing unit (CPU).

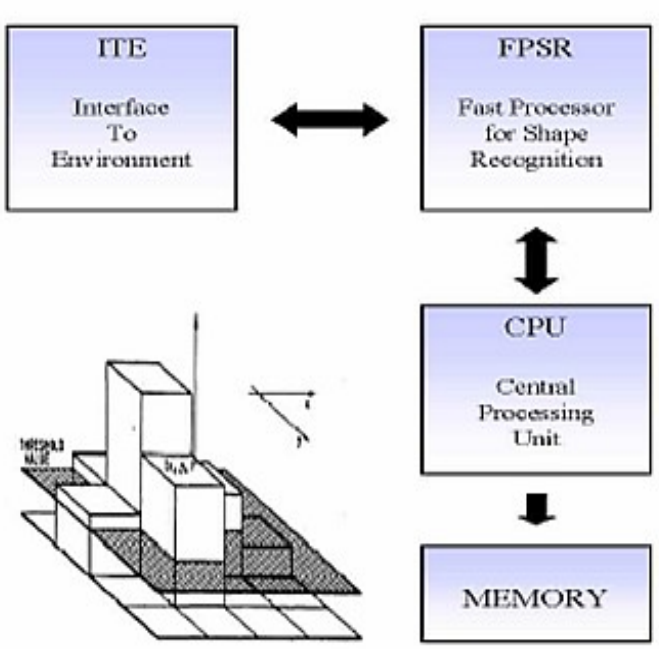

*Figure 1.*The SMART block diagram and (left corner) centroid calculation of the over-threshold points of the cross correlation function.

Hemispheric reflective markers are used for the following reasons:

• They can be easily fixed to the body

• Their image does not change if they rotate on their axis of symmetry

• Their images does not significantly change if they rotate on the other two axes

• The reflective material increases the contrast, thus improving recognition reliability

In order to analyze a spatial movement, the SMART system must be made aware of all relative spatial information contained within the working volume (the space in which the movement will take place).

The spatial calibration is obtained by knowing:

• The position and orientation of all TVC's (television camera) with respect to the laboratory reference system.

• The correction of optical image distortions from each TVC (linearization).

• The dimension of the working volume (3D calibration).

Figure 2 depicts the coordinate based reference system in accordance with the 'right-hand-rule'. During a movement analysis, the positive X axis represents the progression of movement. Consequently, the XY plane represents the lateral view of the motion, the YZ plane depicts frontal movements, and the XZ plane transverse movements.

X Axis The progressive movement axis

Y Axis Vertical, positive in up direction

Z Axis Transverse to the direction of movement

After the first-level processing, the information (marker coordinates) is transferred to the CPU in order to extract information of general interest from raw data.

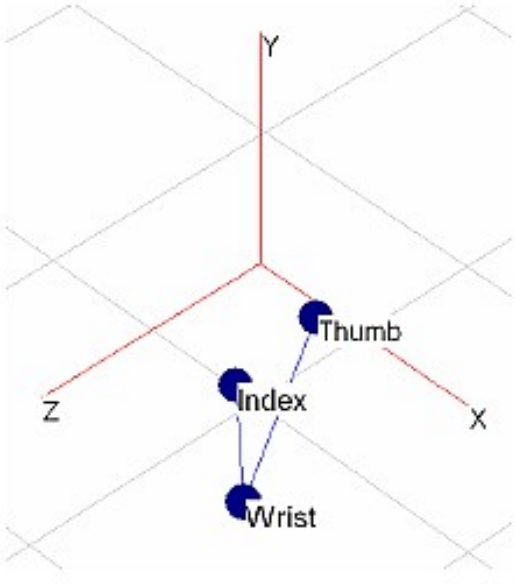

Figure 2. Reference system of hemispheric reflective markers within the spatial calibrated volume.

APPENDIX III:ELECTROENCEPHALOGRAPY

1. Introduction

The purpose of this appendix is to describe the main principles underlying electroencephalography (EEG). The EEG is a record of the oscillations of brain electric potentials recorded from a number of electrodes varying from 20 to 256,attached to the human scalp. Recorded signals are transmitted to amplifiers, then through filtering and artifacts correction and rejection the signal became ready for decoding (Nunez & Srinivasan, 2007). EEG recording procedures are noninvasive, safe and painless; these together with very high temporal resolution constitute the main strengths of this technique. Berger (1929) provided the first human electroencephalography recording outlining three main elements: spontaneous activity measured on the scalp (this activity goes on continuously in the living individual), evoked potentials (components that arise in response to a stimulus, and one must use a train of stimuli and signal averaging to improve the signal-to-noise ratio) and single neuron activity (examined through the use of microelectrodes which measuring activity within the cells of interest) (Malmivuo & Plonsey, 1995).

2. Source of EEG activity

Electroencephalography is a recording of the electric current produced by pyramidal neurons of the cerebral cortex during synaptic excitations. EEG records this current by means of silver electrodes placed on the scalp. Event-related potentials (ERPs), which can be extracted from the EEG signal are related to averaged EEG responses that are time locked to stimuli processing. Furthermore ERP researchers use also evoked potential (EP) ER waveforms, to refer to the waveforms created by averaging together the averaged waveforms of an individual subjects

(Luck, 2005).

Figure 1. describes the generation of voltage recorder from the scalp, through a brief description of all involved steps, from generation of electric potential to signal detection during the recording process.

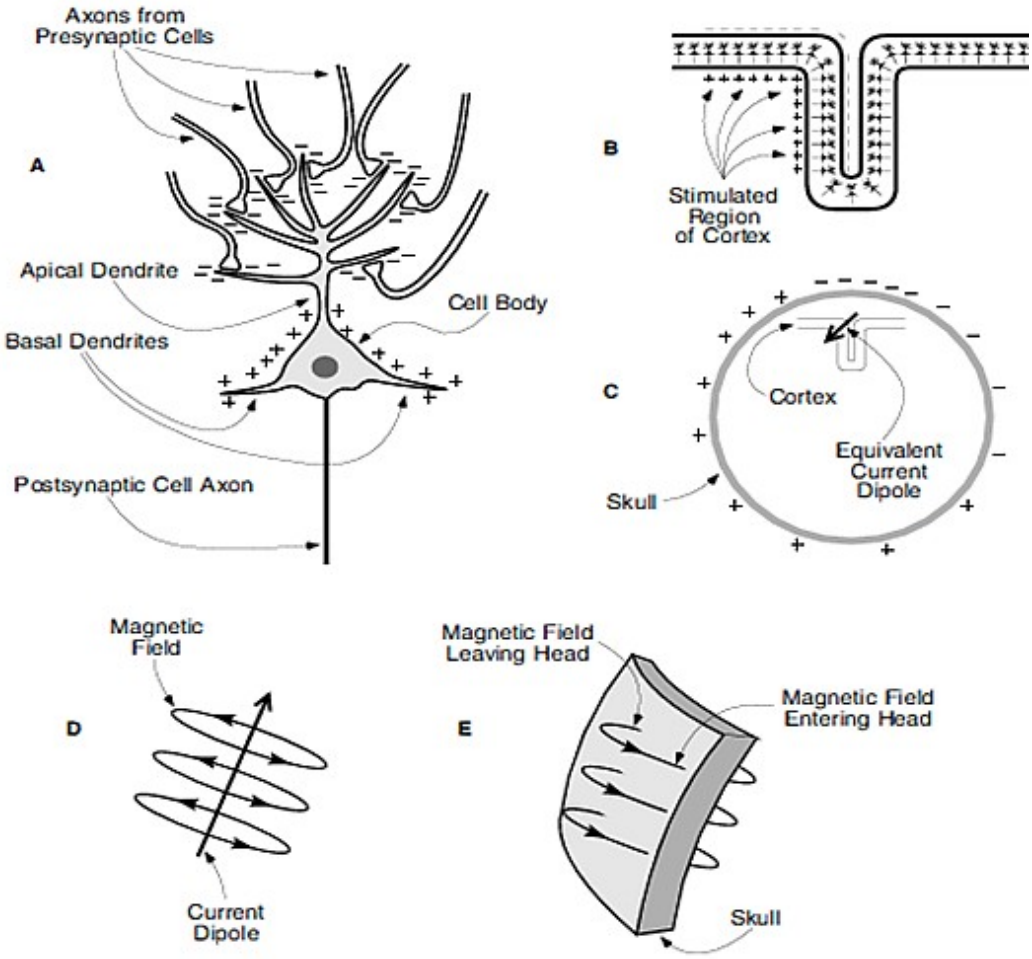

Figure 1. Principles of ERP generation. (A) Schematic pyramidal cell during neurotransmission. An excitatory neurotransmitter is released from the presynaptic terminals, causing positive ions to flow into the postsynaptic neuron. This creates a net negative extracellular voltage (represented by the "-" symbols) in the area of other parts of the neuron, yielding a small dipole. (B) Folded sheet of cortex containing many pyramidal cells. When a region of this sheet is stimulated, the dipoles from the individual neurons summate. (C) The summated dipoles from the individual neurons can be approximated by a single equivalent current dipole, shown here as an arrow. The position and orientation of this dipole determine the distribution of positive and negative voltages recorded at the surface of the head. (D) Example of a current dipole with a magnetic field traveling around it. (E) Example of the magnetic field generated by a dipole that lies just inside the surface of the skull. If the dipole is roughly parallel to the surface, the magnetic field can be recorded as it leaves and enters the head; no field can be recorded if the dipole is oriented radially (Luck & Girelli, 1998).

3. Recording system

The internationally standardized 10-20 system, recommended from the International Federation of Societies for Electroencephalography and Clinical Neurophysiology, is constituted in a series of guidelines for electrodes placement during recording of spontaneous EEG. The locations of electrodes on the scalp are determined starting from nasion (which is the delve at the top of the nose, level with the eyes) and inion (which is the bony lump at the base of the skull on the midline at the back of the head) that represents the reference points to all the skull perimeters measured in transversal and medial plane. (Malmivuo & Plonsey, 1995). The name of this conventional electrode setting, 10-20, indicates that the electrodes along the midline are placed at 10, 20, 20, 20, 20, and 10 % of the total nasion – inion distance, moreover also the electrode numbers are organized in order to indicate the hemisphere, the odd ones on the left and the even ones on the right (Luck, 2005).

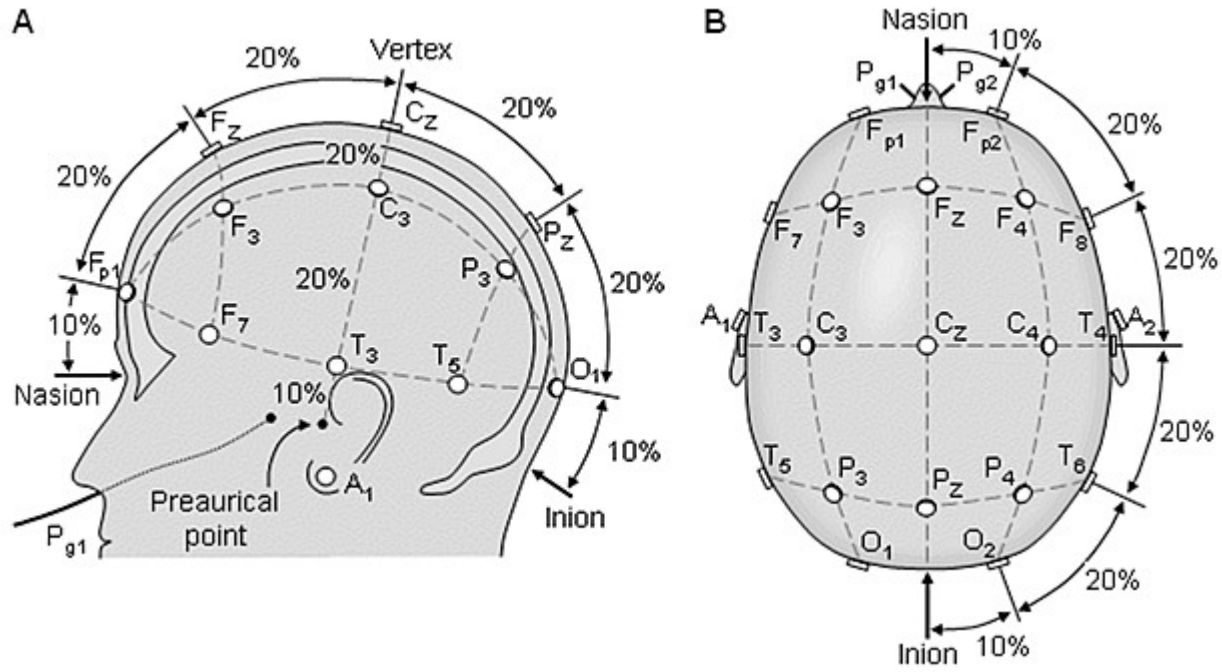

Figure 2. The international 10-20 system seen from (A) left and (B) above the head. A = Ear lobe, C = central, Pg = nasopharyngeal, P = parietal, F = frontal, Fp = frontal polar, O = occipital. (sorce: Malmivuo & Plonsey, 1995).

In addition, one or two reference electrodes (often placed on ear lobes) and a ground electrode (often placed on the nose to provide amplifiers with reference voltages) are required. In referential recordings, potentials between each recording electrode and a fixed reference are measured over time. The distinction between "recording" and "reference" electrodes is mostly artificial since both electrode categories involve potential differences between body sites, allowing closed current loops through tissue and EEG machine. Bipolar recordings measure potential differences between adjacent scalp electrodes. When such bipolar electrodes are placed close together (say 1 or 2 centimeters), potential differences are estimates of tangential electric fields (or current densities) in the scalp between the electrodes. Electrode placements and the different ways of combining electrode pairs to measure potential differences on the head constitute the electrode montage (Nunez & Srinivasan, 2007).

4 Reliability of EEG waveforms

From the EEG signal is possible to designate different waveforms, associated to different frequency range and brain states. Here I provide a brief description of main brain rhythms (depicted in Figures 3., 4., 5., 6., 7., and 8.) categorized through frequency location and trend (Ullsperger & Debener, 2010).

4.1 Delta rhythms

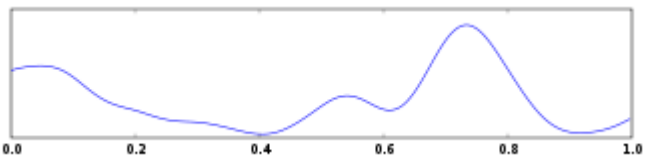

Figure 3. Delta rhythms (Source:http://upload.wikimedia.org/wikipedia/commons/thumb/b/be/Eeg_delta.svg)

The delta waves are defined as rhythms with frequency below 4 Hz. They tend to be the highest in amplitude and the slowest waves. Normally they are detectable in infants and sleeping adults (stages 3 and 4 of sleep), and during some continuous attention task. It is usually most prominent frontally in adults (i.e. FIRDA - Frontal Intermittent Rhythmic Delta) and posteriorly in children (i.e. OIRDA - Occipital Intermittent Rhythmic Delta).

4.2 Theta rhythms

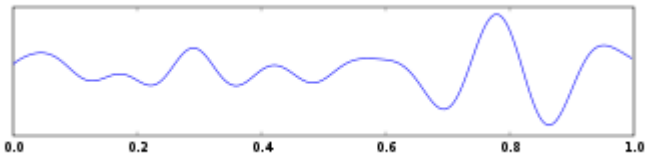

Figure 4. Theta rhythms.(Source:http://upload.wikimedia.org/wikipedia/commons/thumb/3/33/Eeg_theta.svg)

Theta is the frequency range from 4 Hz to 7 Hz. Theta waves are normally detected in young children. This range has been associated with drowsiness or arousal in older children and adults reports of relaxed, meditative, and creative states. Moreover in awake adults, theta activities dominating at mid-frontal electrodes are well described and related to cognitive activities, especially in working memory tasks.

4.3 alpha rhythms

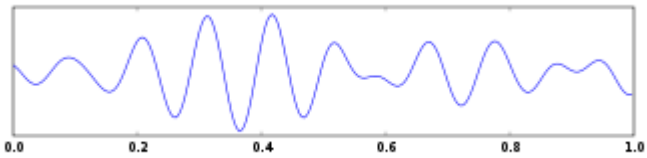

Figure 5. Alpha rhythms(Source:http://upload.wikimedia.org/wikipedia/commons/thumb/e/ee/Eeg_alpha.svg)

Alpha waves are recorded in the frequency range from 8 Hz to 12 Hz. This waves were the first described in EEG oscillation by Berger (1929). Despite such long history, the functional significance and the neuronal generators of these rhythms are still largely

unknown. Normally they are distributed in the posterior regions of the head on both sides, higher in amplitude on the dominant side. They can be measured from an awake person when the eye are closed and attenuates with eye opening or mental exertion (Ullsperger & Debener, 2010).

4.4. Beta rhythms

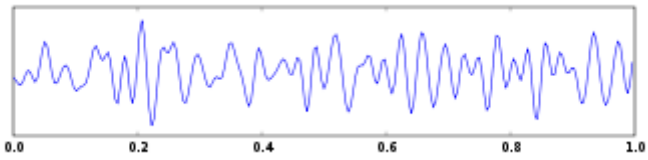

Figure 6. Beta rhythms. (Source: http://upload.wikimedia.org/wikipedia/commons/thumb/2/28/Eeg_beta.svg)

Beta is the frequency range from 12 Hz to about 30 Hz. Usually it can be detectable on both sides in symmetrical distribution and is most evident frontally. Beta activity is closely linked to motor behavior and is generally attenuated during active movements. Furthermore, considering low amplitude with multiple and varying frequencies is generally associated with active, busy or anxious thinking and active concentration.

4.5. Gamma rhythms

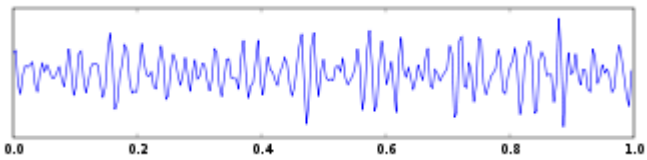

Fgure 7. Gamma rhythms
(Source:http://upload.wikimedia.org/wikipedia/commons/thumb/2/21/Eeg_gamma.svg)

Gamma is the frequency ranging approximately from 30 to100 Hz. Gamma rhythms are thought to represent the binding of different populations of neurons into a network for the

purpose of carrying out a certain cognitive or motor function.

4.6. Mu rhythms

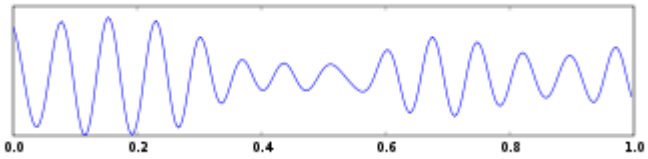

Figure 8. Mu rhythms. (Source: http://upload.wikimedia.org/wikipedia/commons/thumb/b/be/Eeg_SMR.svg)

Mu activity ranges from 8 to 13 Hz, partly overlapping with other frequencies. It is supposed to reflect the synchronous firing of motor neurons in rest state. The beta and gamma frequency should be considered together into the description of their courses forms called event-related desynchronisation (ERD), and the latter event-related synchronization (ERS) (Da Silva, 2010). Generally ERD and ERS, strictly related to movement planning and execution, reflects a decrease or an increase in the synchrony of the underlying neuronal populations.

Considering hand movement, both the mu rhythm and the beta rhythm display ERD. Both activities are localized around the central sulcus but with different distribution. ERS in the gamma frequency band can also be found before movement execution over the central regions. ERS has its maximum after the movement end (Mulert & Lemieux, 2010).

5. Advantage and disadvantage

The signal coming from cortical synaptic action generates electrical change in the 10 to 100 millisecond range. EEG is one of the best available technologies with sufficient temporal resolution to follow these fast dynamic changes. On the other hand, EEG spatial resolutions is poor relative to modern brain structural imaging methods (Nunez & Srinivasan, 2007). This

section outlines the advantages and disadvantages related to ERPs waveforms. First of all ERPs provide an online measure of stimuli processing, and provides the possibility of monitoring online a variety of information processes with excellent temporal resolution.

ERPs, moreover, provide a continuous measure of processing between a stimulus and a response, making it possible to determine which stage or stages of processing are affected by a specific experimental manipulation (Luck, 2005).

On the other hand one of the biggest disadvantages of ERPs is the source localization, because the spatial resolution is quite poor in comparison to the temporal one, but nowadays this problem has been partially circumvented by the development of source analysis. This powerful temporal resolution in the order of 1 ms allows to address with ERPs some question that would be difficult to tackle with others neuroimaging techniques. A second disadvantage of the ERP technique is that ERPs are so small that it usually requires a large number of trials to measure them accurately (Luck, 2005).

6. Major components

ERP waveforms consist in a sequence of positive and negative voltage deflections, which are called peaks, waves, and more frequently components. To better characterize each components, one of the most popular convention suggests to plot ERP waveforms with negative voltages upward and positive voltages downward (Luck, 2005). It is also common to label such components with a precise latency reference (i.e. P300, positive deflection in voltage with a latency of roughly 300 milliseconds). All the others components that does not use letters and numbers are referred with acronyms (i.e. CNV, contingent negative variation). Because ERP peaks reflects the flow of information through the brain, components are defined primarily on the basis of their polarity, latency, and general scalp distribution (Luck, 2005). Below a very brief

overview of the main ERP components is reported.

C100*:* Exceptionally this component is not labeled with a P or an N because its polarity can vary. The C100 wave appears to be generated around area V1 (primary visual cortex), typically onsets 40–60 ms post-stimulus and peaks 80–100 ms post-stimulus, and it is highly sensitive to stimulus parameters, such as contrast and spatial frequency (Luck, 2005).

P100*:* P1 wave is largest at lateral occipital electrode sites and typically onsets 60–90 ms post-stimulus with a peak between 100–130 ms; latency will vary substantially depending on stimulus contrast. This wave is sensitive to variations in stimulus parameters, like direction of spatial attention and subject's state of arousal (Luck, 2005).

N100*:* There are several visual subcomponents attached to this negative component. The earliest subcomponent peaks 100–150 ms post-stimulus at anterior electrode sites, and there appear to be at least two posterior N1 components that typically peaks 150–200 ms post-stimulus, one arising from parietal cortex and another arising from lateral occipital cortex. Moreover lateral occipital N1 subcomponent appears to be larger when subjects perform discrimination instead detection tasks, which led to the proposal that this may reflect discriminative processing (Luck, 2005).

P200*:* This component follows the N100 wave at anterior and central scalp sites. It is larger for stimuli containing target features, and this effect is enhanced when the targets are relatively infrequent. Usually P200 is difficult t to distinguish given the overlapping with N100, N200, and P300 waves in the posterior sites (Luck, 2005).

Mismatch negativity*:* The mismatch negativity (MMN) elicits a negative-going wave that is largest at central midline scalp sites and typically peaks between 160 and 220 ms. Generally it is observed when subjects are exposed to a repetitive train of identical stimuli with occasional mismatching stimuli. MMN is thought to reflect a fairly automatic process that compares

incoming stimuli to a sensory memory trace of preceding stimuli (Luck, 2005).

N200: Many components in this range have been identified: the first is bilateral but not automatic, anterior response that is present even when the deviant item is not a target; the second one N200b is present only if the deviant item is a target, this subcomponent is bilateral and probability sensitive; the third and last one called N200pc is observed at posterior electrode sites contralateral to the location of the target, and it reflects the focusing of spatial attention onto the target location (Luck, 2005).

P300*:* Within the range of P300 wave there are several different ERP subcomponents, namely the P300a (frontal distributed) and the P300b (parietal distributed). Both are elicited by unpredictable, infrequent shifts in tone pitch or intensity, but the P3b component is present only when these shifts are task-relevant, The P300 amplitude depends on the probability of the task defined category of a stimulus (usually is larger when subjects devote more effort to a task, and smaller when the subject is uncertain of whether a given stimulus is a target or a non-target). The P300 wave is generated after the stimulus has been categorized according to the rules of the task (Luck, 2005).

Readiness Potential*:* The readiness potential (RP) are recorded if subjects make a series of occasional manual responses; in this case responses are preceded by a slow negative shift at frontal and central electrode sites that usually starts one second before the actual response. Scalp topography of the readiness potential depends on which effectors has been used to make the response; with differences between the two sides of the body and differences within a given side (i.e. lateralized portion is called the lateralized readiness potential, LRP). Usually this component shows a superimposed positive-going followed by a negative-going during response to end up with another positive-going deflection after the response (Luck, 2005).

CNV*:* The contingent negative variation (CNV) consists of a negativity following the warning stimulus, a return to baseline, and then a negativity preceding the target stimulus. For this component two phases can be distinguished, the first phase is usually regarded as reflecting processing concerned with the warning stimulus. The second phase is usually regarded as reflecting the readiness potential that occurs as the subject prepares to respond to the target (Luck, 2005).

7. Artifacts

There are several types of artifacts (electrical signal recorded by EEG but not originating from cerebral sites) that can contaminate EEG recordings. They can be sudivided in biological (endogenous) and environmental (exogenous) artifacts. Endogenous artifacts are likely to affect the signal of neural electric activity. The most common are blink and eye movements, heartbeat, skin conductance and participants movements.

Considering the artifacts originating outside the body, considerable attention must be given to electrical isolation of the recording apparatus and isolation of the recording room (i.e. Faraday cage). Furthermore it is a good practice to pay enough attention to the positioning of the recording cables. They must be displaced in very well aligned disposition to avoid additional artifacts.

There are two main techniques for eliminating the artifacts effects: the first is called artifact rejection and provide an exclusion of contaminated trials from the averaged ERP waveforms; the second, called artifact correction, works through an estimation of the artifacts influence on the ERPs and then use correction procedures to subtract away the estimated contribution of the artifacts (Luck, 2005).

APPENDIX IV:fMRI

This section describes some principles of magnetic resonance imaging (MRI). Images are sampled using an MR Scanner, which consists of a (superconducting) main magnet, gradient coils and the radio frequency system (Figure 1.).

Firstly, the basic principles of magnetic resonance imaging are explained: those principles include the physics of spins and their alignment with an external magnetic field, the influence of radio frequency pulses and consequently the relaxation phenomena and the localization of the MR signal in 3D space through selective excitation. Next, the phenomenon of functional magnetic resonance imaging, which uses blood as an intrinsic contrast agent (blood oxygenation level dependent contrast, BOLD), is described.

The understanding of fMRI principles is particularly important since the experimental studies presented in this thesis are based on images collected through this technique.

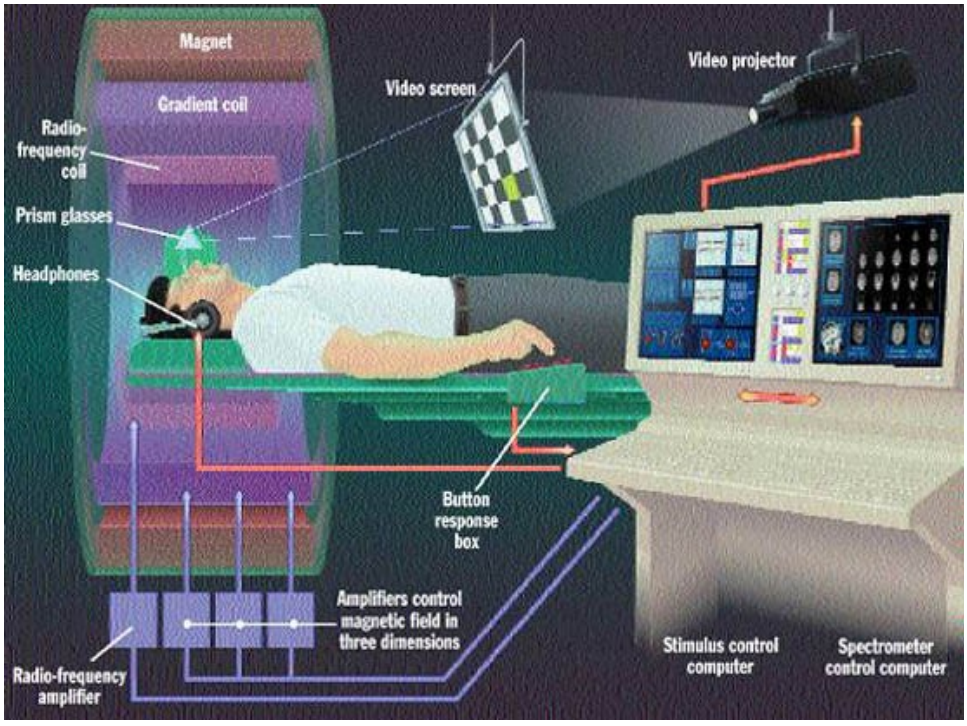

Figure 1. Main components of a magnetic resonance scanner are a main magnet, the gradient coils with the power supply, and a radio frequency coil (Source: Jody Culham web slides).

1. Introduction

In the last years the development in the field of neuroscience has been enormous: beside new techniques investigating molecular and genetic processes, also the comprehension of complex cognitive functions has made huge progresses. A significant contribution has been given by the development of imaging techniques. Imaging techniques not only gave the possibility to have a non-invasive measure of brain function, beyond animal models (neurophysiological studies), but also allowed for the study of a healthy brain, without the need to resort to a damaged one (neuropsychology) to speculate on its functioning in normal state. These imaging methods have identified many specific areas in the brain, and some of them seem to find an homologue in other species' brain, like in the case of the macaque monkey (Grill-Spector & Malach, 2004).

Among imaging techniques, magnetic resonance imaging (MRI) met the widest approval, especially thanks to its non-invasiveness and its technical properties. In cognitive neuroscience, MRI is used to indirectly infer the functional activity of the brain, in which case it is referred to as functional Magnetic Resonance Imaging (fMRI).

As its name implies, the technique exploits magnetic properties of atomic nuclei to create images of biological tissues. Between 1920 and 1940 physics has demonstrated that atomic nuclei have magnetic properties, and that these properties can be manipulated. In fact nuclei of many atoms, as sodium, hydrogen and phosphorus, can behave as small magnetic dipoles, and can assume either high-energy states (behaving as if oriented against the applied field) or low-energy states (in alignment with the applied magnetic field). Atoms with this property have by definition a "nuclear spin". The transition between these two states is associated either the absorption or emission of energy in the radiofrequency range. The frequency of the energy emitted by an excited nucleus is proportional to the strength of the magnetic field in which the nucleus is placed . The strength of the magnetic fields created by MR scanners typically ranges from 1.5 to 4 Tesla (1 Tesla= 10,000 Gauss; earth's magnetic field is approximately 0.00005 Tesla), raising

up until 7 Tesla in some cases (Jezzard & Clare, 2002).

2. Outside the magnetic field

The measure of a brain in a magnetic field will produce atomic nuclei alignment according to the forces present in this field: this occurs to all nuclei that are electrically charged and spin around their axis. Of the many types of nuclei in the brain, hydrogen nuclei are the most commonly measured in MRI (Jezzard & Clare, 2002), because of their massive presence in the human brain, and their strong MR signal.

Hydrogen nuclei are positively charged particles that, under normal conditions, spin around themselves (see Figure 2): spin motion of a proton generates an electrical current, because protons carry positive charges.

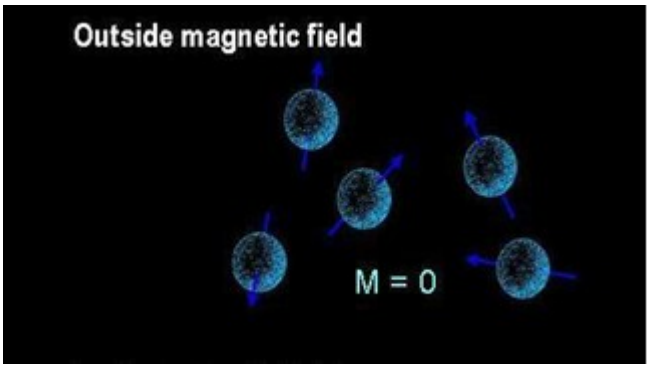

Figure 2. Representation of atomic nuclei spinning around themselves; M: net magnetization (Source: Robert Cox web slides).

3. Inside the magnetic field

As outlined above, before the brain is placed in a magnetic field, spins point randomly in space, and consequently nuclei are not aligned: (Figure 2.).When the brain enters the magnetic field, the protons align themselves in the direction of the main magnetic field (Figure 3.): they reach this position by performing a gyroscopic movement, the precession.

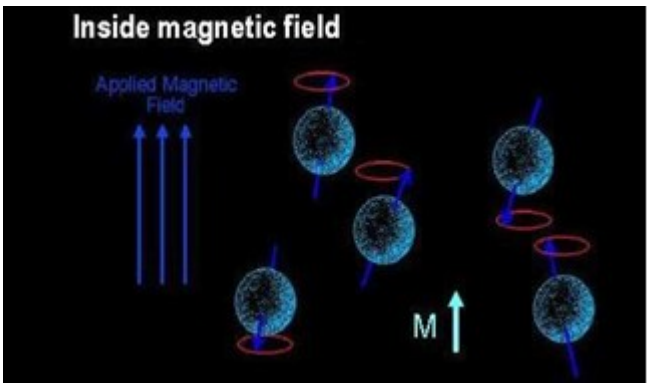

Figure 3. representation of atomic nuclei alignment within the magnetic field (**Source**: Robert Cox web slides)

This phenomenon is also known as *magnetic moment* (μ) (see Figure 4.). The frequency of this precession depends first of all on the type of nucleus: this means that precession frequency of an hydrogen nucleus will be different to the one possessed by a sodium nucleus. Both percentage of nuclei aligning with the magnetic field and precessing frequency are strongly dependent to the strength of the magnetic field: the stronger the magnetic field is, the higher the percentage of alignment to the magnetic field and the speed of precessing frequency (Jezzard & Clare, 2002).

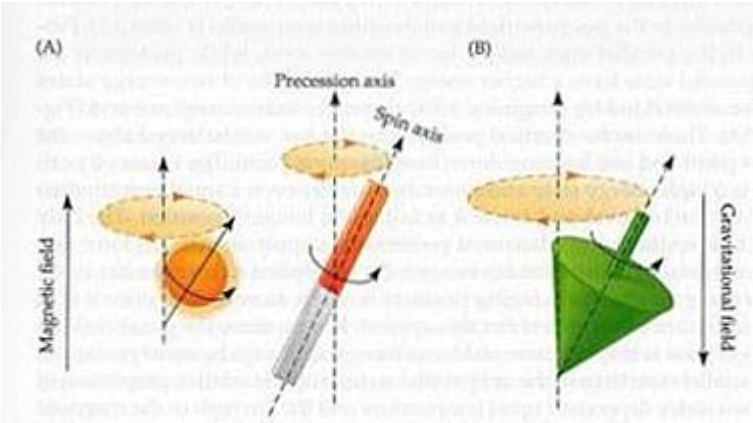

Figure 4. Precession:the movement of a rotating magnet within a magnetic field (A) is similar to the movement of a top in earth's gravitational field (B) representation of atomic nuclei alignment within the magnetic field. In addition, the spin axis moves around a vertical axis (precession). (Source: Huettel et al., 2004)

Furthermore, because protons have an odd-numbered mass, its spin will be the result of the product of the mass of a spinning body multiplied by its angular velocity (*angular momentum*, J):

Both μ and J can be conceived as vectors pointing in the same direction, along the spin axis (right-hand rule) (Huettel et al., 2004).

Each proton has a magnetic moment and an angular momentum that are the potential source of the MR signal. However, outside a magnetic field, the spins of hydrogen nuclei are randomly oriented, and therefore tend to nullify each other.

Consequently, if spins are randomly oriented, their sum (*net magnetization*) will be pretty small. The net magnetization can be conceived as a vector with *longitudinal* and *transverse* components: the vector representing the longitudinal component can be either parallel or antiparallel to the magnetic field, whereas the transverse component is perpendicular. Given the huge amount of spins, the transverse component tend to be canceled out, while the larger the amount of spin parallel to the magnetic field, the stronger the longitudinal magnetization will be.

4. How the MR signal is produced

The net magnetization constitutes the basis for the MR signal. To obtain a measure of it, we need to perturbate the equilibrium state of spins, in order to observe how they react to perturbations. This perturbation is introduced in the magnetic field by the application of a RadioFrequency (RF). The RF pulse is typically an electromagnetic wave, produced by the application of an alternating current perpendicular to the direction of the main magnetic field (90˚ RF-pulse - Jezzard & Clare, 2002). The goal of this 90˚ RF-pulse is thus to change the spin orientation of the hydrogen nuclei.

As outlined in the first paragraph, all spins can take either low- or high-energy state within the magnetic field when changing their orientation as a consequence of the RF pulse: when the excitation pulse is switched off, the spins start returning to their equilibrium and emit a signal, denoted as *free induction decay*. During this energy decreases, a photon will be emitted, with the

same amount of energy as the one released during the change of state: this process is known as *relaxation*. Basically, there are two relaxation mechanisms: the *longitudinal relaxation*, which describes the return to equilibrium along the positive z axis; and *transverse relaxation* (or spin-spin relaxation), characterized by decay of phase-coherence of the spins, which causes a decay of net magnetization in the x-y plane (Figure 5.). This decay of phase-coherence mainly results from an energy exchange between the spins due to their magnetic interactions, causing continuous changes in precession frequencies.

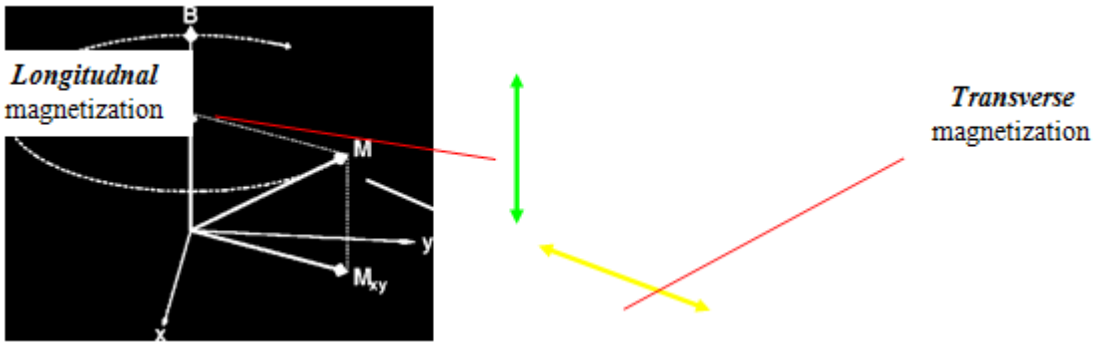

Figure 5. Relaxation mechanisms (Source: Huettel et al., 2004).

Vice versa, a spin growing up to the high-energy state will absorb a photon energy matching the energy difference between the two states: this process is known as *excitation.* Since the excitation process provoked by the RF pulse disrupts the thermal equilibrium, there will be a number of spins immediately releasing energy to recover the equilibrium: during this stage, the spins emit electromagnetic energy that can be detected by the radiofrequency coils, and that provide the data for our images.

5. Relaxation times

The release of energy occurring during relaxation originates the MR signal: as we explained above, the transverse magnetization has to go back to the initial direction (before the RF pulse),

the consequence is a decrease of the transverse magnetization, and thus a loss of MR signal. The time within which this recovery occurs is called T_1 recovery.

Immediately after having been tipped into the transverse plane, the net magnetization is coherent in the sense that spins are precessing along the same vector and simultaneously (in phase): over time spins become out of phase (transverse relaxation), because spins can interfere with each other: the loss of energy occurring at this stage is called *T_2 decay*. Moreover precession frequency of each spin depends also on local field strength, varying from point to point. This effect, combined with the spin-spin interaction, is known as *T_2* decay*, and by virtue of the combination of these two effects, it is usually faster than T_2 (Figure 6.).

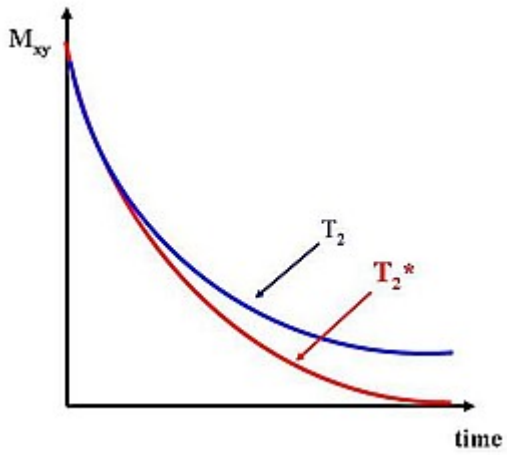

Figure 6. T2 and T2* relaxation times (Source: Huettel et al., 2004).

6. Relaxation times as the basis for image contrasts

Different tissues have different relaxation times: this property can be exploited to create image contrasts derived from differences in T1, T2 and T2*. By varying some acquisition parameters, like the time between the RF pulse and the measurement of the signal (echo time, TE) or the time between two consecutive RF pulses (repetition time, TR), it is thus possible to acquire images selective for these effects. For example, images exploiting properties of the T1 contrast are known as T1-weighted scans, and are particularly indicated for anatomical images, because they

show a good contrast between the grey and the white matter (Figure 7 a). Scans maximizing the T2 contrast are instead known as *T2-weighted scans*, suitable to detect brain damage because of the brightness shown by the lesion (Figure 7 b) (Jezzard et al., 2002). *T2** weighted images, as a consequence of features of the T2* contrast, are particularly indicated for detecting changes in the local field: for example, if we consider a region adjacent to a vessel (in which paramagnetic hemoglobin is predominantly flowing – Figure 7 c), the T2* relaxation time will be pretty short, because of the paramagnetic substance flowing near to it (Jezzard & Clare, 2002). This property of the T2* contrast offers a possibility to measure the Blood-Oxygenation-Level-Dependent signal, known as BOLD and representing the source of the signal measured in functional magnetic resonance (fMRI) imaging studies.

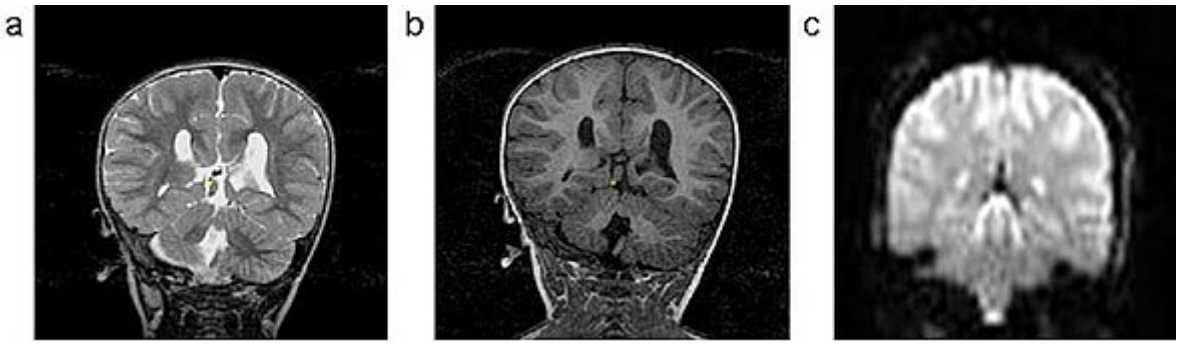

Figure 7. Images created with a) T1-contrast; b) T2-contrast; c) T2*-contrast.

7. The BOLD signal

The BOLD fMRI technique measures changes in the inhomogeneity of the magnetic field, which are a result of changes in the level of oxygen present in the blood (blood oxygenation). Deoxyhaemoglobin (red blood cells which do not contain any oxygen molecule – Figure 8.) has magnetic properties and will cause inhomogeneities in the magnetic field surrounding it. Oxyhaemoglobin (red blood cells which do contain oxygen molecules – Figure 8.) has instead weak magnetic properties and therefore has very little effect on the surrounding magnetic field. Consequently, a high level of deoxyhaemoglobin in the blood will result in a greater field

inhomogeneity, and thus in a decrease of the fMRI signal (Heeger & Ress, 2002; Jezzard & Clare, 2002).

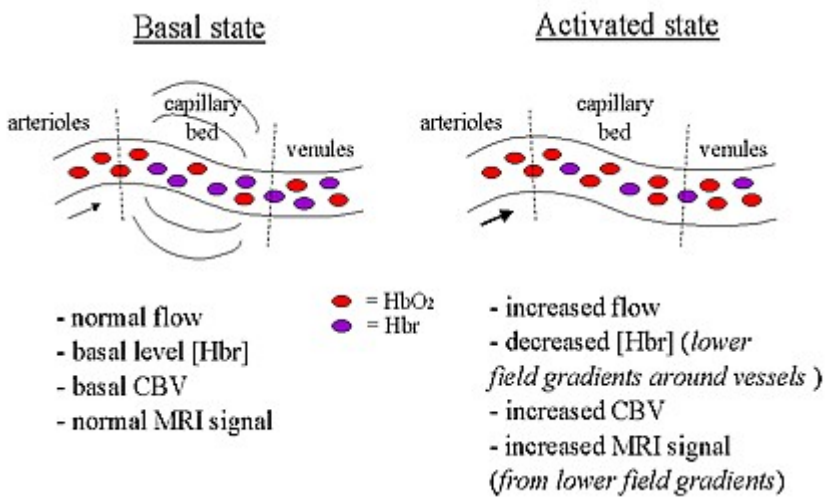

Figure 8. During activation the cerebral blood flow (CBF) increases and the deoxyhemoglobin (purple) concentration falls. Blood becomes more oxygenated (red). Reduced field inhomogeneities (i.e., lower field gradients) lead to a longer T2* and therefore to an increased MRI signal. (**Source**: Brief Introduction to fMRI by Irene Tracey).

The fMRI signal against time in response to a temporary increase in neuronal activity is known as the Haemodynamic Response Function (HRF). The HRF goes through three stages (see Figure 9.) (Heeger & Ress, 2002).

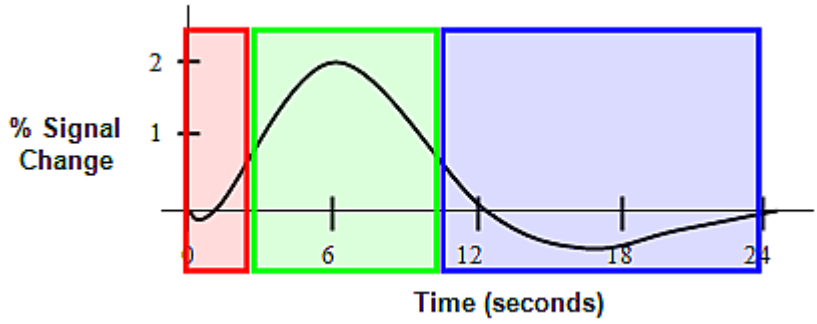

Figure 9. Time course of HRF as a response to a short increase in neuronal activity (time = 0)

The fMRI signal initially decreases, because the active neurons use oxygen at disposal at time=0, and therefore the relative level of deoxyhaemoglobin in the blood increases. This decrease,

however, is quite small, and also difficult to detect (Uğurbil et al., 2003).

Following the initial decrease, there is a large increase in the fMRI signal which reaches its maximum after approximately 6 seconds. This increase is due to a massive oversupply of oxygen-rich blood.

There are two main hypotheses for this increase in blood flow: first, it would compensate for the oxygen being used by the active neurons. However, the supply in oxygen by the increase in blood flow is much larger than the amount of oxygen used by the active neurons. Second, the increase in blood flow would instead compensate for the amount of glucose being used by the neurons and not the amount of oxygen (Heeger & Ress, 2002). This is because the increase in blood flow is proportional to the amount of glucose being used by the active neurons. In any case, this overflow of oxygen results in a large decrease in the relative level of deoxyhaemoglobin, which originates the fMRI signal.

Finally, the last stage of the HRF is a slow return to the a level of deoxyhaemoglobin similar to the first one, and a decay of the fMRI signal until it has reached its original baseline level after an initial undershoot after approximately 24 seconds (Heeger & Ress, 2002).

8. Some notes on BOLD

It is important to outline that the BOLD signal represents an indirect measure of the underlying neuronal activity, relying on the assumption that neuronal activity and haemodynamics are directly related. Furthermore, the fMRI signal reflects the sum of the activity of a large group of neurons (Heeger & Ress, 2002), and therefore can be the result of either of a large activation of a small group of neurons, or of a small increase in activation of a large group of neurons (Heeger & Ress, 2002). This relies on the assumption that neurons responsible for the same function will be adjacent in the brain. Moreover, as outlined above, the BOLD signal can be influenced by

nearby blood vessels: therefore the relative decrease in deoxyhaemoglobin is larger in large veins than in small veins. This means that the maximum BOLD fMRI signal is often obtained in the large veins that can be a few millimetres away from the site of neural activation. (Jezzard & Clare, 2002; Uğurbil et al., 2003). Related to this aspect, blood vessels have to cross more than one brain region to reach the "demanding region" and supply it with oxyhaemoglobin. This "unspecificity" of blood flow results in an image where the "demanding region" appears larger than it is (Jezzard & Clare, 2002; Uğurbil et al., 2003) Finally, it is also important to note that the haemodynamic response is much slower than the underlying neuronal activity. Because of this slowness in the response, fMRI technique has a relatively poor temporal resolution when compared to methods that more directly measure neuronal activity such as EEG (Heeger & Ress, 2002).

APPENDIX V: INDIPENDENT COMPONENT ANALYSIS

1. What is it

One of the commonest problems in data processing is finding a suitable representation of multivariate data. The indipendent component analysis (ICA) essentially gives the possibility to reveal the driving forces underlying a set of observed phenomena (Stone, 2004).

One of the best know example of the principle underlying the use of ICA is the cocktail party problem (Hyvärinen et al., 2001) or nutshell example showed in Figure 1. (Stone, 2004). In these circumstances a large amount of data are measured from *n* source, and it is know that each measured signal depends on several distinct underlying factors. It follows that each measured signal is a mixture of the underlying factors. Generally the problem is to establish how the sources and the weights of these sources for each observation have to be estimated (Ullsperger & Debener, 2010).

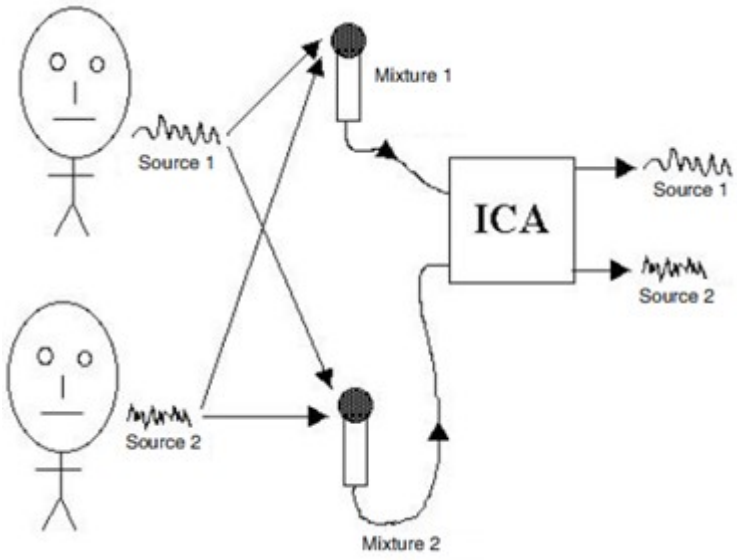

Figure 1. ICA in a nutshell. If two people speak at the same time in a room containing two microphones then the output of each microphone is a mixture of two voice signals. Given these two signal mixtures, ICA can recover the two original voices or source signals. This example uses speech, but ICA can extract source signals from any set of two or more measured signal mixtures, where each signal mixture is assumed to consist of a mixture of source signals (reported from Stone, 2004).

ICA is a statistical and computational technique for revealing hidden factors underlying sets of random variables, measurements, or signals (Hyvärinen et al., 2009). ICA is a linear decomposition technique that aims to reveal the underlying statistical sources of mixed signals (Ullsperger & Debener, 2010).

ICA defines a generative model for the observed multivariate data, in which the data variables are assumed to be linear mixtures of some unknown latent variables, and the mixing system is also unknown. The latent variables are assumed non-Gaussian (non –normal) and mutually independent, and they are called the independent components of the observed data or sources or factors (Hyvärinen et al., 2009).

ICA belongs to blind source separation (BSS) methods for separating data into underlying informational components, where such data can take the form of images, sounds, telecommunication channels or different sources. The term "blind" implies that such methods can separate data into source signals even if very little is known about the nature of those different sources (Stone, 2004).

2. How ICA works

ICA is based on assumption that if different independent signals are from different physical sources indeed this basic assumption can be reversed in order to delineate the ICA job: separate signal mixtures into statistically independent signals. If this main assumption is valid each of the signals extracted by ICA should be generated by a different physical source or process (Stone, 2004).

Logically, it follows that ICA is related to conventional methods for analyzing large data sets, such as principal component analysis (PCA) and factor analysis (FA) but differs from them

because it uses the non-Gaussian structure of the data, which is crucial for recovering the underlying components that created the data (Stone, 2004; Hyvärinen et al., 2009). ICA can be applied even if the desired output is unknown or hypotheses are constrained or simplistic, or even if the main goals are to divide the measurements in different conditions.

Mathematically ICA can be represented like an observed random vector X modeled by a linear latent variable model (Jutten & Herault, 1991),

$$x_i(t) = \sum_{j=1}^{m} a_{ij} s_j(t), \quad \text{for all } i = 1, \ldots, n.$$

or like a matrix form: x = As

where the mixing matrix A is constant, s*j* are latent random variables (independent component), and it is allow estimate both A and s observing only x (Hyvärinen et al., 2009).

The main basic proprieties of the ICA model show that the components are mutually statistically independent therefore their joint density function is factorizable. As already explained the components have non-Gaussian distribution, they are not ordered and they are defined only up to a multiplicative constant (Hyvärinen, 2013). Moreover the mixing matrix is square and invertible (Hyvärinen et al., 2009).

3. Applications

ICA may help for the detection of signal sources that cannot be identified at the raw data level using other, more conventional techniques (Ullsperger & Debener, 2010). ICA has been applied to problems in research fields such as speech processing, brain imaging electrical brain signals, telecommunications, and stock market prediction (Stone, 2004).

Considering EEG, the application of ICA has become popular for two key features: it is a

powerful way to remove artifacts from EEG, and to disentangle otherwise mixed brain signals (Ullsperger & Debener, 2010). Moreover these characteristics encouraged the progress in multimodal data integration such as EEG-fMRI (Debener et al., 2006).

In terms of the present thesis one of the most used exploratory integration approach considering fMRI is ICA. This analysis could account for spatial or temporal independence of brain activity patterns.

Beyond the analysis of multi-channel EEG and fMRI data, ICA it is applied to different levels of data analysis such as EEG informed fMRI analysis, fusion of EEG and fMRI by parallel group, integration of separately or simultaneously recorded neuroimage for instance.

During the last years, ICA has become a standard tool for signal processing. Applications have become very widespread, they can be found in almost every field of science owing to the generality of the model (Hyvärinen, 2013).

APPENDIX VIa: EDIMBURGH HANDEDNESS INVENTORY

Your Initials:_

Please indicate with a check (✓) your preference in using your left or right hand in the following tasks.

Where the preference is so strong you would never use the other hand, unless absolutely forced to, put two checks (✓ ✓).

If you are indifferent, put one check in each column (✓ | ✓).

Some of the activities require both hands. In these cases, the part of the task or object for which hand preference is wanted is indicated in parentheses.

Task / Object	Left Hand	Right Hand
1. Writing		
2. Drawing		
3. Throwing		
4. Scissors		
5. Toothbrush		
6. Knife (without fork)		

7. Spoon		
8. Broom (upper hand)		
9. Striking a Match (match)		
10. Opening a Box (lid)		
Total checks:	LH =	RH =

Cumulative Total	CT = LH + RH =
Difference	D = RH – LH =
Result	R = (D / CT) x100 =
Interpretation: (Left Handed: R < -40) (Ambidextrous: -40 ≤ R ≤ +40) (Right Handed: R > +40)	

Scoring:

Add up the number of checks in the “Left” and “Right” columns and enter in the “TOTAL” row for each column. Add the left total and the right total and enter in the “Cumulative TOTAL” cell. Subtract the left total from the right total and enter in the “Difference” cell. Divide the “Difference” cell by the “Cumulative TOTAL” cell (round to 2 digits if necessary) and multiply by 100; enter the result in the “Result” cell.

Interpretation (based on Result):

- below-40=left-handed
- between -40 and +40=ambidextrous
- above +40=right-handed

APPENDIX VIb: INFORMED CONSENT

UNIVERSITÀ DEGLI STUDI DI PADOVA
DIPARTIMENTO DI PSICOLOGIA GENERALE

CORRELATI NEURALI DEL MOVIMENTO DI RAGGIUNGIMENTO E PRENSIONE.

Responsabili della ricerca: Prof. U. Castiello, Dott. C. Begliomini; Dott. T. De Sanctis

CONSENSO INFORMATO

Con questo studio vogliamo studiare l'andamento dell'attività cerebrale (rilevata tramite l'elettroencefalogramma e risonanza magnetica funzionale) durante compiti di raggiungimento e prensione verso oggetti tridimensionali.

Ti sarà chiesto di eseguire con velocità naturale tre differenti tipi di movimento verso l'oggetto che troverai dinanzi a te. I tipi di movimento prevedono:

- prensione dell'oggetto tramite l'utilizzo delle dita pollice-indice;
- prensione dell'oggetto tramite l'utilizzo dell'intera mano;
- raggiungimento dell'oggetto da parte delle nocche delle dita.

Ad indicare quale movimento eseguire ci saranno dei suoni, uno per ogni tipo di movimento: subito dopo si udirà un secondo suono diverso dal precedente volto a dare il segnale di via al movimento.

E' fondamentale non iniziare il movimento prima di questo suono

L'esperimento dura circa 40 minuti, suddivisi in quattro blocchi da 10 minuti ciascuno intervallati da una breve pausa. Successivamente acquisiremo un'immagine anatomica (5 minuti) ed immagini di connettività strutturale (25 minuti). Durante queste ultime due fasi non dovrai eseguire alcun compito e potrai chiudere gli occhi e rilassarti.

L’esperimento vero e proprio sarà preceduto sa una fase di familiarizzazione con i movimenti ed i suoni nella quale potrai trovare risposta agli eventuali dubbi.

E’ FONDAMENTALE NON MUOVERSI ALL’INTERNO DELLO SCANNER

Il sottoscritto, _____

acquisite oralmente le informazioni di cui all’art. 13 del D.lgs 196/2003, conferisce al dott. _____il proprio consenso al trattamento dei suoi dati personali e sensibili.

Padova, _____

Nome, cognome e telefono del Partecipante:_____
_____

Nome, cognome e telefono dello Sperimentatore:
_____
_____

Firma del Partecipante _____

Firma dello Sperimentatore _____

APPENDIX VIc: MRI INFORMED CONSENT

ISTITUTO DI RADIOLOGIA – POLICLINICO
Istruzioni operative di preparazione

RISONANZA MAGNETICA (RM)
SCHEDA INFORMATIVA DI CONSENSO

COGNOME_____
NOME_____
DATA DI NASCITA_____

La Risonannza Magnetica serve a rendere visibili al Medico alterazioni patologiche. Al posto di radiazioni ionizzanti o sostanze radioattive per la formazione di immagini vengono usate onde radio in campi magnetici. Dal Vostro corpo viene captato un segnale di eco con antenne molto sensibili, e viene trasferito ad un computer, con il quale si ottengono immagini della zona corporea studiata. Con i campi magnetici in uso (con forza fino a 3 Tesla) si sono riscontrati solo disturbi collaterali brevissimi, che comunque non portano danni.

Attenzione! Corpi metallici, quando posti in un campo magnetico possono provocare disturbi! AIUTATECI AD EVITARLI! Per questo prima di entrare nella stanza di Risonanza Magnetica toglietevi tutti i seguenti oggetti:

- Lenti a contatto, apparecchi acustici, protesi dentarie
- Orecchini, anelli, collane, braccialetti
- Fermagli per capelli, piercings
- Bancomat e carte di credito; tessere magnetiche in genere. Tali supporti vengono smagnetizzati e diventano pertanto inservibili.
- Accessori metallici (cinture, fibbie…)
- Monete, penne, chiavi ed altri corpi metallici
- Il giorno dell'esame è da evitare l'uso di cosmetici quali lacche, gel, ombretti, mascara ecc ecc.

METODO DI ESAME
L'esame viene eseguito in una stanza apposita. Voi sarete sdraiati su un lettino che scorre all'interno della macchina in un'apertura circolare di 70-100 cm. La durata dell'esame varia dai 30 ai 90 minuti. Durante l'esecuzione dell'esame dovete cercare di rimanere rilassati e di non muovere la testa. Durante l'esame sentirete dei rumori, tipo forti battiti, dovuti al funzionamento normale della macchina per Risonanza Magnetica. Avrà a disposizione un dispositivo di allarme da azionare nel caso desideri interrompere l'esame per qualche motivo.

PER FAVORE CHIEDETECI!
Se non avete capito qualosa, se volete avere maggiori informazioni sulla metodica e sul suo significato. Noi siamo a disposizione per spiegazioni, domande e chiarimenti

DICHIARAZIONE DEL PAZIENTE
Il sottoscritto/La sottoscritta_____
Ha partecipato ad un consulto informativo in cui ha potuto fare tutte le possibili domande
- Non ha bisogno di porre altre domande e non necessita di tempi di riflessione
- È consapevole che l'indagine ha finalità di ricerca e non è mio stesso beneficio
- Acconsente con ciò all'esecuzione dell'esame proposto

Il rifiuto ad eseguire l'esame o la sua interruzione non comportano ripercussione alcuna.

LIMITAZIONI
Solo una ristretta cerchia di persone non può sottoporsi a questa metodica. Per questa ragione si prega di rispondere alle seguenti domande.

Soffre di claustrofobia?	**SI**	**NO**
Ha mai lavorato (o lavora) come saldatore, tornitore o carrozziere?	**SI**	**NO**
Ha mai subito incidenti stradali, incidenti di caccia?	**SI**	**NO**
E' stato vittima di traumi da esplosione?	**SI**	**NO**
E' in stato di gravidanza?	**SI**	**NO**
Ultime mestruazioni avvenute		
Ha subito interventi chirurgici su: TESTA ADDOME COLLO ESTREMITA' TORACE ALTRI		
E' portatore di:		
• Schegge di frammenti metallici?	**SI**	**NO**
• Clips su aneurismi (vasi sanguigni), aorta, cervello?	**SI**	**NO**
• Valvole cardiache?	**SI**	**NO**
• Distrattori della colonna vertebrale?	**SI**	**NO**
• Pompe ad infusione per insulina o altri farmaci?	**SI**	**NO**
• Pace-maker cardiaco o altri tipi di catetere cardiaco?	**SI**	**NO**
• Corpi metallici nelle orecchie o impianti per udito?	**SI**	**NO**
• Neurostimolatori?	**SI**	**NO**
• Elettrodi impiantati nel cervello o subdurali?	**SI**	**NO**
• Corpi intrauterini?	**SI**	**NO**
• Deviazione spinale o ventricolare?	**SI**	**NO**
• Protesi metalliche (per pregresse fratture, interventi correttivi articolari, etc.), viti, chiodi, filo, etc.?	**SI**	**NO**
In caso di risposta affermativa, dove?		
• Protesi dentarie, fisse o mobili?	**SI**	**NO**
• Protesi del cristallino?	**SI**	**NO**
• Piercings non removibili?	**SI**	**NO**
• Tatuaggi?	**SI**	**NO**
• Cerotti medici (nicotina, anticoncezionale)?	**SI**	**NO**
E' affetto da anemia falciforme?	**SI**	**NO**

Data_____

Firma del paziente_____

Medico_____

Firma del Medico_____